

ISTANBUL TECHNICAL UNIVERSITY ★ GRADUATE SCHOOL

**INVESTIGATING THE VALORISATION POTENTIAL
OF HAZELNUT BY-PRODUCTS: TRANSFORMING WASTE
INTO FUNCTIONAL FOOD INGREDIENTS**



Ph.D. THESIS

Fatma Duygu CEYLAN

Department of Food Engineering

Food Engineering Programme

DECEMBER 2022

ISTANBUL TECHNICAL UNIVERSITY ★ GRADUATE SCHOOL

**INVESTIGATING THE VALORISATION POTENTIAL
OF HAZELNUT BY-PRODUCTS: TRANSFORMING WASTE
INTO FUNCTIONAL FOOD INGREDIENTS**

Ph.D. THESIS

**Fatma Duygu CEYLAN
(506152501)**

Department of Food Engineering

Food Engineering Programme

Thesis Advisor: Prof. Dr. Esra ÇAPANOĞLU GÜVEN

DECEMBER 2022

İSTANBUL TEKNİK ÜNİVERSİTESİ ★ LİSANSÜSTÜ EĞİTİM ENSTİTÜSÜ

**FINDIK YAN ÜRÜNLERİNİN POTANSİYEL KATMA
DEĞERİNİN İNCELENMESİ: ATIK KONUMUNDAN
FONKSİYONEL GIDA BİLEŞENİNE DÖNÜŞÜM**

DOKTORA TEZİ

**Fatma Duygu CEYLAN
(506152501)**

Gıda Mühendisliği Anabilim Dalı

Gıda Mühendisliği Programı

Tez Danışmanı: Prof. Dr. Esra ÇAPANOĞLU GÜVEN

ARALIK 2022

Fatma Duygu CEYLAN, a Ph.D. student of ITU Graduate School student ID 506152501 successfully defended the thesis entitled “INVESTIGATING THE VALORISATION POTENTIAL OF HAZELNUT BY-PRODUCTS: TRANSFORMING WASTE INTO FUNCTIONAL FOOD INGREDIENTS”, which she prepared after fulfilling the requirements specified in the associated legislations, before the jury whose signatures are below.

Thesis Advisor : **Prof. Dr. Esra ÇAPANOĞLU GÜVEN**
Istanbul Technical University

Jury Members : **Assoc. Prof. Dr. Aşlı CAN KARAÇA**
Istanbul Technical University

Prof. Dr. Aliye ARAS
Istanbul University

Assoc.Prof. Dr. Derya KAHVECİ KARINCAOĞLU
Istanbul Technical University

Assist. Prof. Dr. Zehra GÜLSÜNOĞLU KONUŞKAN
Istanbul Aydın University

Date of Submission : **30 November 2022**

Date of Defense : **9 December 2022**





To My Beloved Family



FOREWORD

First of all, I would like to express my special thanks and sincere gratitude to my supervisor and mentor, Prof. Dr. Esra ÇAPANOĞLU GÜVEN who helped me in countless ways, educated me in the scientific and academic field, and supervised me to carry out this PhD thesis. She is an exceptional scientist and a person who has a fantastic sense of affection, and I am truly fortunate to be her student, which is an honour to carry and a motivation to succeed.

I would like to express my gratitude to Prof. Dr. Aliye ARAS and Assoc. Prof. Dr. Aslı CAN KARAÇA who shared their scientific views and recommendations with me during this study.

This PhD dissertation was carried out in Food Engineering Department at Istanbul Technical University. Some parts of the thesis were completed at the University of Wisconsin-Madison Food Science Department. So, I would like to express my sincere gratitude to Assoc. Prof. Dr. Bradley BOLLING for his guidance, dedication, and understanding during my stay in his lab and for allowing me to join his team. It was an unforgettable experience for me where I spent the beginning of the Covid-19 pandemic. I would also like to express my special gratitude to my close friends Elisa ALE, Grace LIU, Serena WU and Dasol CHOI from UW Madison, with whom I have made lifelong friendships even though we are in three different continents, for their help and support in my dissertation and the unforgettable memories we have collected together.

This thesis was financially supported by Istanbul Technical University, Scientific Research Projects (BAP) Unit (Project numbers: 43465 and 43489). I also would like to acknowledge here: Doctoral Research Scholarship by The Council of Higher Education of Turkey (YOK-YUDAB)- University of Wisconsin Madison, The United States of America, August 2019-August 2020. I am grateful for the samples provided by Giresun Fındık Araştırma Enstitüsü and Altaş Yağ San. ve Tic. A.Ş.

It is my pleasure to express my thanks to Assist. Prof. Dr. Hilal YILMAZ and Dr. Büşra GÜLTEKİN SUBAŞI for their scientific contribution to the this thesis. I would also like to special thank Dr. Deniz GÜNAL KÖROĞLU who was always there to help me with her smiling face whenever I needed it, day and night during the article preparation process. I am grateful to Doğa BİLİCAN and BEYZA VAHAPOĞLU for their assistance with the SEM and FTIR analyses. Speacial thanks to Nalan DEMİR, Evren DEMİRCAN and Ümit ALTUNTAŞ for their help in practical issues.

Also, I would like to extend my gratitude to all my lab colleagues and research assistants at Istanbul Technical University, Food Engineering Department. Special thanks to my office mates Elif Feyza AYDAR, Hümeyra ÇAVDAR and Zehra MERTDİNÇ who always give me joy and energy.

As part of our barrel of monkey group, I would also like to express my gratitude to Gizem SOYDAN and Hakan ALAKOCA for the wonderful celebrations that followed

the tough times. On the other hand, Serkan IŐIK aka MSI deserves a gold medal for his dedication to help me to format the thesis day and night. It would not have been possible without him.

I have special thanks to my close friends Atefeh KARİMİDASTJERD, Burcu GÜLDİKEN, Hande YÜCE, Sena BAKIR and Ponçıksu for all their support and help as well as all the good memories that we shared together during my Ph.D. life and we will continue from now on.

I have reserved the most special thanks for my fellow and best buddy Gizem ÇATALKAYA who was always there for me in any case, no matter what, to support me during all these years.

Last but not the least, I would like to thank my beloved family; my parents Mukadder and Mesut CEYLAN, my younger brother, sister-in-law and newborn nephew Çağrı, Büşra and Çağan Berk CEYLAN, my grand parents Cevriye and Mehmet CEYLAN and my whole extended family members for their endless love, support and prayers throughout my education and life. Lastly, I would like to extend my deepest and special appreciation to my partner and my best friend Nabil ADRAR for his priceless support, encouragement, patience and love. I am grateful to have you as a part of my life.

December 2022

Fatma Duygu CEYLAN
(Food Engineer, M.Sc.)

TABLE OF CONTENTS

	<u>Page</u>
FOREWORD	x
TABLE OF CONTENTS	xii
ABBREVIATIONS	xiii
SYMBOLS	xv
LIST OF TABLES	xvii
LIST OF FIGURES	xx
SUMMARY	xxi
ÖZET	xxv
1. INTRODUCTION	1
1.1 Purpose of Thesis	4
2. VALORISATION OF HAZELNUT BY-PRODUCTS: CURRENT APPLICATIONS AND FUTURE POTENTIAL	5
2.1 Introduction	5
2.2 Chemical Composition of Hazelnut By-products	7
2.2.1 Proximate composition and nutritional value	7
2.2.1.1 Proximate composition of the shell	7
2.2.1.2 Proximate composition of the skin	9
2.2.1.3 Hazelnut skin is a rich source of vitamin E, Oleic, and Linoleic Acids	9
2.2.1.4 Proximate composition of the meal	10
2.2.2 Polyphenols and other bioactive components in hazelnuts by-products	12
2.2.2.1 Bioactive compounds of hazelnut skin	12
2.2.2.2 Bioactive compounds of hazelnut shell	13
2.2.2.3 Bioactive compounds of hazelnut meal	14
2.3 Insights Into Current and Valorisation of Hazelnut By-products	16
2.3.1 Valorisation of hazelnut shell	16
2.3.2 Valorisation of hazelnut skin	22
2.3.3 Valorisation of hazelnut meat	27
2.4 Conclusions and Perspectives	32
3. COMBINED NEUTRASE-ALCALASE PROTEIN HYDROLYSATES FROM HAZELNUT MEAL, A POTENTIAL FUNCTIONAL FOOD INGREDIENT	35
3.1 Introduction	35
3.2 Materials and Methods	36
3.2.1 Enzymes and chemicals	36
3.2.2 Hazelnut meal characterization	36
3.2.3 Protein extraction from hazelnut meal	37
3.2.4 Preparation of hazelnut protein hydrolysates	37
3.2.5 SDS-PAGE analysis	39
3.2.6 Molecular Weight (MW) distribution	39
3.2.7 Amino acid profile	39
3.2.8 Fourier-Transform Infrared spectroscopy (FTIR)	40
3.2.9 Scanning Electron Microscopy (SEM)	40
3.2.10 Dynamic light scattering analysis	40
3.2.11 Determination of emulsifying properties	41
3.2.12 Assessment of FFA Release Inhibition	41
3.2.13 In-vitro Antioxidant Activity	42
3.2.14 Statistical Analysis	43
3.3 Results and Discussion	43
3.3.1 Protein Hydrolysis Efficiency	43
3.3.1.1 Degree of protein hydrolysis and SDS-PAGE patterns	43

3.3.2	Molecular Weight (MW) Distribution of Protein Isolates and Hydrolysates.....	46
3.3.3	Amino Acid Profile of Hazelnut Protein Isolates and Hydrolysates ...	47
3.3.4	Fourier-Transform Infrared (FTIR) Spectroscopy	48
3.3.5	Scanning Electron Microscopy (SEM).....	52
3.3.6	Particle Size, Size Distribution and ζ -potential	53
3.3.7	Emulsifying Properties.....	54
3.3.8	Inhibition of FFA Release	58
3.3.9	In-vitro Antioxidant Activity of Protein Isolates and Hydrolysates ...	59
3.3.9.1	DPPH Radical Scavenging Activity	59
3.3.9.2	ABTS Radical Scavenging Activity	60
3.4	Conclusion	62
4.	INTERACTIONS BETWEEN HAZELNUT (<i>CORYLUS AVELLANA L.</i>) PROTEIN AND PHENOLICS AND IN VITRO GASTROINTESTINAL DIGESTIBILITY	63
4.1	Introduction	63
4.2	Materials and Methods	64
4.2.1	Materials.....	64
4.2.2	Preparation of hazelnut skin extracts (HSE)	65
4.2.3	Preparation of protein isolate from hazelnut meal)	65
4.2.4	Amino acid profile of the hazelnut protein isolate.....	66
4.2.5	Preparation of protein-phenolic complex solutions.....	67
4.2.5.1	Particle size, size distribution, and ζ -potential determination	67
4.2.5.2	Fluorescence quenching.....	67
4.2.5.3	Stern-Volmer equationg	68
4.2.5.4	Thermodynamic parameters	69
4.2.5.5	Fourier Transform Infrared (FTIR) spectroscopy	69
4.2.6	Assessment of hazelnut protein digestibility by pancreatin	70
4.2.7	Simulated in-vitro gastrointestinal digestion for HSE bioaccessibility	71
4.2.7.1	Spectrophotometric analyses.....	71
4.2.7.2	HPLC-DAD analysis of phenolic compounds	71
4.2.8	Statistical analysis.....	73
4.3	Results and Discussion	73
4.3.1	Effect of dephenolisation on protein purity and protein recovery and amino acid profile	73
4.3.2	Average particle size, size distribution, and ζ -charge	74
4.3.3	Fluorescence quenching	76
4.3.3.1	Stern-Volmer plot.....	79
4.3.3.2	Thermodynamic parameters	81
4.3.4	Fourier Transform Infrared (FTIR) spectroscopy.....	83
4.3.5	Effect of polyphenols on hazelnut protein digestibility	86
4.3.6	Simulated in vitro gastrointestinal digestion.....	88
4.3.6.1	Spectrophotometric analyses.....	88
4.3.6.2	HPLC-DAD analysis of phenolic compounds	89
4.4	Conclusions	93
5.	CONCLUSIONS	95
5.1	Status and Main Outcomes of This Thesis	95
5.1.1	Valorisation of hazelnut by-products: current applications and future potential.....	95
5.1.2	Combined Neutrase-Alcalase protein hydrolysates from hazelnut meal, a potential functional food ingredient	96
5.1.3	Interactions between hazelnut (<i>Corylus Avellana L.</i>) protein and phenolics and in vitro gastrointestinal digestibility.....	96
	REFERENCES	99
	CURRICULUM VITAE	123

ABBREVIATIONS

A375	: Primary human melanoma cancer cell line
ABTS	: 2,2'-azino-di-(3-ethylbenzthiazoline sulfonic acid
ACE	: Angiotension I-converting enzyme
AH	: Alcalase hydrolysates of PI
AMPK	: Adenosine monophosphate-activated protein kinase
ANOVA	: Analysis of variance
AXOS	: Arabino-xylooligosaccharides
BCAA	: Branched-chain amino acids
C	: Catechin
CEO	: Clove essential oil
ChCl	: Choline chloride
CUPRAC	: Cupric ion reducing antioxidant capacity
(DPP)-IV	: Dipeptidyl peptidase
DES	: Deep eutectic solvents
DH	: Degree of hydrolysis
DHC	: Defatted hazelnut meal
DHCP	: Defatted hazelnut meal protein
DHF	: Defatted hazelnut flour
DHFP	: Defatted hazelnut flour protein
dHPI	: Dephenolised hazelnut meal protein isolates
DLS	: Dynamic light scattering
DPPH	: 2,2-Diphenyl-1-picrylhydrazyl
EAA	: Essential amino acids
EAI	: Emulsifying activity index
EC	: Epicatechin
EGC	: (-)-Epigallocatechin
EGCG	: (-)-Epigallocatechin gallate
ESI	: Emulsifying stability index
FFA	: Free fatty acid
FTIR	: Fourier-Transform Infrared Spectroscopy
GA	: Gallic acid
GCG	: Gallocatechin gallate
GI	: Gastrointestinal
H2SO4	: Sulfuric acid
HeLa	: Cervical cancer cell line
HPH	: High-pressure homogenisation
HP-SEC	: A high-performance size-exclusion chromatograph
HS	: Hazelnut skin
HSE	: Hazelnut skin phenolic extracts
HSPE	: Hazelnut skin phenolic extract
IC50	: The 50% inhibitory concentration values

kDa	: Kilodalton
LC/APCI-MS	: Liquid chromatography/ atmospheric pressure chemical ionization–tandem mass spectrometry
LC-Q-TOF/MS	: Liquid Chromatography Quadrupole Time-of-Flight Mass Spectrometry
MAE	: Microwave-assisted extraction
MFAH	: Alcalase hydrolysates of MFPI
MFANH	: Hydrolysates obtained with sequential hydrolysis by respectively, Alcalase and Neutrase of MFPI
MFNAH	: Hydrolysates obtained with sequential hydrolysis by respectively, Neutrase and Alcalase of MFPI
MFNH	: Neutrase hydrolysates of MFPI
MFPI	: Microfluidized protein isolates
MTT	: 3-(4,5-dimethylthiazol-2-yl)-2,5-diphenyltetrazolium bromide
MUFA	: Monounsaturated fatty acid
MW	: Molecular weight
NADES	: Natural deep eutectic solvents
NaOH	: Sodium hydroxide
NEAA	: Non-essential amino acids
NH	: Neutrase hydrolysates of PI
PBS	: Phosphate-buffered saline
PCA	: Protocatechuic acid
PDA	: Photo diode array
PDI	: Polydispersity index
PES	: Polyethersulfone
Phen	: Phenylalanine
PI	: Hazelnut protein isolates
PL	: Pancreatic lipase
PLA	: Poly(lactic acid)
PMT	: Photon counting photomultiplier
PP	: Poly(propylene)
PUFA	: Polyunsaturated fatty acid
Q3R	: Quercetin 3-O-rhamnoside
QUE	: Quercetin
RI	: Recovery index
SCE	: Supercritical carbon dioxide extraction
SD	: Standard deviation
SDS	: Sodium dodecyl sulfate
SEC	: Size exclusion chromatography
SEM	: Scanning Electron Microscopy
SK-Mel 28	: Metastatic human melanoma cancer cell line
TFA	: Trifluoroacetic acid
TPC	: Total Phenolic content
Trp	: Tryptophane
Tyr	: Tyrosine
UAE	: Ultrasound-assisted extraction
US	: Ultrasound
XOS	: Xylooligosaccharides
α-TTP	: α -tocopherol transfer protein

SYMBOLS

α	: The average degree of dissociation of the α -NH ₂ groups released during hydrolysis
β	: Beta
γ	: Gamma
ζ	: Zeta
ϕ	: The volumetric fraction of the oil
ΔH	: Enthalpy change
ΔS	: Entropy change
ΔG	: Gibbs free energy change
n	: Slope of the plot
K_A	: Intercept of the plot
τ_0	: The lifetime of the fluorophore in the absence of quencher
Q	: Concentration of phenolic extract



LIST OF TABLES

	<u>Page</u>
Table 2.1 : Proximate composition of hazelnut (<i>Corylus avellana</i> L.) by-products (wt%, db).	8
Table 2.2 : Amino acid profile of hazelnut proteins (Shahidi and Miraliakbari, 2006).	11
Table 3.1 : Amino acid profile of hazelnut meal protein isolates (mg/g protein)..	47
Table 3.2 : Secondary structure content (%) of protein samples from FTIR data.	51
Table 4.1 : Protein content and protein recovery from defatted hazelnut meal (dry basis).	74
Table 4.2 : Amino acid profile of hazelnut meal protein isolate (mg/g protein). ...	74
Table 4.3 : Stern-Volmer constants and thermodynamic parameters of dHPI-HSE complex at different temperatures.	82
Table 4.4 : Intensity values of major FTIR bands and Secondary structure content (%) of dHPI-phenolic complexes from FTIR data.	85
Table 4.5 : Total phenolic content (TPC), recovery index of phenolic compounds (RI) and antioxidant capacities (DPPH and CUPRAC methods) in gastrointestinal digestion phases.....	90
Table 4.6 : Phenolic profiles of initial gastric and intestinal phases of solutions after in vitro GI digestion.	91



LIST OF FIGURES

	<u>Page</u>
Figure 2.1 : Fates of in-shell hazelnut and its by-products obtained after industrial processing. The numbers are approximate (citations in sections 1 and 2), ND: not determined.....	6
Figure 2.2 : Chemical structures of major phenolic compounds found in hazelnut by-products. The asterisks: *,**,*** refer respectively to major phenolic compounds of the skin, the shell, and the meal. Data were collected from the Phenol-Explorer database (http://phenol-explorer.eu/) except for quinic acid, chlorogenic acid, and rutin, which were from Chemspider (https://www.chemspider.com/), and glansreginin A and B which were from Greenmolbd (https://www.greenmolbd.gov.bd/). Esterification of syringic acid with a random hexose was made using Chemdraw online program (https://chemdrawdirect.perkinelmer.cloud/js/sample/index.html). All data was openly accessed on 10.05.2022.	15
Figure 3.1 : Degree of hydrolysis (A) and changes in SDS-PAGE profiles of microfluidized and non-microfluidized hazelnut protein isolates and their hydrolysates, prepared with Alcalase, Neutrase, or the combination of both (B, C). M: Marker, 1:PI, 2: MFPI, 3:NH, 4:MFNH, 5:AH 6:MFAH, 7:MFNAH, 8:MFANH.....	45
Figure 3.2 : Molecular weight distribution of hazelnut protein isolates and their hydrolysates, prepared with Alcalase, Neutrase, or the combination of both.	46
Figure 3.3 : FTIR spectra of hazelnut protein isolates and their hydrolysates, prepared with Alcalase, Neutrase, or the combination of both in the range of 500-4000 cm^{-1} (A), 2800-3500 cm^{-1} (B) and 1200-1800 cm^{-1} (C).	50
Figure 3.4 : Morphologies of microfluidized and non-microfluidized hazelnut protein isolates and their hydrolysates, prepared with Alcalase, Neutrase, or the combination of both.	54
Figure 3.5 : Average particle size (a), size distribution (b) and (c) surface charge of microfluidized and non-microfluidized hazelnut protein isolates and their hydrolysates, prepared with Alcalase, Neutrase, or the combination of both. Different letters (a-d) indicate statistically significant differences ($P < 0.05$).....	55

Figure 3.6 : Emulsifying properties of microfluidized and non-microfluidized hazelnut protein isolates and their hydrolysates, prepared with Alcalase, Neutrase, or the combination of both. Results are expressed as emulsifying activity index (EAI) and emulsion stability index (ESI). Small letters (a-f) indicate significant differences between ESI groups ($p < 0.05$). Capital letters (A-D) indicate significant differences between EAI groups ($p < 0.05$).	57
Figure 3.7 : Inhibition of FFA (%) of microfluidized and non-microfluidized hazelnut protein isolates and their hydrolysates, prepared with Alcalase, Neutrase, or the combination of both.	59
Figure 3.8 : DPPH (A) and ABTS (B) radical scavenging activities of microfluidized and non-microfluidized hazelnut protein isolates and their hydrolysates, prepared with Alcalase, Neutrase, or the combination of both. Different letters (a-d) indicate statistically significant differences ($P < 0.05$).	61
Figure 4.1 : Flow diagram of simulated in vitro gastrointestinal digestion. pH adjustment was made with 0.1 M HCL or 1 M NaOH for each phase.	72
Figure 4.2 : DLS results of hazelnut protein isolates (HPI), dephenolized HPI (dHPI), and dHPI-HSE/Catechin complexes at different concentrations of polyphenols (mM). A: Average size and polydispersity index (PDI). B: ζ -potential.	75
Figure 4.3 : Fluorescence emission spectra (at λ_{ex} 280 nm) of dHPI HSE.complex at 298 (a), 308 (b), and 318 K (c) in phosphate buffer solution at pH 7 with an increase in HSE concentration (0-0.5 mM). Each curve represents a triplicate assay after correction for phenol extract fluorescence.	77
Figure 4.4 : Fluorescence intensity results of dHPI at the excitation wavelength of 295 nm with an increase in HSE concentration (0-0.5 mM) in PBS at pH 7 and room temperature.	78
Figure 4.5 : Stern-Volmer plots (a). the double logarithm regression curves (b). and Van't Hoff plots (c) for dHPI-HSE mixtures at different temperatures (blue: 298 K; red: 308 K; black: 318 K) to calculate the number of binding sites (n). binding constant (K_A). and thermodynamic parameters.	80
Figure 4.6 : FTIR spectra of dHPI. dHPI-HSE complex and dHPI-catechin complex. dHPI: dephenolyzed protein isolate; dHPI+C: hazelnut meal protein isolate-catechin solution; dHPI+HSE: hazelnut meal protein isolate-hazelnut skin extract solution.	84
Figure 4.7 : Degree of hydrolysis of hazelnut protein isolates (HPI), dephenolized HPI (dHPI), and dHPI-HSE/Catechin (C) complexes at different concentrations of polyphenols (mM). *The actual concentrations are 16.67 times higher but protein/polyphenol ratios are kept the same as what was used in the other parts of the study. ..	87

INVESTIGATING THE VALORISATION POTENTIAL OF HAZELNUT BY-PRODUCTS: TRANSFORMING WASTE INTO FUNCTIONAL FOOD INGREDIENTS

SUMMARY

Hazelnuts are one of the most widely consumed nuts around the world. Considering the nutritional value of hazelnuts, a wide range of hazelnut-based food products are available in the market. Nevertheless, the processing of hazelnuts generates a large number of by-products and waste. The most valuable by-products of the hazelnut industry are shell, skin, and meal. These by-products are rich in bioactive compounds, protein, dietary fibre, mono- and polyunsaturated fatty acids, vitamins, minerals, phytosterols, and squalene. The current utilisation of hazelnut by-products is mostly limited to animal feed supplementation of hazelnut meal and skin and use as a low-value heat source for the shells. However, disposing of these by-products or using them as a low-value heat source or animal feed supplementation results in significant waste of a natural resource rich in nutritional components. Consequently, valorising hazelnut by-products as bioactive ingredients in diverse fields such as food, pharmaceuticals and cosmetics has stimulated interest among scientists, producers, and consumers.

In light of the above, a research strategy to investigate the valorisation potential of hazelnut by-products has been developed. The objectives of this Ph.D. dissertation were (i) to valorise hazelnut meal and explore the potential anti-obesity and antioxidant activities of its protein hydrolysates; (ii) to investigate the effect of the hydrolysis strategy (single or sequential hydrolysis) using Alcalase and Neutrase, as well as the application of microfluidization pretreatment on the antioxidant and anti-obesity activities and the functional properties of the protein isolates and hydrolysates; (iii) to examine the formation of the protein-polyphenol complex from dephenolised hazelnut meal protein isolates (dHPI) and hazelnut skin phenolic extracts (HSE); (iv) to monitor the bioaccessibility of hazelnut proteins and polyphenols after protein-polyphenol complexation.

Two different research studies (Chapters 3-4) were conducted in line with these purposes. Firstly, hydrolysates of hazelnut proteins obtained with Alcalase and Neutrase were mainly examined for their physicochemical properties, potential anti-obesity effects, antioxidant capacities, and emulsifying properties (Chapter 3). Later on, protein-polyphenol complexes formed from dephenolised hazelnut meal protein isolates (dHPI) and hazelnut skin phenolic extracts (HSE) were investigated as well as their effects on bioaccessibility (Chapter 4). The background and objectives of this Ph.D. dissertation are introduced in the first chapter. Following that, an overview of current scientific knowledge about the main and most valuable hazelnut by-products and their actual valorisation, focusing on their chemical composition to inspire new

applications of these valuable resources and fully exploit their potential, has been reviewed in the second part.

In the third part, hazelnut meal protein hydrolysates obtained by a single or combined hydrolysis by Alcalase and Neutrase were mainly characterised for their physicochemical properties (SDS-PAGE, particle size distribution, Fourier transform infrared, molecular weight distribution, etc.) and potential anti-obesity effect (FFA release inhibition), antioxidant activity (DPPH and ABTS methods), and emulsifying properties. The impact of microfluidization pretreatment was also investigated. The combination of Alcalase with Neutrase permitted the highest degree of hydrolysis (DH) ($15.57 \pm 0.0\%$) of hazelnut protein isolate, which resulted in hydrolysates with the highest amount of low molecular weight peptides, as indicated by size exclusion chromatography (SEC) and SDS-PAGE. There was a positive correlation between the degree of hydrolysis and the inhibition of FFA release by pancreatic lipase, with a significant positive effect of microfluidization when followed by Alcalase hydrolysis. Microfluidization enhanced the emulsifying activity index (EAI) of protein isolates and hydrolysates. Low hydrolysis by Neutrase had the best effect on the EAI (84.32 ± 1.43 (NH) and 88.04 ± 2.22 m²/g (MFNH)), while a negative correlation between the emulsifying stability index (ESI) and the DH was observed. Again, the combined Alcalase-Neutrase hydrolysates displayed the highest radical scavenging activities ($96.63 \pm 1.0\%$ DPPH and $98.31 \pm 0.46\%$ ABTS). FTIR results showed that the application of microfluidization caused the unfolding of the protein structure. The individual or combined application of the Alcalase and Neutrase enzymes caused a switch from the β -sheet organization of the proteins to α -helix structures. In conclusion, hazelnut meal may be a good source of bioactive and functional peptides. The control of its enzymatic hydrolysis, together with an appropriate pretreatment such as microfluidization, may be crucial to achieve the best suitable activity.

In the fourth part, the formation of the protein-polyphenol complex from dephenolised hazelnut meal protein isolates (dHPI) and hazelnut skin phenolic extracts (HSE), as well as its effect on the bioaccessibility of both hazelnut proteins and polyphenols, were investigated. The dHPI+HSE complexes were of considerable size and dependent on HSE concentration due to the occurrence of aggregation. Although catechin was the main component of HSE, it did not cause aggregation, except for a slight rise in particle size. According to fluorescence quenching, the hazelnut protein-phenolic extract complex had a linear Stern-Volmer plot expressing static quenching between 0-0.5 mM concentrations, and the interaction was mainly dependent on hydrogen bonding and van der Waals forces ($\Delta H < 0$ and $\Delta S < 0$) and the reaction was spontaneous ($\Delta G < 0$). According to Fourier Transform Infrared (FTIR) Spectroscopy results, higher phenolic extract concentration caused an increase in irregular structures in hazelnut protein, while the lowest phenolic concentration and catechin altered the regular structure. Skin extracts did not alter the digestibility of dephenolised proteins, but dephenolisation reduced the degree of hydrolysis by pancreatin. The formation of the protein-polyphenol complex had a beneficial effect on the bioaccessibility of hazelnut skin polyphenols predominantly on the gallolated form of the catechins such as gallocatechin gallate and epigallocatechin gallate.

The final part presents the general discussions and conclusions, as well as future perspectives on the valorisation of hazelnut by-products, based on the findings of the previous chapters. A by-product of the hazelnut oil industry, hazelnut meal, was valorised as a source of bioactive peptides with an emphasis on their potential anti-obesity and antioxidant properties. First, hazelnut meal protein isolates were treated with microfluidization to improve their hydrolysis and functional properties. Then, sequential or individual hydrolysis by Neutrase and Alcalase was performed to prepare the protein hydrolysates. Finally, by combining Alcalase and Neutrase hydrolysis, we achieved the highest degrees of hydrolysis (DH), inhibiting FFA release by pancreatic lipase and scavenging free radicals. Regarding anti-obesity and antioxidant properties, hazelnut protein hydrolysates have the potential as functional food ingredients. Therefore, it is important to understand the process for protein processing (pretreatment, degree of hydrolysis, etc.) based on its intended application. Protein-polyphenol interactions improved the bioavailability of hazelnut skin polyphenols, particularly the gallolated form of catechins like gallic catechin gallate (GCG) and epigallocatechin gallate (EGCG). In recent years, researchers have focused on polyphenolic compounds and plant-based proteins isolated from natural sources. It is essential in vegan formulations such as foam-like products (mousse) or emulsions (mayonnaise), where the functional properties of proteins are crucial. Additionally, there is no consensus on whether protein-phenolic interactions affect polyphenol bioavailability positively or negatively. Consequently, more research needs to be conducted on this subject and reported in the literature



FINDIK YAN ÜRÜNLERİNİN POTANSİYEL KATMA DEĞERİNİN İNCELENMESİ: ATIK KONUMUNDAN FONKSİYONEL GIDA BİLEŞENİNE DÖNÜŞÜM

ÖZET

Fındık, dünya çapında en çok tüketilen kuruyemişlerden biridir. Fındığın besin değeri de göz önüne alındığında, piyasada çok çeşitli fındık bazlı gıda ürünleri mevcuttur. Bununla birlikte, fındığın işlenmesi çok sayıda yan ürün ve atık oluşturmaktadır. Fındık endüstrisinin en değerli yan ürünleri kabuk, zar ve küspedir. Bu yan ürünler, biyoaktif bileşikler, protein, diyet lifi, tekli ve çoklu doymamış yağ asitleri, vitaminler, mineraller, fitosteroller ve skualen açısından zengindir. Fındık yan ürünlerinin mevcut kullanımı, fındık küspesi ve zarının hayvan yemi takviyesi, kabuklar için ise düşük değerli bir ısı kaynağı olarak kullanımı ile sınırlıdır. Bununla birlikte, bu yan ürünlerin bertaraf edilmesi veya düşük değerli bir ısı kaynağı veya hayvan yemi takviyesi olarak kullanılması, besin bileşenleri açısından zengin bir doğal kaynağın önemli ölçüde israfına neden olmaktadır. Sonuç olarak, fındık yan ürünlerinin gıda, eczacılık ve kozmetik gibi farklı alanlarda biyoaktif bileşenler olarak değerlendirilmesi bilim adamları, üreticiler ve tüketiciler arasında ilgi uyandırmaktadır.

Bu tez çalışması yukarıdaki bilgiler ışığında, fındık yan ürünlerinin katma değer kazanma potansiyelini araştırılması üzerine kurgulanmıştır. Bu doktora tezinin amaçları sırasıyla (i) fındık küspesine katma değer kazandırmak ve fındık posasından elde edilen protein hidrolizatlarının potansiyel anti-obezite ve antioksidan aktivitelerinin araştırması; (ii) Alkalaz ve Nötraz enzimleri kullanılarak hidroliz stratejisinin (tek veya kombine hidroliz) yanı sıra mikroakışkanlaştırma ön işleminin antioksidan ve anti-obezite aktiviteleri ve protein izolatları ile hidrolizatların fonksiyonel özellikleri üzerindeki etkisini araştırmak; (iii) Fenolik bileşikleri uzaklaştırılmış fındık küspesi protein izolatlarından (dHPI) ve fındık zarı fenolik ekstraktlarından (HSE) protein-polifenol kompleksinin oluşumunun incelenmesi; (iv) protein-polifenol kompleksi oluşumu sonrası fındık proteinlerinin ve polifenollerin biyoerişilebilirliğinin izlenmesidir.

Bu amaçlar doğrultusunda iki farklı araştırma çalışması (Bölüm 3-4) yapılmıştır. İlk olarak, Alcalase ve Neutrased enzimleri ile elde edilen fındık protein hidrolizatlarının temel olarak fizikokimyasal özellikleri, potansiyel anti-obezite etkileri, antioksidan kapasiteleri ve emülsifiye edici özellikleri incelenmiştir (Bölüm 3). Sonrasında defenolize fındık küspesi protein izolatlarından (dHPI) ve fındık zarı fenolik ekstraktlarından (HSE) oluşan protein-polifenol kompleksleri ve bunların biyoerişilebilirlik üzerindeki etkileri araştırılmıştır (Bölüm 4).

İlk bölümde bu doktora tezinin araştırma çerçevesi ve hedefleri tanıtılmıştır. Ardından, ikinci bölümde, başlıca fındık yan ürünleri, bu değerli kaynakların yeni uygulamalarına ilham vermek ve potansiyellerinden tam olarak yararlanmak için

kimyasal bileşimlerine odaklanılarak mevcut bilimsel bilgilere genel bir bakış açısı oluşturulmuştur.

Ardından, ikinci bölümde, başlıca fındık yan ürünleri ve bunların değerlendirilmesi hakkında mevcut bilimsel bilgilere genel bir bakış, bu değerli kaynakların yeni uygulamalarına ilham vermek ve potansiyellerinden tam olarak yararlanmak için kimyasal bileşimlerine odaklanılarak bahsedilmiştir.

Üçüncü bölümde, Alkalaz ve Nötraz enzimleri kullanılarak tek veya kombine hidroliz ile elde edilen fındık küspesi protein hidrolizatlarının temel olarak fizikokimyasal özellikleri (SDS-PAGE, parçacık boyutu dağılımı, Fourier dönüşümü kızılötesi (FTIR), moleküler ağırlık dağılımı vb.) ve potansiyel anti-obeze etkisi, antioksidan aktivite (DPPH ve ABTS yöntemleri) ve emülsifiye edici özellikleri karakterize edilmiştir. Ayrıca bu özelliklerin üzerine mikroakışkanlaştırma ön işleminin etkisi de araştırılmıştır. Alkalaz'ın Nötraz ile kombinasyonu, boyut dışlama kromatografisi (SEC) ve SDS-PAGE sonuçları ile belirtilmek üzere, en yüksek miktarda düşük moleküler ağırlıklı peptidlere sahip hidrolizatlarla sonuçlanan fındık protein izolatında en yüksek hidroliz derecesine (DH) ($15,57 \pm 0,0$) sahip olduğu rapor edilmiştir. Hidroliz derecesi ile pankreatik lipaz tarafından serbest yağ asitleri salınımının inhibisyonu arasında pozitif bir korelasyon vardır ve ardından Alkalaz hidrolizi ile birlikte mikroakışkanlaştırmanın önemli bir pozitif etkisi olduğu görülmüştür. Mikroakışkanlaştırma, protein izolatlarının ve hidrolizatların emülsiyon aktivite indeksini (EAI) artırmıştır. Nötraz ile elde edilen düşük hidroliz derecesinin EAI üzerinde en iyi etkiye sahip olduğu görülürken ($84,32 \pm 1,43$ (NH) ve $88,04 \pm 2,22$ m²/g (MFNH)), emülsiyon stabilite indeksi (ESI) ile DH arasında negatif bir korelasyon gözlenmiştir. Yine, kombine Alkalaz-Nötraz hidrolizatları en yüksek radikal yakalama aktivitelerini göstermiştir (96.63 ± 1.06 DPPH ve 98.31 ± 0.46 ABTS). FTIR sonuçları, mikroakışkanlaştırma ön uygulamasının protein yapısının açılmasına neden olduğunu göstermiştir. Alkalaz ve Nötraz enzimlerinin bireysel veya kombine uygulaması, proteinlerin β -tabaka organizasyonundan α -heliks yapılarına geçişe neden olmuştur. Bu çalışma ile, fındık küspesinin iyi bir biyoaktif ve fonksiyonel peptit kaynağı olabileceği ve mikroakışkanlaştırma gibi uygun bir ön işleme birlikte enzimatik hidrolizasyonun kontrolünün, en iyi biyoaktiviteyi elde etmek için çok önemli olabileceği sonuçlarına varılmıştır.

Dördüncü bölümde, defenolize fındık küspesi protein izolatlarından (dHPI) ve fındık zarı fenolik ekstraktlarından (HSE) protein-polifenol kompleksinin oluşumu ve hem fındık proteinlerinin hem de polifenollerin biyoerişilebilirliği üzerindeki etkisi incelenmiştir. dHPI±HSE komplekslerinin boyutları dikkate değer büyüklükte olduğu görülmüş ve agregasyonun meydana gelmesi nedeniyle HSE konsantrasyonuna bağlı olduğu rapor edilmiştir. Kateşin, HSE'nin ana bileşeni olmasına rağmen, partikül boyutunda hafif bir artış dışında agregasyona neden olmamıştır. Floresan söndürme sonuçlarına göre, fındık proteini-fenolik ekstrakt kompleksi, 0-0.5 mM konsantrasyonları arasında statik söndürmeyi ifade eden doğrusal bir Stern-Volmer grafiğine sahiptir, etkileşim, esas olarak hidrojen bağına ve van der Waals kuvvetlerine ($\Delta H < 0$ ve $\Delta S < 0$) bağlıdır ve reaksiyon kendiliğinden olmuştur ($\Delta G < 0$). FTIR sonuçlarına göre, yüksek fenolik ekstrakt konsantrasyonu fındık proteininde düzensiz yapılarda artışa neden olurken, en düşük fenolik konsantrasyon ve kateşin düzenli

yapıyı deęiřtirmiřtir. Fındık zarı ekstraktları, defenolize proteinlerin sindirilebilirlięini deęiřtirmemiřtir, ancak defenolizasyon, pankreatin hidrolizi derecesini azaltmıřtır. Protein-polifenol kompleksinin oluřumu, fındık zarı polifenollerinin biyolojik olarak eriřilebilirlięi gz nne alındıęında, aęırlıklı olarak gallokateřin gallat ve epigallokateřin galat gibi kateřinlerin gallatlanmıř formu zerinde yararlı bir etkiye sahip olduęu grlmřtir.

Son blm, nceki blmlerde elde edilen veriler dikkate alınarak, genel tartıřmalar ve sonuların yanı sıra fındık yan rnlerinin deęerlendirilmesine iliřkin gelecekteki arařtırmalar iin tavsiyeler sunmaktadır. Fındık yaęı endstrisinin bir yan rn olan fındık kspesti, potansiyel anti-obezite ve antioksidan zelliklerine vurgu yapılarak biyoaktif peptit kaynaęı olarak deęerlendirilmiřtir. İlk olarak, fındık kspesti protein izolatları, hidrolizasyon ve fonksiyonel zelliklerini iyileřtirmek iin mikro-akıřkanlařtırma iřlemine tabi tutulmuřtur. Daha sonra, protein hidrolizatlarını hazırlamak iin Ntraz ve Alkalaz ile kombine veya bireysel hidroliz gerekleřtirilmiřtir. Alkalaz ve Ntraz hidroliz kombinasyonu ile, en yksek hidroliz derecesine, pankreatik lipaz tarafından serbest yaę asidi salınımı nleme ve serbest radikal sprme kapasitesine ulařılmıřtır. Anti-obezite ve antioksidan zellikleri gz nne alındıęında, fındık protein hidrolizatları, fonksiyonel gıda bileřeni olma potansiyele sahiptir. Bu nedenle, amalanan uygulamaya baęlı olarak protein iřleme srecini (n iřlem, hidroliz derecesi, vb.) anlamak nemlidir. Protein-polifenol etkileřimleri, fındık kabuęu polifenollerinin, zellikle de gallokateřin gallat (GCG) ve epigallokateřin gallat (EGCG) gibi kateřinlerin gallatlı formlarının biyoeriřilebilirliklerini iyileřtirmiřtir. Son yıllarda arařtırmacılar, doęal kaynaklardan izole edilen polifenolik bileřikler ve bitki bazlı proteinler zerinde yoęunlařmıřlardır. Ancak, protein-fenolik etkileřimlerin polifenol biyoeriřilebilirlięini olumlu veya olumsuz etkileyip etkilemedięi konusunda fikir birlięi yoktur. Sonu olarak, bu konuda daha fazla arařtırma yapılması ve literatrde rapor edilmesi gerekmektedir.



1. INTRODUCTION

It is well-known that animals and humans have been consuming nuts since ancient times because of their high energy content. Nuts are generally considered to be a healthy source of plant protein (10%–25%), polyunsaturated (PUFA) and monounsaturated (MUFA) fatty acids, dietary fiber, vitamins (e.g., niacin, folate, E), minerals (e.g., magnesium, copper, selenium, potassium), and antioxidants. There has been an upward trend in the global consumption of nuts over the past few decades, which may be due to media reports linking consumption of nuts to health benefits based on favorable scientific findings (Wien, 2017).

One of the world's most popular tree nuts, the hazelnut, or *Corylus avellana* L., is also rich in nutrients, fat-soluble bioactives, and phenolics/phytochemicals (Pelvan et al., 2018). It is particularly rich in flavan-3-ols and proanthocyanidins. In comparison with other tree nuts, hazelnuts have the highest proanthocyanidin content as well as a high level of hydrolysable tannins (Lainas et al., 2016). The Food and Drug Administration (FDA) and the European Food Safety Authority (EFSA) both recommend the consumption of nuts, including hazelnuts, on a daily basis to reduce the risk of coronary heart disease (Pelvan et al., 2018).

Hazelnut production (with shell) exceeded one million metric tons worldwide in 2020 (1,072,308 MT). Turkey remains the top producer with 62% (865,500 MT), followed by Italy (33%), and the USA (6%). Fresh consumption accounts for around 10% of hazelnut intake, with the rest mainly processed industrially (approximately 90%), predominantly to produce hazelnut oil, leaving huge quantities of by-products. The in-shell hazelnuts are cracked before further processing or consumption, resulting in a considerable residual biomass. According to global production statistics, the shells (endocarps) account for approximately 50 to 55% of the weight of the mature nut (Fuso et al., 2021). The oil content in hazelnut is approximately 60 % (Król and Gantner, 2020), so the residual hazelnut meal obtained from cold press oil extraction represents

around 40% of the kernel mass. In terms of chemical composition, the meal should be similar to that of the whole nut but without the oils. Around 2.5% of the hazelnut kernel's weight is made up of brown skin (also known as testa, perisperm, or pericarp), which is discarded during roasting (Alasalvar et al., 2009) and found in the meal when the kernels are pressed raw.

Hazelnut meal is rich in proteins (38-54%) (Acan et al., 2021; Aydemir et al., 2014) and is thus an economical way to obtain protein. Furthermore, after being hydrolyzed by enzymes, hazelnut meal can be transformed into bioactive peptides used in various food formulations. There are many plant-based proteins that have compact quaternary and tertiary structures, making them more resistant to proteolysis (Hu et al., 2011). Food macromolecules are processed using microfluidization in a continuous, low-temperature process with reduced nutrient component loss and fast processing times (Zhang et al., 2021). Additionally, microfluidization as a pretreatment may enhance the functional properties of proteins and their enzymatic hydrolysis, by releasing the folded structure of proteins, exposing the core groups within them (Hu et al., 2011; Zhang et al., 2021; Chen et al., 2016; Liu et al., 2017b).

There are several noncommunicable chronic diseases associated with obesity and overweight. These include cardiovascular diseases, a leading cause of death worldwide; diabetes; musculoskeletal disorders; and even certain cancers, including liver, prostate, endometrial, breast, ovarian, gallbladder, colon, and kidney, among other diseases (WHO, 2021). World Health Organization statistics indicate that 1.9 billion adults are overweight and 650 million are obese worldwide (WHO World Health Statistics, 2021). The pancreatic lipase (PL) is the primary digestive enzyme that hydrolyzes dietary fats (50–70%). Thereby, it promotes the absorption of fats from the diet (Birari and Bhutani, 2007). Thus, inhibiting PL is an effective strategy for limiting intestinal absorption of lipids and thereby contributing to weight loss. Furthermore, plant-derived PL inhibitors provide a source of potential future drug candidates that can complement the limited number of currently available anti-obesity medications (Rajan et al., 2020; de la Garza et al., 2011). The peptides derived from edible plants have recently emerged as very promising and safe candidates as PL inhibitors, which may also be used in functional food formulations with anti-obesity

properties (Coronado-Cáceres et al., 2020; Wang et al., 2022; Fan et al., 2018; Esfandi et al., 2022).

The interaction between proteins and phenolic compounds occurs during food processing or following consumption of other foods containing phenolic compounds (Rohn, 2014). The type of interaction between proteins or phenolic compounds can be either covalent or non-covalent and is affected by several factors, such as temperature, pH, protein type, and concentration (Ozdal et al., 2013). Even though it has been widely investigated in recent years, few studies have been conducted on the interaction of plant-based proteins with phenolics. Studies on the interactions of proteins obtained from nuts have so far been limited to walnuts or peanuts to the best of our knowledge.

Fluorescence quenching occurs due to interactions between proteins and ligands that involve collisional effects, formation of ground-state complexes, non-radical energy transfer, etc., that decrease protein fluorescence intensity. In addition shifts in λ_{max} may indicate important molecular events (folding/unfolding and position of fluorophore) caused by the interactions between phenolics and proteins. Moreover, fluorescence spectroscopy technique may help to understand how many phenolics molecules can bind to the protein and the thermal stability of this binding and interaction. After all, using fluorescence spectroscopy technique to investigate the protein-phenolics interaction is very useful and novel approach in order to understand the many features of the interactions effectively in a sample-size and time friendly way. FTIR is one of the spectroscopic methods that provide information about the secondary structures of proteins. Moreover, dynamic light scattering (DLS) and ζ -potential are practical complementary techniques for determining the changes in proteins with the formation of the protein-phenolic complex by monitoring the alteration in hydrodynamic radius and charge distribution of the proteins, respectively.

It has been stated that protein-phenolic complexes formed as a result of interaction suppress the antioxidant effects of phenolic compounds during gastrointestinal digestion and form indigestible complexes (Ozdal et al., 2013; Rawel and Rohn, 2010). However, phenols interacting with proteins during gastrointestinal digestion are thought to be protected from oxidation (Jakobek, 2015). Therefore, as the gastric

chyme waits for a certain time, the appearance of phenolic compounds in the blood may be delayed as a result of protein-phenolic interaction during digestion, and phenolics can be separated from the complexes in the gastrointestinal tract without any change in the total amount of phenolic substances (Zhang et al., 2014).

In fact, there is no literature available to study the interaction between the protein isolate, prepared with hazelnut meal obtained from cold press oil extraction after removing its remaining oil (defatting), and phenolic compounds obtained from the hazelnut skin by using fluorescence spectroscopy technique. In this study, we have also showed how to combine the effects of the interaction ability of hazelnut protein and phenolics on their gastrointestinal digestibility for the first time

1.1 Purpose of Thesis

The objectives of this thesis;

1. To valorise hazelnut meal and explore the potential anti-obesity and antioxidant activities of its protein hydrolysates;
2. To investigate the effect of the hydrolysis strategy (single or sequential hydrolysis) using Alcalase and Neutralse, as well as the application of microfluidization pretreatment on these activities and the functional properties of the protein isolates and hydrolysates;
3. To examine the formation of the protein-polyphenol complex from dephenolised hazelnut meal protein isolates (dHPI) and hazelnut skin phenolic extracts (HSE);
4. To monitor the bioaccessibility of hazelnut proteins and polyphenols after protein-polyphenol complexation.

2. VALORISATION OF HAZELNUT BY-PRODUCTS: CURRENT APPLICATIONS AND FUTURE POTENTIAL

2.1 Introduction

Hazelnuts are very appreciated worldwide for their pleasant crispness and their unique and delicate flavour due to the presence of a variety of volatile compounds (Alasalvar et al., 2006). Hazelnuts and foods containing this nut have been labelled as functional foods because their consumption is associated with human health benefits owing to high amounts of nutrients and bioactive compounds such as monounsaturated and polyunsaturated fatty acids, vitamins, minerals, dietary fibres, phytosterols (β -sitosterol), squalene, and a variety of polyphenols (Alasalvar and Shahidi, 2008; Köksal et al., 2006). Regular consumption of hazelnut has been reported to improve cardiometabolic risk factors and thus prevent cardiovascular disease events by reducing LDL and total cholesterol levels in the blood (Brown et al., 2022; Perna et al., 2016). Hazelnut consists of several species and varieties (cultivars). *Corylus avellana* L. or the European hazel, are the most common commercially grown hazelnut shrubs and trees. This species was propagated from a selection of wild populations on the basis of its large nut size with thinner shells, and the superior quality of the kernels (Erdogan and Mehlenbacher, 2000). This may explain why most research has focused on this species. All the data presented in this review are from *Corylus avellana* L. studies.

In 2020, the annual production of hazelnut (with shell) exceeded one million metric tons worldwide (1,072,308 MT) with Turkey remaining the main producer with 62% of the total production (665,000 MT), followed by Italy (13%) and the USA (6%) (FAOSTAT, 2022b). Fresh consumption represents only a small part of the fate of hazelnuts (approx. 10%) while most is processed industrially (approx. 90%) (Baldi, 2010), mainly to produce hazelnut oil, leaving huge quantities of by-products (Figure 2.1). In-shell hazelnuts are cracked before further processing or consumption of the kernel (cotyledons/seed), which results in large residual biomass. Indeed, the

shells (endocarps) represent approximately 50 to 55% of the weight of the whole mature nut (Fuso et al., 2021) which represents a very large volume considering the global production. The oil content in hazelnut is approximately 60% (Król and Gantner, 2020), so the residual hazelnut meal obtained from cold press oil extraction represents around 40% of the kernel mass. The chemical composition of the meal should be similar to the whole nut minus the oils' components. Nevertheless, very less attention is given to this very valuable resource which could be a potential ingredient for functional food preparations due to its high content of bioactive molecules and nutrients, especially proteins (up to 54%) (Aydemir et al., 2014). The brown skin (also known as testa or perisperm) surrounding the hazelnut kernel represents around 2.5% of the total kernel weight, which is discarded as a by-product upon roasting (Alasalvar et al., 2009) and is also found in the meal as the kernels are pressed raw.

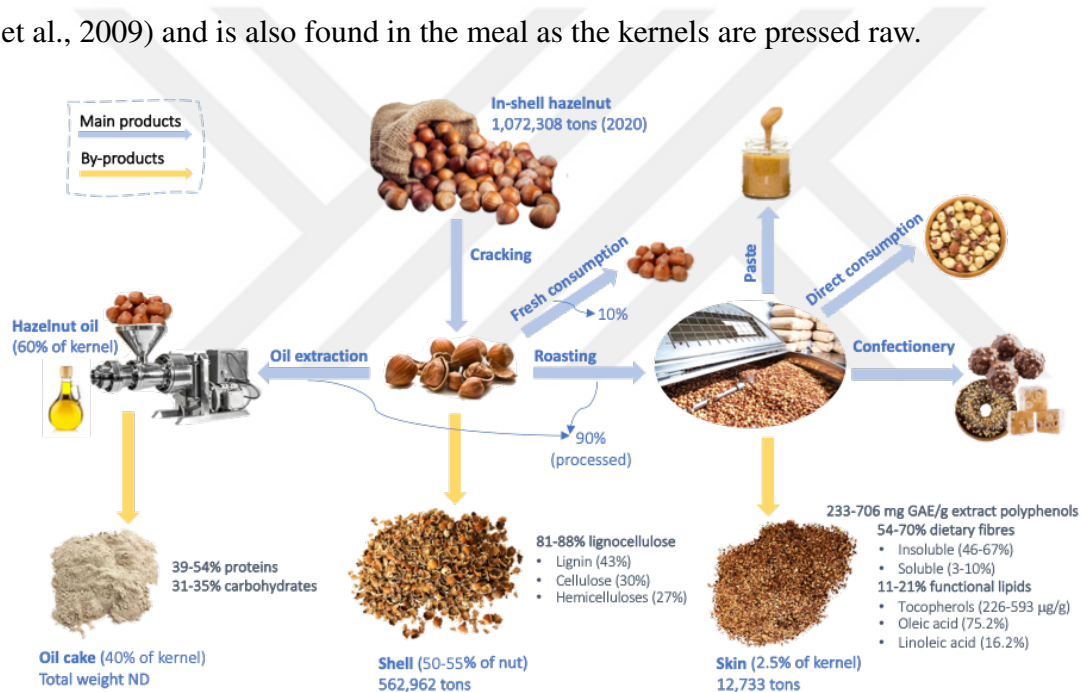


Figure 2.1 : Fates of in-shell hazelnut and its by-products obtained after industrial processing. The numbers are approximate (citations in sections 1 and 2), ND: not determined.

This article reviews the current scientific knowledge concerning the main and the most valuable hazelnut by-products, i.e., the meal, skin, and shell, and their actual utilisation, with a highlight on their chemical composition to inspire new applications of these valuable resources and exploit their full potential.

2.2 Chemical Composition of Hazelnut By-products

2.2.1 Proximate composition and nutritional value

2.2.1.1 Proximate composition of the shell

Fibres are the predominant components in hazelnut shells, ranging from 80.9 to 88.2% wet basis (wt%) (Xu et al., 2012; Yuan et al., 2018) (Table 2.1). Hazelnut shells contain between 2.1 and 6.7 wt% proteins; 0.2-1.55 wt% fat and 0.8-2.0 wt% ash, of which 27.7% is potassium and 16.9% calcium (Gozyaydin and Yuksel, 2017; Lopes et al., 2012; Xu et al., 2012; Yuan et al., 2018). The moisture content of hazelnut shells is estimated between 7.24 and 8.93% (Gozyaydin and Yuksel, 2017; Yuan et al., 2018).

The fibres in the hazelnut's shell constitute the structural non-extractive woody material (lignocellulosic biomass) and are composed of three main polymers: 43% lignin, 30% cellulose, and 27% hemicelluloses (Demirbaş, 2005). The presence of smaller amounts of galactan (1.6% db. of shell) and arabinan (0.3%) in hazelnut shells has been reported as well (Surek and Buyukkileci, 2017).

Unlike cellulose, which is a linear polymer of glucose units with α -1,4-linkages, hemicellulose is a heteropolysaccharide composed of different hexoses, pentoses, and glucuronic acid, with more frequent branches. Lignin is not a carbohydrate; its structure is more complex than hemicellulose. It is a highly irregular polymer consisting of non-repeating phenylpropanoid subunits (i.e., p-hydroxyphenyl, guaiacyl, and syringyl units). Cellulose, hemicellulose, and lignin are linked together by a variety of covalent and non-covalent linkages, making the hydrolysis of lignocellulose even more difficult (Malherbe and Cloete, 2002). Hazelnut hemicellulose is mainly composed of heteroxylyan, which is made up of a backbone of xylose units, substituted with arabinose, acetyl groups, uronic acid, and possibly some phenolic compounds (Fuso et al., 2021; Pérez-Armada et al., 2019). Xylooligosaccharides (XOS) and arabino-xylooligosaccharides (AXOS), a valuable source of prebiotics, are two abundant oligosaccharides that can be obtained from the hydrolysis of the hemicellulosic fraction of hazelnut shell (Fuso et al., 2021; Surek et al., 2021).

Increasing attention has been given to the recovery of mono/oligosaccharides and bioactive compounds from hazelnut shells for utilisation in different products (Hoşgün and Bozan, 2020; Pérez-Armada et al., 2019). Thermochemical pre-treatment and enzymatic hydrolysis are required to obtain these products and thus add energy and material costs that should be considered to determine the feasibility of a given application (Hoşgün and Bozan, 2020). The complex structure of lignocellulose and its recalcitrance to physical, chemical, or biological degradation has been the main challenging aspect impeding its full valorisation from hazelnut shells. Even though, progress is being made in the recovery of energy-rich molecules and bioactive molecules from this biomass with new methods and applications (Beisl et al., 2017; Bjelić et al., 2022; Gu et al., 2021; Shen and Sun, 2021). For example, lignin has been used as nano and micro encapsulating material for diverse drugs or for the improvement of mechanical properties of other polymer nanocomposites, as a UV blocker, a source of bioactive compounds (antimicrobial and antioxidant), surfactant in Pickering emulsions, and as carbonized nanostructures for energy storage (supercapacitors) (Beisl et al., 2017).

Table 2.1 : Proximate composition of hazelnut (*Corylus avellana* L.) by-products (wt%, db).

	Moisture	Ash	Proteins	Lipids	Total fibres	References
Shell	7.24-8.93	0.8-2.0	2.1-6.7	0.2-1.55*	80.9-88.2	(Gozaydin and Yuksel, 2017; Lopes et al., 2012; Xu et al., 2012; Yuan et al., 2018)
Skin	4.31-8.56	1.7-4.5	7.5-9.39	10.98-21.2	54.28-69.78 (insoluble: 46.45-67.1% ; soluble: 2.68-10.0)	(Bertolino et al., 2015; Ivanović et al., 2020; Montella et al., 2013a; Ozdemir et al., 2014; Tunçil, 2020)
Meal	4.13-7.77	5.01-7.41	38.68-54.43	1.1-15.93	30.67-35.5 (carbo- hydrates)	(Acan et al., 2021; Atalar, 2019; Aydemir et al., 2014)

*1.55% was calculated from wet basis value (1.44%) by considering moisture content (7.24%) of the same reference (Yuan et al., 2018).

2.2.1.2 Proximate composition of the skin

The dried hazelnut skin is a very rich source of dietary fibres. They contain 54.28 to 69.78 wt% of dietary fibres, of which 46.45-67.1% are insoluble and 2.68-10.0% are soluble (Bertolino et al., 2015; Montella et al., 2013a; Ozdemir et al., 2014; Tunçil, 2020). Dietary fibres are defined as “the edible parts of plants or analogous carbohydrates that are resistant to digestion and absorption in the human small intestine with complete or partial fermentation in the large intestine” (AACCI Report, 2001). Insoluble fibres act to speed up the transit of food materials through the small intestine while soluble fibres may reduce transit rates and delay gastric emptying (Cummings, 2001). Generous dietary fibre consumption has been linked to improved immune function and lower risks of developing several diseases, i.e., cardiovascular diseases, diabetes, obesity, hypertension, cancer, and certain gastrointestinal disorders (Anderson et al., 2009). Lipids are also abundant in hazelnut skin, constituting 10.98 to 21.2 wt% (db), but may be from oil absorption from the kernel during the roasting process (Bertolino et al., 2015; Ivanović et al., 2020; Montella et al., 2013a; Ozdemir et al., 2014; Tunçil, 2020). Hazelnut skin contains between 7.5 and 9.39 wt% proteins, 17.45 and 19.09 wt% net carbohydrates, 1.7 and 4.5 wt% ash, and between 4.31 and 8.56 wt% moisture (Bertolino et al., 2015; Ivanović et al., 2020; Montella et al., 2013a; Ozdemir et al., 2014; Tunçil, 2020). Hazelnut skin is a rich source of essential minerals, i.e., magnesium (114 mg/100g), calcium (85.8 mg/100g), sodium (60.5 mg/100g); phosphorous (52.6 mg/100g), potassium (15.9 mg/100g), iron (4.19 mg/100g), manganese (1.45 mg/100g), zinc (1.1 mg/100g), copper (0.44 mg/100g), and selenium (23.9 μ g/100g), while toxic metals like lead, arsenic and mercury were not detected in this by-product (Ivanović et al., 2020).

2.2.1.3 Hazelnut skin is a rich source of vitamin E, Oleic, and Linoleic Acids

α -Tocopherol is a potent fat-soluble antioxidant that protects unsaturated fatty acids in cell membranes and lipoproteins by preventing lipid peroxidation and scavenging free radicals (Niki and Traber, 2012; Schneider, 2005). Hazelnut skin contains twice the total tocopherols ($\alpha + \beta + \gamma$) as the kernel without skin (226 to 593 vs 130 to 281 μ g/g

of skin, according to variety) with a predominance of α -tocopherol (168.2 to 443.8 $\mu\text{g/g}$) (Taş and Gökmen, 2015). Although the biological activity of tocopherols may have similarities in-vitro, α -tocopherol is the only one retained at high levels in plasma and tissues due to the selectivity of the hepatic α -tocopherol transfer protein (α -TTP), while the other isomers are metabolised and excreted at higher rates (Szewczyk et al., 2021). It is also the only isomer that is recognised to meet human requirements for vitamin E (Monsen, 2000) Hazelnut skin content in tocopherols reported by others (Taş and Gökmen, 2015) is comparable to levels in sunflower oil (585 $\mu\text{g/g}$ oil) and is higher than both refined and extra virgin olive oils (67 and 211 $\mu\text{g/g}$ oil) (Aksoz et al., 2020).

The oil fraction of hazelnut skin (10.98-21.2 wt% db.) is very rich in monounsaturated fatty acid (MUFA) oleic acid (C18:1n-9) (75.2%) and the essential ω 6 polyunsaturated fatty acid (PUFA) linoleic acid (C18:2n-6) (16.2%) (Ozdemir et al., 2014). Ivanović et al. (2020) have reported similar results with up to 74.81% oleic acid and 16.33% linoleic acid of total fatty acids of hazelnut skin. The authors have also reported the presence of traces of linolenic acid (C18:3n-3), essential ω 3 fatty acid, and eicosenoic acid (C20:1n-9) (<0.2%). Besides being the most energy-dense of all macronutrients (9 calories per gram, also true for saturated fatty acids), unsaturated fatty acids are known to be beneficial for health as they are associated with reduced risks of cardiovascular disease and certain cancers (i.e., colon, breast, and prostate) as well as the promotion of neuronal development and cognitive function (Lunn and Theobald, 2006).

2.2.1.4 Proximate composition of the meal

Few studies have assessed the composition of hazelnut meal. This component is a very rich source of proteins, containing between 38.7 and 54.4% protein (Acan et al., 2021; Atalar, 2019; Aydemir et al., 2014). These levels are similar to the protein content of soybean meal (45.0-48.8%, 12% moisture weight basis) (Thakur and Hurburgh, 2007). This could explain the recent interest in finding uses for this by-product, focusing on using hazelnut meal for generating bioactive peptides via hydrolysis methods (Cağlar et al., 2021b,a; Göksu et al., 2022b; Li et al., 2021; Wang et al., 2020). Furthermore, hazelnut proteins have been reported to be of high quality because of their amino acid

profile. Indeed, all essential amino acids, including branched-chain and limiting amino acids, are present in hazelnut proteins in appreciable amounts (Table 2.2) (Shahidi and Miraliakbari, 2006).

Table 2.2 : Amino acid profile of hazelnut proteins (Shahidi and Miraliakbari, 2006).

Amino acid	Content (%)
Isoleucine ^{a,b}	3.75
Valine ^{a,b}	4.37
Phenylalanine ^b	4.53
Lysine ^{b,c}	2.63
Methionine ^{b,c}	1.07
Threonine ^{b,c}	2.95
Tryptophan ^b	1.42
Histidine ^b	2.16
Cystine ^d	1.51
Arginine ^d	14.2
Tyrosine ^d	2.99
Alanine ^d	4.67
Aspartic acid ^d	10.5
Glutamic acid ^d	23.3
Glycine ^d	4.65
Proline ^d	3.36
Serine ^d	4.41

a Branched-chain amino acids,

b Essential amino acids,

c Limiting amino acids,

d Non-essential amino acids

To our best knowledge, there is no data on the dietary fibre content of hazelnut meal, but it should contain at least the fibres of the skin as hazelnuts are mostly pressed with their skin. Carbohydrates are the second most abundant nutrient in hazelnut meal, representing between 30.67 and 35.5% of mass (Atalar, 2019; Aydemir et al., 2014). The main simple sugars found in the meal are saccharose (3.97%); glucose (0.8%); fructose (0.57%) and xylose (0.34%) (Acan et al., 2021). Hazelnut meal contains also appreciable amounts of lipids (3.1-15.93%) and ash (5.01-7.4%), while moisture content is estimated between 4.13 and 7.77% (Acan et al., 2021; Atalar, 2019; Aydemir et al., 2014). The fat contained in hazelnut meal remains from oil extraction, thus and due to lack of data, the qualitative fat profile in hazelnut meal is assumed to be the same as described in the literature for hazelnut kernels: oleic acid (C18:1 ω 9) \approx 80%;

linoleic acid (C18:2 ω 6) \approx 9%; palmitic (C16:0) \approx 5%; stearic (C18:0) \approx 3%; vaccenic (C18:1 ω 7) acid \approx 1%; others < 1% (Amaral et al., 2006).

2.2.2 Polyphenols and other bioactive components in hazelnuts by-products

A study that exploited the Phenol-Explorer database (www.phenol-explorer.eu) has ranked hazelnut as the 21st richest food in polyphenols among 452 common foods (including fruits, vegetables, seeds, nuts, cereals, oils, and beverages) with an estimated polyphenol content of 495 mg/100 g (as the sum of the content of individual polyphenols as determined by chromatography) (Pérez-Jiménez et al., 2010). Chestnut was the only nut ranked higher than hazelnut (11th, 1215 mg/100 g). The actual chemical composition of hazelnut by-products may vary quantitatively and qualitatively due to many factors including the nut variety, origin and climate, the extraction techniques and conditions, the type of solvents used, and the analytical method employed to identify and quantify the different compounds (Herrera et al., 2020; Król et al., 2020; Nazzaro et al., 2012; Slatnar et al., 2014). Maceration before extraction was reported to have a positive effect on the extraction of phenolic compounds from hazelnut shells regardless of the method performed (Michele et al., 2021).

2.2.2.1 Bioactive compounds of hazelnut skin

Hazelnut skin is the richest source of phenolic compounds among hazelnut by-products, having 233 to 706 mg GAE/g extract (Ivanović et al., 2020; Ozdemir et al., 2014; Taş and Gökmen, 2015). Furthermore, hazelnut skin had a high flavonoid content, containing up to 664 mg catechin equivalent/g extract (Montella et al., 2013b). The predominant phenolics present in hazelnut skin are (+)-catechin, gallic acid, quercetin, kaempferol, (-)-epicatechin, p-hydroxybenzoic acid, procyanidin B2, and procatechuic acid (Ivanović et al., 2020; Król et al., 2020; Montella et al., 2013b) (Figure 2.2). Other identified phenolics in hazelnut skin include ferulic acid, caffeic acid, p-coumaric acid, rutin (quercetin-3-O-rutinoside), resveratrol, naringenin, procyanidin B1, procyanidin C2 trimer, prodelphinidin beta-type dimers, procyanidin beta 1 dimer, Procyanidin beta-type trimers, procyanidin beta-type

gallate, myricetin-rhamnoside, quercetin-3-O-rhamnoside, phloretin-2-O-Glucoside, kaempferol-rhamnoside, epigallocatechin, kaempferol-3-O-glucoside, apigenin, galocatechin gallate, 3-coumaric acid (Bertolino et al., 2015; Ivanović et al., 2020; Król et al., 2020; Spagnuolo et al., 2021). Proanthocyanidins also constitute a considerable part of hazelnut skin polyphenols (29.0 mg CE/g extractable + 7.7 mg CE/g bound) (Lainas et al., 2016). Proanthocyanidins are condensed tannins consisting of oligo- or polymers of flavan-3-ols produced at the end of flavonoid biosynthetic pathway, which are shown to possess important biological activities, i.e., antioxidant, antimicrobial, antidiabetic, neuroprotective, and anticancer activities (Rauf et al., 2019). Nevertheless, their known astringency may dictate the way hazelnut skin can be used and the amount which can be introduced into a functional food formulation. Hazelnut skin also contains an appreciable amount of serotonin (up to 4.1 $\mu\text{g/g}$ in some varieties), a neurotransmitter acting on both the central and peripheral nervous system which is implicated in the regulation of mood, sleep, anxiety, appetite, and blood pressure (Taş et al., 2019).

2.2.2.2 Bioactive compounds of hazelnut shell

Even though hazelnut shells have lower total phenolic content than the skin, their presence in this by-product is still considerable (4.5 to 159.70 mg GAE/g extract; flavonoid content up to 64.83 mg rutin equivalent/g extract) and are certainly more diverse (Herrera et al., 2020; Salem et al., 2022; Xu et al., 2012). The polyphenols present in hazelnut shells include the phenolic acids (gallic acid, 4-hydroxybenzoic acid, vanillic acid, syringic acid, p-coumaric acid, guaiacol, ellagic acid, coumaroylquinic acid, protocatechuic acid, caffeic acid, ferulic acid, 3-hydroxybenzoic acid, sinapic acid, vanillic acid), esters of phenolic acids (galloylquinic acid, coumaroylquinic acid, pentose esters of coumaric acid, hexose ester of syringic acid, chlorogenic acid (3-O-caffeoylquinic acid)), phenolic aldehydes (3,4-dihydroxybenzaldehyde (protocatechuic aldehyde), vanillin, 3-methoxy-4-hydroxy-cinnamaldehyde), flavonoids ((+)-catechin, (-)-epicatechin, myricetin, epicatechin gallate, naringenin, taxifolin, quercetin, prodelphinidin dimer, procyanidin dimers, procyanidin trimer, kaempferol,

diosmetin, apigenin, luteolin, pinobanksin, galocatechin), flavonoid glycosides (Kaempferol rhamnoside, Myricitrin, Phlorizin, Rutin, Isoquercitin), stilbenes (Pinosylvin); lignans (Todolactol), and other phenols (Dihydroconiferyl alcohol, 1-guaiacyl-3-OH-1-propanone, 1-guaiacyl -2,3-diOH-1-propanone, 1,3-(bis-guaiacyl)-1,2-propandiol, Coniferyl alcohol, Monomethyl pinosylvin, 4,4'-diOH-3,3'-dimethoxystilbene, glucopyranoside2[-4(OH)phe]) (Michele et al., 2021; Herrera et al., 2020; Pérez-Armada et al., 2019; Shahidi et al., 2007; Yuan et al., 2018).

Gallic acid is the most abundant phenolic compound in hazelnut shells (Ciemniewska-Żytikiewicz et al., 2015; Michele et al., 2021; Shahidi et al., 2007), while (+)-catechin was reported as the most abundant by others (Yuan et al., 2018). Epicatechin gallate, chlorogenic acid, rutin, protocatechuic acid, vanillin and todolactol are the other major phenolics found in hazelnut shells (Michele et al., 2021; Yuan et al., 2018) (Figure 2.2).

2.2.2.3 Bioactive compounds of hazelnut meal

The presence of polyphenols in hazelnut meal is between 0.53 and 15.96 mg GAE/g extract, which is appreciable, but considerably less than the skin and shell (Acan et al., 2021; Simsek et al., 2017; Slatnar et al., 2014). This may explain why the studies on polyphenols in this by-product are very limited and rather, much focus has been given to its protein content. Interestingly, it was found that the phenolic contents in hazelnut meal extracts are considerably higher than those of the unprocessed flours of the kernels (Bener et al., 2022; Slatnar et al., 2014), including individual phenolics from the flavan-3-ol group and hydrolysable tannins (Slatnar et al., 2014). The major phenolics in hazelnut meal are quinic acid, quercetin-3-O-rhamnoside, (+)-catechin, catechol, glansreginin A, glansreginin B; hexose ester of syringic acid and procyanidin dimers, trimers, and tetramers. The following phenolics were also identified at different levels: protocatechuic acid, quercetin-3-O-glucoside, myricetin-3-O-rhamnoside, 4-hydroxybenzoic acid, B-type dimer gallate, caffeic acid, (-)-epicatechin, (-)-epicatechin gallate, ferulic acid, gallic acid, p-coumaric acid hexoside, quercetin, rutin, salicylic acid, sinapic acid, p-coumaric acid, vanillin,

vanillic acid, and chlorogenic acid (Bener et al., 2022; Simsek et al., 2017; Slatnar et al., 2014).

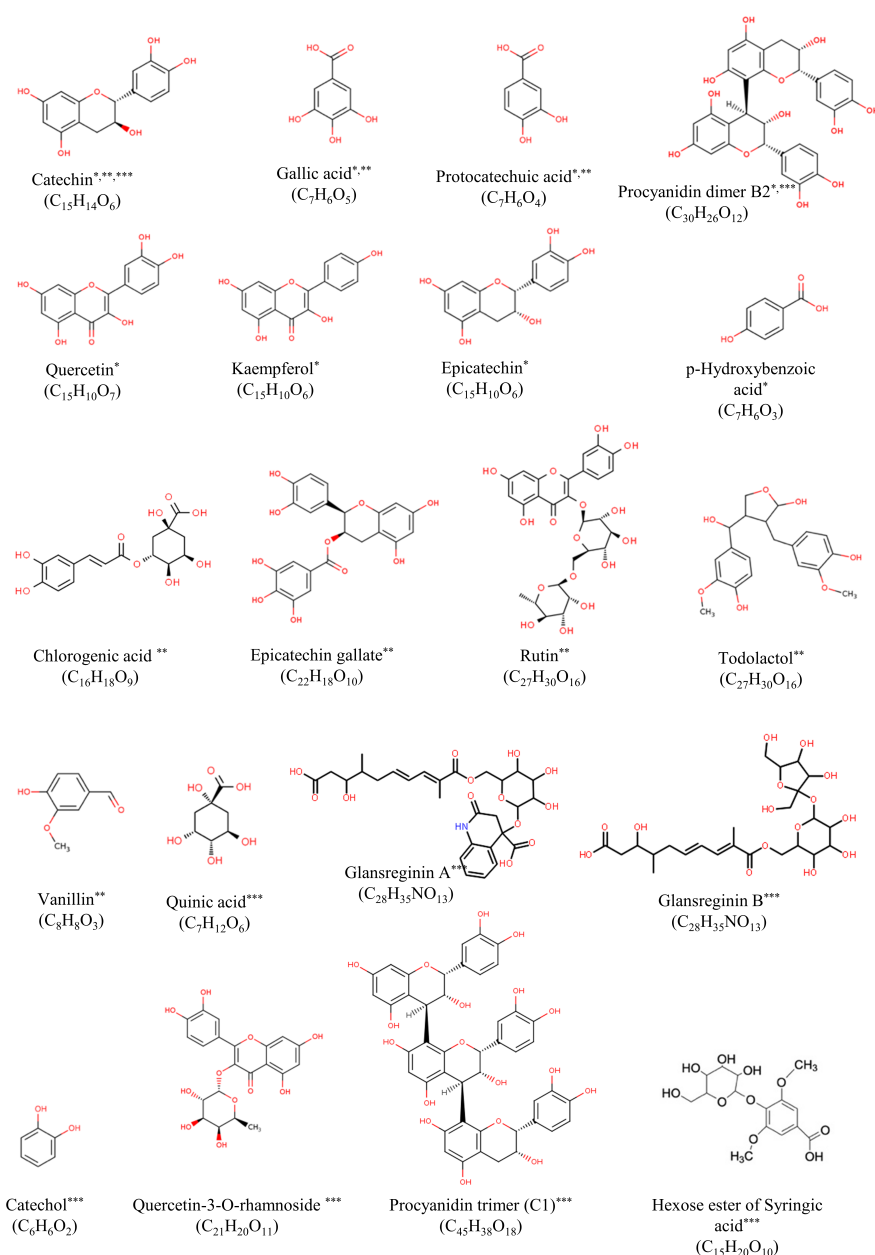


Figure 2.2 : Chemical structures of major phenolic compounds found in hazelnut by-products. The asterisks: *,**,*** refer respectively to major phenolic compounds of the skin, the shell, and the meal. Data were collected from the Phenol-Explorer database (<http://phenol-explorer.eu/>) except for quinic acid, chlorogenic acid, and rutin, which were from Chemspider (<https://www.chemspider.com/>), and glansreginin A and B which were from Greenmolbd (<https://www.greenmolbd.gov.bd/>). Esterification of syringic acid with a random hexose was made using Chemdraw online program (<https://chemdrawdirect.perkinelmer.cloud/js/sample/index.html>). All data was openly accessed on 10.05.2022.

2.3 Insights Into Current and Valorisation of Hazelnut By-products

The shell, skin and meal are the main valuable by-products of the hazelnut industry. These by-products are rich sources of diverse bioactive compounds, protein and dietary fibre with great potential to become a valuable source of functional food and ingredients. Therefore, studies investigating the valorisation of hazelnut by-products have increased in recent years (Acan et al., 2021; Anil, 2007; Montella et al., 2013b; Puliga et al., 2022; Saricaoglu et al., 2018; Uzuner and Cekmecelioglu, 2014). The majority of the studies on shells are principally focused on recovery of phenolic compound (Esposito et al., 2017; Masullo et al., 2017; Pérez-Armada et al., 2019; Yuan et al., 2018), cellulosic compounds (Arslan et al., 2012; Hoşgün et al., 2017; Hoşgün and Bozan, 2020; López et al., 2020; Puliga et al., 2022; Rivas et al., 2020; Uzuner et al., 2017, 2018; Uzuner and Cekmecelioglu, 2014) and activated carbon (Balci et al., 1994; Cimino, 2000; Demirbas, 2002; Demirbas et al., 2009; Demirbaş et al., 2008; Kobya, 2004; Sencan et al., 2015). Similarly, studies on the application of hazelnut skin have focused on isolation of phenolic compounds (Bertolino et al., 2015; Contini et al., 2012; Ivanović et al., 2020; Mocchiari et al., 2019; Papirio, 2020; Zeppa et al., 2015), dietary fibre (Bertolino et al., 2015; Papirio, 2020; Renna et al., 2020; Yılmaz and Şebnem Tavman, 2016) and the pigment (Ozdemir et al., 2014). For hazelnut meal, research has predominantly concentrated on protein hydrolysates (Moure et al., 2002; Sen and Kahveci, 2020; Simsek, 2021; Tatar et al., 2015) and bioactive peptides (Cağlar et al., 2021b,a; Göksu et al., 2022b,a; Gülseren and Çakır, 2019).

2.3.1 Valorisation of hazelnut shell

The main by-product of hazelnut production is hazelnut shells. However, disposing of the shells or using them as a low-value heat source results in a significant waste of a natural resource rich in phenolic and cellulosic compounds and lignin. Consequently, utilising hazelnut shells as alternative source of bioactive ingredients in diverse fields such as food, pharmaceuticals and cosmetics has stimulated interest among scientists, producers, and consumers (Yuan et al., 2018).

Studies in the literature on the valorisation of hazelnut shells into ingredients which contains natural polyphenols frequently centre upon the extraction procedure, characterisation and identification of the phenolic composition (Michele et al., 2021; Masullo et al., 2017; Pérez-Armada et al., 2019; Yuan et al., 2018). The optimal method for obtaining phenolics from hazelnut shell by conventional extraction in methanol or ethanol was 55.7% aqueous ethanol and 108.7 min at 20°C (Stévigny et al., 2007). Yuan et al. (2018) optimised the ultrasound-assisted extraction process parameters of phenolic compounds from hazelnut shells using response surface methodology. The factors of the study were solvent type (methanol, ethanol and acetone), concentration of solvents (20, 35, 50, 65 and 80%) temperature (30, 40, 50 °C), solid to liquid ratio (10, 20, 30, 40, 50 g/L), and extraction time (10 min, 20 min, 30 min, 1h, 2h, 3h, 4h). The optimal conditions were reported as 61% acetone and 4 hours of extraction time and 10 g/L ratio for the maximum recovery of phenolics. Regarding extraction speed, ultrasound-assisted extraction is an effective alternative to conventional extraction techniques for phenolic recovery from hazelnut shells. Since acetone and methanol, two of the most efficient extraction solvents, are very toxic, they may not be the most suitable solvent for extraction in the food industry. Thus, more environmentally friendly solvents should be specified to extract phenolic compounds from hazelnut shells using ultrasound assistance. Furthermore, several novel extraction techniques have been developed using less toxic solvents, such as ethanol, water, and resin. Three methods were used to obtain phenolic extracts from hazelnut shells: ultrasonic bath, maceration and high-power ultrasonic using ethanol as a solvent. Study results revealed that maceration positively impacts the extraction of different phenolic compounds regardless of the method employed (Michele et al., 2021). Pérez-Armada et al. (2019) also extracted the phenolic compounds from hazelnut shells by using green processes. Hydrothermal autohydrolysis and polymeric resins were applied to release and recover the polyphenols respectively. The combination of autohydrolysis and resin adsorption resulted in a practical approach for recovering polyphenols with antioxidant activity from hazelnut shells. In other respects, biological activities of hazelnut shell extract were investigated by Esposito et al. (2017). The 3-(4,5-dimethylthiazol-2-yl)-2,5-diphenyltetrazolium bromide (MTT) bioassay was

used to assess the antiproliferative activity of hazelnut shell extract and its key components against human melanoma (primary and metastatic, A375 and SK-Mel 28, respectively) and cervical cancer (HeLa) cell lines. As a result of these studies, hazelnut shell extracts may be useful as potentially expandable health-promoting agents in functional foods, nutraceuticals, or dietary supplements. However, more information is needed about the dose response and biological effects in vivo, considering hazelnut polyphenols are extensively metabolised after oral consumption.

As described above, the main constituent of hazelnut shell is lignin. Because of the polymeric structure of their components, hazelnut shells are so complex that fractionation is necessary to yield valuable products, like all lignocellulosic biomass wastes. In this regard, the hazelnut shell is an excellent candidate for a biorefinery, which relies on the selective separation of the main components of the raw materials and their conversion into new materials, chemicals and energy (Fuso et al., 2021). Activated carbon has been utilised for many decades for gas purification, gas mixture separation, exhaust air purification, solvent recovery, heavy metal removal, solution decolorisation, and water purification (Cuhadar, 2005). Several applications have been conducted on obtaining activated carbon from hazelnut shell by utilising its high lignin content and using this activated carbon to absorb heavy metals such as lead (Ahmed et al., 2019b; Pehlivan et al., 2009; Sencan et al., 2015), chromium (Bayrak et al., 2006; Cimino, 2000; Kobya, 2004), cadmium (Jamali et al., 2009), zinc (Kazemipour et al., 2008), nickel (Demirbas, 2002), copper (Demirbaş et al., 2008; Milenković et al., 2009) and arsenic (Sert et al., 2017) from the environment (especially from aqueous solutions) but also dyes (Ferrero, 2007) and CO₂ (Lewicka, 2017).

Other potential valorisation applications have investigated the possible use of hazelnut shell to produce fermentable sugar, ethanol or hydrogen. The transformation of lignocellulosic biomass to ethanol occurs in two stages: the hydrolysis of cellulose into sugars, followed by fermentation by yeasts or bacteria to transform fermentable sugars into ethanol. The hydrolysis process utilises either acid or enzymatic hydrolysis techniques. The high lignin content makes shells extremely resistant to decomposition. When lignin and hemicellulose co-exist, cellulolytic enzymes cannot access the cellulose for fermentation of sugar, so hydrolysis efficiency is reduced. There are

several ways to change the macromolecular structure and increase the surface area and pore size of lignocellulosic biomass before pre-treatment, which allows enzymes to attach to the carbohydrate matrix and produce sugars, which can then be fermented by bacteria or yeast. Physical, chemical, and biological processes are applied as pre-treatment. While biological pre-treatment procedures can be time consuming, physical pre-treatment methods have been shown to be energy inefficient. Chemical pre-treatments, on the other hand, attracted great attention (Chen et al., 2007; Xu et al., 2010). Although various chemical pre-treatment methods have been identified for lignocellulosic materials, their effectiveness varies depending on the raw material. As a result, an optimum pre-treatment must be developed for each raw material (Uzuner et al., 2017).

According to Arslan et al. (2012), sulfuric acid was used to hydrolyze hazelnut shell hemicellulose at various temperatures and acid concentrations. A kinetic model was developed as a function of process variables to predict the concentration of reducing sugar produced by hydrolysis and 0.4M sulfuric acid concentration was found to be most suitable according to proposed model. In a previous study of same group, lignin was removed using alkali pre-treatment (1–3% NaOH) and afterwards hydrolysed using 0.7 M sulfuric acid at constant conditions of 90°C, 220 min and a solid/liquid ratio of 1/5 (w/v). The hydrolysate was fermented by *Pichia Stipitis* to obtain ethanol (Arslan and Eken-Saraçoğlu, 2010). In their studies, enzymatic hydrolysis was not performed, and to our knowledge, no other study was recorded on the hydrolysis of hazelnut shells. Only the hemicellulosic fraction may be effectively dissolved by dilute acid, whereas alkali pre-treatment dissolves lignin and hemicellulosic sugars. As a result, a significant amount of residual cellulose remains unutilised, thus enzymatic hydrolysis becomes crucial. Accordingly, Uzuner and Cekmecelioglu (2014), designed a study to observe the effect of single and combined enzymatic and chemical hydrolysis on the formation of fermentable sugars from hazelnut shells. The optimised conditions were a temperature of 130°C, an acid concentration of 3.42 percent (w/w) and an optimum reducing sugar content of 16.65 g/L were achieved over a period of 31.7 min, resulting in a saccharification yield of 62.8% and low acetic acid levels. The total sugar yield of the combined acid and enzymatic hydrolysis was 72.4% of the

theoretical value. Combining dilute acid with enzymatic hydrolysis has also been shown to be more effective than acid hydrolysis alone. Uzuner et al. (2017) also investigated the influence of alkali pre-treatment and enzymatic hydrolysis on the production of fermentable sugars from hazelnut shells. Different sodium hydroxide (NaOH) concentrations, solid-liquid ratios, and pre-treatment times were used, and optimal solid recovery, lignin removal, and reducing sugar production conditions were predicted using response surface methodology. A response surface model was developed to predict the optimal reducing sugar production using 3% NaOH, a solid-to-liquid ratio of 1:13 and a pre-treatment period of 63 minutes at 121°C. Uyan et al. (2020), on the other hand, used separated hydrolysis and fermentation method and selected a near-critical water pre-treatment method (liquid hot water) due to its unique economic and environmental properties to produce bioethanol using *Saccharomyces cerevisia*. The maximum ethanol yield was 44.9% at 72 h with 0.5 g solid loading. Another research group investigated the effect of different pre-treatment methods on the enzymatic hydrolysis of hazelnut shells. First, they investigated the effect of saturated steam pre-treatment parameters (from 160 to 200 °C and 0-30 min) on the hemicellulose removal and enzymatic hydrolysis of hazelnut shells. These conditions gave the maximum 83% removal of hemicellulose at 200°C for 30 min, maximum 46% cellulose digestibility at 180°C for 30 min and produced 177 mg/g substrate of fermentable sugar (Hosgun and Bozan, 2014). Afterward, for the conversion of hazelnut shell cellulose to fermentable sugars and ethanol, low-temperature alkali (NaOH) pre-treatment, enzymatic saccharification, and ethanol fermentation were investigated by same group (Hoşgün et al., 2017). A 6% NaOH pre-treatment for 72 h and 1/10 solid/liquid ratio led to the maximum glucose recovery of 48.3 g/100 g cellulose. The removal of lignin and hemicellulose was 41.2 and 37.79%, respectively, for these conditions, and 3.77 g of ethanol was produced from 100 g of untreated hazelnut shells. Next, they compared the effect of three different thermochemical pre-treatment methods (steam, dilute H₂SO₄, and dilute NaOH) on the glucose recovery from hazelnut shells while assessing the energy consumption and energy efficiency of the process (e.g. the amount of glucose generated per MJ of energy consumed) for each treatment (Hoşgün and Bozan, 2020). For this study,

pre-treatments were applied as 1% H₂SO₄, 2.25% NaOH and steam at different temperatures (120, 150 and 200 °C) and different pre-treatment times (15, 30, 60 min) following enzymatic hydrolysis with a mixture of cellulase and β -glucosidase. The highest lignin removal (73.28%) was obtained with 2.25% NaOH pre-treatment at 200 °C for 60 min compared to acid and steam pre-treatment. After pre-treatment of hazelnut shells with 1% H₂SO₄ at 200 °C, over 60% cellulose and 100% hemicellulose were solubilised. The highest cellulose recovery (76.3%) was achieved with steam pre-treatment at 200°C for 60 min. Glucose recovery was highest (58.7%) in the biomass pre-treated with 2.25% NaOH at 150 °C for 60 min. The energy efficiencies of pre-treatments were 1.53, 4.75, and 4.98 g glucose/ MJ for steam, acid and alkali pre-treatments, respectively. They concluded that alkaline pre-treatment of hazelnut shells is superior to other methods (acid and steam) in terms of glucose recovery and energy efficiency.

Most recently, it was investigated the effect of different individual pre-treatment methods (dilute acid, alkaline and liquid hot water) and the combination of these methods on the chemical compositions and enzymatic hydrolysis yield (Hoşgün et al., 2021). Overall, the use of a two-step pre-treatment on hazelnut shells revealed the improved effect of the second pre-treatment; therefore, the sequence of pre-treatment methods had a significant effect on both substrate properties and enzymatic hydrolysis efficiency of biomass. Combination of alkali-liquid hot water pre-treatments removed 60.7% of lignin, while a liquid hot water-dilute acid pre-treatment combination removed the most hemicellulose (93.8%), and a combination of dilute acid-liquid hot water pre-treatment gave the highest cellulose recovery (94.0%) and the maximum glucose recovery (54.9%). The total energy requirement of this combination was approximately 1.8 MJ to recover 10.2 g glucose. According to these findings, the authors concluded that the complete removal of the physical barrier of lignin and hemicellulose may not be necessary; partial displacement of lignin and alteration of cellulose structure may also be effective in increasing the sugar recovery from lignocellulosic biomass. On the other hand, another comparison study on applying individual or combined pre-treatments was conducted by López et al. (2020). Raw or autohydrolysed hazelnut shells were fractionated using

different organosolv (a pulping technique that uses an organic solvent to solubilise lignin and hemicellulose) processes including alkali, alkali-organosolv, organosolv or acid-catalysed organosolv processes. A comparative study of the findings revealed that acid-catalysed organosolv delignification achieved maximum lignin removal (65.3%) by allowing limited cellulose losses. Other studies have investigated the possible use of hazelnut shells to obtain prebiotic compounds such as oligosaccharides (Rivas et al., 2020; Surek et al., 2021). The dissolution of the hemicelluloses is achieved by a hydrothermal pre-treatment, while the lignin and cellulose remain in the solid phase almost unchanged, allowing their further processing for a complementary valorisation of the shells. The study conducted by Rivas et al. (2020) applied an optimised hydrothermal pre-treatment at 210°C to transform hemicellulose into soluble substituted oligosaccharides in liquid phase. Membrane filtration was performed to refine the oligosaccharides, which constituted for up to 90.9 wt% of the non-volatile solutes in the refined solution. The autohydrolysis step also yielded solids containing up to 93.13% Klason lignin and glucan, representing recovery yields of these components of greater than 85% and 90%, respectively. Besides, Surek et al. (2021) designed a sophisticated study to produce xylooligosaccharides (XOS) with a low degree of polymerisation (DP 2-6) from hazelnut shells. *Aureobasidium pullulans* xylanase was used for the autohydrolysis of hazelnut shells. The maximal XOS (DP 2-6) synthesis was 22.5 g/L with an enzyme concentration of 240 U/g XOS and a substrate concentration of 72 g/L at pH 5.0 and 40°C.

Due to their high lignin contents, hazelnut shells make an excellent substrate for the growth of edible and medicinal fungi. In this regard, *Ganoderma lucidum*, *Lentinula edodes*, and *Pleurotus cornucopiae* were grown on hazelnut shell substrates in order to evaluate their potential as alternative growth substrates (Puliga et al., 2022). The use of hazelnut shells as a substrate for mushroom growth is an eco-friendly alternative to the valorisation of agricultural by-products.

2.3.2 Valorisation of hazelnut skin

Hazelnut skin is a by-product of the roasting process of hazelnut industry, representing 2.5% of total hazelnut kernel weight (Alasalvar et al., 2009). The skins detach from

kernels during roasting, and then discarded as a waste. Roasted hazelnut skins are rich sources of polyphenolic compounds, dietary fibres as well as vitamin E, oleic and linoleic acids. Hence, the valorisation of such a rich biomass is promising. Valorisation applications of hazelnut skin have primarily focused on the extraction, characterisation and identification of phenolic compounds and dietary fibres, as in hazelnut shells (Alasalvar et al., 2009; Fanali et al., 2021; Ivanović et al., 2020; Košťálová and Hromádková, 2019; Lelli et al., 2021; Montella et al., 2013a; Odabaş and Koca, 2016; Tunçil, 2020; Yılmaz and Şebnem Tavman, 2016).

In a feasibility study to obtain phenolic extracts from hazelnut skin, Contini et al. (2008) applied long maceration extraction technique at room temperature using 80% (v/v) of aqueous methanol, ethanol or acetone, resulting in about 30% extraction yield and up to 502 mg gallic acid equivalents/g total phenolic content. Odabaş and Koca (2016), on the other hand, optimised the recovery of polyphenols from hazelnut skin using ultrasound-assisted (UAE), microwave-assisted (MAE) and supercritical carbon dioxide extraction (SCE) methods. They also compared these novel methods with applying the maceration method. According to their findings, UAE was reported (with the optimum following conditions; 45 min and 67.2-67.6% ethanol concentration) to be the best technique for extracting polyphenols from hazelnut skin, with the highest total phenolic content and antioxidant capacity values. Deep eutectic solvents (DES) are promising alternative green solvents to conventional solvents for the extraction of bioactive compounds from biomasses due to their outstanding physicochemical properties, such as thermal stability, non-volatility, excellent solubility and conductivity. They are also inexpensive, biodegradable, less toxic and more synthetically accessible. In this regard, 15 different DES and natural deep eutectic solvents (NADES) were studied in order to extract phenolic compounds from hazelnut skin (Fanali et al., 2021). Among the solvents tested, choline chloride (ChCl) and lactic acid-based NADES was reported as the most promising solvent with the optimum conditions of a 35% water solution of ChCl and lactic acid (molar ratio 1:2) and 1:25 g/ml solid: solvent ratio at 80°C. When compared to a conventional organic solvent, the optimized conditions enabled for the recovery of 39% more phenolic compounds (Fanali et al., 2021).

In addition to determining the optimum conditions for the extraction of phenolic compounds, the characterisation of the bound polyphenols (especially proanthocyanidins) is also essential in valorising the hazelnut skin. It might provide information on food processing and health studies on delivering proanthocyanidins in functional foods, characterising phenolic bioactivity in hazelnuts, and determining polyphenol metabolism after hazelnut intake (Lainas et al., 2016). Within this context, the effects of roasting on bound and extractable polyphenols (proanthocyanidins) on hazelnut skin were investigated by Lainas et al. (2016) resulting 21% recovery of bound proanthocyanidins (mainly dimers, trimers and tetramers) with the alkaline hydrolysis application.

Polysaccharides (Košťálová and Hromádková, 2019), water and alkali-soluble oligosaccharides (Montella et al., 2013a) and water-insoluble dietary fibres from hazelnut skin (Tunçil, 2020) were identified and characterised by several researchers. UAE has been optimised by Yılmaz and Şebnem Tavman (2016) in the extraction of polysaccharides from hazelnut skin. Sonication times were evaluated, and maximum ethanol insoluble extracts were obtained in 60 min, while the highest dry matter content was obtained in 120 min with UAE (Yılmaz and Şebnem Tavman, 2016). Furthermore, Montella et al. (2013b) evaluated the potential prebiotic activity of bioactive extracts from hazelnut skin. The functional activity of extracts was demonstrated by utilizing them as ingredients in a medium used to grow two probiotic strains (*Lactobacillus plantarum* P17630 and *Lactobacillus crispatus* P17631).

Valorisation applications then focused on the fortification of model food products with hazelnut skin and investigation of their sensory, functional and biological properties etc. In a study to develop a novel coffee-based functional beverage, the addition of crude hazelnut skin phenolic extract (HSPE) to increase the antioxidant capacity of the espresso coffee brew (EC) was investigated by Contini et al. (2012). They added HSPE before and after brewing the coffee and evaluated theirs in vitro (total phenolic content and antiradical ability) and in vivo (antioxidant potential of plasma in rats) antioxidant capacities. It was observed that adding HSPE to EC pre- or post-brewing increased the antioxidant activity of the brew in vitro and in vivo. In vivo experiments indicated that HSPE phenolics possessed higher antioxidant activity in

rats than phenolics naturally present in coffee; also, synergic effects between HSPE and EC phenolics may have occurred. In another study investigating the acute absorption and bioavailability of phenolic compounds of a hazelnut skin beverage in healthy subjects, the acute effect of these compounds on vascular/endothelial function was evaluated (Mocciaro et al., 2019). Forty-one healthy adults consumed hazelnut skin drinks prepared using the infusion method. After blood and urine samples were collected, ten plasma and twenty-four urine metabolites were detected. Although the determined bioavailability was around 27%, the circulating metabolites had no significant effect on vascular/endothelial function. Bertolino et al. (2015) evaluated the effects of hazelnut skin addition on the antioxidant capacity, physicochemical properties and sensory characteristics of yoghurt. Skins from three different hazelnut varieties (San Giovanni, Georgia and Tonda Gentile Trilobata) were utilized at two concentrations (3% and 6%) to enhance the polyphenol and dietary fibre content of the yoghurt.

The antioxidant capacities of fortified yoghurts increased compared to the control group (plain yoghurt) during storage; however, no changes in the phenolic compounds were reported. Moreover, yoghurts enriched with 6% hazelnut skin had the best functional ability, whereas yoghurts containing 3% San Giovanni and Tonda Gentile Tribolata hazelnut skin had the highest consumer rating. A similar study was carried out by Dinkçi et al. (2021) to evaluate the physicochemical, rheological, microbiological biochemical and sensory properties of functional yoghurt enriched with hazelnut skin (2%, 3% and 4%). Their findings showed that enrichment of yoghurt with hazelnut skin significantly improved the total solid and total fat contents, titratable acidity, the viability of yoghurt bacteria, water holding capacity and antioxidant activity of yoghurts. In the meantime, the sensory properties of yoghurts fortified with hazelnut skin were similar to those of control yoghurts, which increases the consumption potential of yoghurts enriched with hazelnut skin. In another study in which dairy products were fortified with hazelnut by-products, the effect of hazelnut skin (1%, 2% and 3%) and flour (1.5%, 3% and 4.5%) addition on the physicochemical and sensory properties of vanilla ice cream was investigated by Dervisoglu (2006). Their results revealed that hazelnut flour and skin could be good functional ingredients

to produce a non-fat ice cream at addition levels of 3% and 1%, respectively. In addition to dairy products, there are also studies in which bakery products are enriched with hazelnut skin. Cikrikci et al. (2016) evaluated potential utilisation of hazelnut skin as a functional ingredient in cake formulation. Firstly, they applied microfluidisation to ameliorate the functional properties of hazelnut skin. The effects of different proportions (10%, 15% and 20%) of microfluidised hazelnut skin on the rheological behaviour of cake batter and texture, colour parameters and storage qualities of cakes were investigated. Microfluidisation resulted in a highly branched fibrous structure with higher water binding capacity from hazelnut skin. This structure gave gluten-like strength and elasticity, increasing springiness and firmness scores. The results of this study indicated that microfluidised HS could be a potential functional ingredient candidate in bakery products. Recently, using various vegetables, vegetable juices and legumes as an ingredient in pasta production has become widespread to improve pasta's nutritional value. Zeppa et al. (2015) assessed the future use of hazelnut skins (4 different origins and 3 different quantities) to enhance the nutritional value of fresh egg pasta. Concentration of skin affected all assessed physicochemical characteristics and customer preferences with the pasta, although there were also significant variations between the four varieties. The results indicated that it is possible to utilise hazelnut skin in fresh pasta manufacture to produce fortified pasta with high antioxidant activity and fibre content. An example is the use of hazelnut skin in poultry meat and meat product aimed to evaluate the antioxidant, qualitative and sensory properties and shelf life of chicken burgers (Longato et al., 2019). Hazelnut skins could be used as a functional ingredient in the production of chicken burgers, which improved the cooking characteristics and antioxidant capabilities. Another study investigated the potential use of hazelnut skin powder as a natural and functional colourant with a high amount of dietary fibre and phenolic compounds (Ozdemir et al., 2014). They reported that high shear homogenisation was used to generate a desirable low micron particle size for hazelnut skin to integrate into food formulations; however, no significant change was observed in phenolic content and antioxidant activity.

Besides the use of hazelnut skin as a food ingredient, valorisation potential in other fields has also been investigated. Esposito et al. (2020) aimed to develop bioactive

pullulan-based packaging films loaded with phenolic-rich extracts from hazelnut skin via solvent casting method. Fabricated films showed thermal stability up to 200°C, good UV-light barrier properties and mechanical performance, additionally antioxidant and antibacterial activities. Another study aimed to separate different fractions, such as reinforcing filler, antioxidants and plasticizers, through diethyl ether and ethanolic extraction from hazelnut skin for high-added value poly(lactic acid) (PLA) and poly(propylene) (PP) (Battezzore et al., 2014). The dynamic mechanical thermal analysis findings suggested that the first fraction (obtained after diethyl ether extraction) was partly plasticised PLA. The second fraction (supernatant phase of ethanolic extraction) was composed of UV absorbers and thermal stabilisers that prolonged the induction time of PP oxidation (30%). The third fraction (solid phase of ethanolic extraction) increased the storage modulus of PLA and PP by 30 and 20%, respectively.

Considering the studies in which hazelnut skin was used as an ingredient in animal feed, the effect of dietary hazelnut skin on production and composition of milk was investigated by Campione et al. (2020). Dietary hazelnut skin had no negative impact on dry matter intake or milk production. However, it tended to increase fat and slightly decrease protein percentage in milk, indicating that it could be used to replace dried beet pulp in a commercial formulation for lactating ewes with minor adverse effects. Similar study focused on effect of inclusion of hazelnut skin in the diet of dairy ewes on the chemical and sensory profile of cheese (Caccamo et al., 2019). The sensory profile of cheeses manufactured with milk from ewes fed with hazelnut skin revealed a minor production of off-flavours associated with spicy and acid characteristics. Lipolysis levels in the prolonged ripening phase could enhance sensitivity to polyunsaturated fatty acid (PUFA) oxidation.

2.3.3 Valorisation of hazelnut meat

The defatted hazelnut meal obtained from oil extraction can be considered as another valuable by-product due to its nutritional value and high protein content. Depending on its characteristics, the meal could benefit various applications in the food and beverage industry. Valorisation studies of defatted hazelnut meal primarily focused on using it

in animal feeding (Buyukcapar and Kamalak, 2007; Emre et al., 2008; Xu and Hanna, 2011; Yalçin et al., 2005). Subsequently, the functional and rheological properties of isolated proteins from hazelnut meal were explored, since hazelnut meal protein could be utilised as a new plant-based protein source in the food industry. In this context, Tatar et al. (2015) evaluated the functional and rheological aspects of hazelnut meal (DHC) and flour (DHF) (by-products of hot and cold press oil extraction), and protein concentrates obtained from meal (DHCP) and flour (DHFP) as well as the influence of the oil extraction technique on hazelnut protein characteristics. The results showed that the emulsifying stability and fat absorption capacity of defatted hazelnut meal (DHC) and defatted hazelnut meal protein (DHCP) were lower than those of defatted hazelnut flour (DHF) and defatted hazelnut flour protein (DHFP). According to their results, authors indicated that protein concentrates isolated from both meal and flour had suitable emulsifying properties and water and oil absorption capacities to use as a functional ingredient in different food products such as soups, cakes, meat products and bread.

Non-thermal technologies such as high-pressure homogenisation (HPH) have been reported to improve the functional properties of sarcoplasmic proteins (Villamonte et al., 2016). Based on this, Saricaoglu et al. (2018) investigated the effect of HPH treatment on functional and rheological properties and molecular structure of hazelnut meal proteins. Their findings revealed that HPH treatment above 75 MPa unfolded the proteins, resulting in a slight band intensity reduction. Functional properties of hazelnut meal protein suspensions, such as emulsifying, solubility and foaming, increased after HPH treatment up to 100 MPa due to increased protein-solvent interaction. Pressures above 100 MPa, on the other hand, could promote further unfolding of the protein, resulting in the formation of hydrophobic and -SH residues and increased protein aggregation and decreased solubility, emulsifying and foaming capabilities. Hence, HPH treatment up to 100 MPa appeared to be a potential strategy for improving the functional and rheological characteristics of hazelnut meal proteins. The same group produced hazelnut milk from defatted hazelnut meal and applied multi-pass HPH to evaluate the effects of HPH conditions on the physicochemical properties of hazelnut milk (Gul et al., 2022). They reported that

homogenisation pressure, hazelnut meal concentration and temperature significantly affected the physicochemical, rheological and colour properties of hazelnut milk. Optimised hazelnut milk production conditions were determined as 12.97% hazelnut meal concentration, 1,140 bar homogenisation pressure and 38.1°C homogenisation temperature with 72.4% efficiency. In another study using novel technologies, the effects of osmotic dehydration pre-treatment and ultrasound-assisted extraction on the functional properties of hazelnut meal protein were investigated by Geow and Tan (2021). The results demonstrated that osmotic dehydration pre-treatment had no significant effect on the functional properties of the defatted meal. The parameters of ultrasound assisted-extraction process, on the other hand, have a considerable impact on the functional properties of the defatted meal. It was concluded that defatted meal extracted from higher parameter settings is ideal for foods with high juiciness and tenderness requirements, whereas defatted meal extracted from lower parameter settings is appropriate for milk-based drinks.

Bioactive peptides can be formed during the digestion or processing of protein-containing foods (Vermeirssen et al., 2004). Likewise, they can be produced in vitro through applying proteases to intact dietary proteins. Enzymatic formation of bioactive peptides is particularly beneficial since organic solvents and hazardous chemicals can be avoided. The formed peptides are appropriate for use in various fields, including food, pharmaceutical and cosmetics (Agyei and Danquah, 2011). In the light of this information, researches on the bioactivities of peptides obtained from hazelnut meal protein has drawn attention. Gülseren (2018) conducted an in-silico study to assess the potential biological functionality of peptides generated from hazelnut, applying three different gastrointestinal (GI) and three non-GI enzymes. The predicted functions of the generated hazelnut peptides were Angiotension I-converting enzyme (ACE)-inhibitory and Dipeptidyl peptidase (DPP)-IV-inhibitory, while anti-oxidative activity was a considerably less probable third category. A further study was carried out to evaluate the in vitro inhibition properties of tryptic hazelnut peptides by the same group (Gülseren and Çakır, 2019). They reported that at relatively low protein content, ACE-inhibitory was around 40%. They verified their results by conducting Liquid Chromatography Quadrupole Time-of-Flight Mass

Spectrometry (LC-Q-TOF/MS) and in silico identification of ACE-inhibitory activities of peptides. One hundred seventy-nine individual peptides were identified in ACE inhibitory fractions. Their potential inhibitory ability was assessed in silico on 22 thermolysin-generated peptides, 3 for chymotrypsin and 4 for trypsin. The same group continued their investigation, focusing on determining in vitro and in silico DPP-IV inhibitory activities of peptides from hazelnut meal protein (Cağlar et al., 2021a). According to their findings, hydrophobic interactions might be the main form of interaction between hazelnut peptides and DPP-IV. Their overall results indicating that hazelnut meal might be a potential source of ACE-inhibitory and DPP-IV-inhibitory peptides that can be used in functional food formulations. Similar study was conducted to determine the potential bioactive activities of protein hydrolysates from hazelnut meal (Simsek, 2021). Alcalase and Trypsin + Chymotrypsin were used to hydrolyse the protein isolates. The peptide fractions above and below 5 kDa were examined in order to inhibit angiotensin I-converting enzyme (ACE), dipeptidyl peptidase-IV (DPP-IV), and -glucosidase activities in vitro. Peptide fractions > 5 kDa were more effective in inhibiting ACE, whereas peptide fractions 5 kDa were more effective in inhibiting DPP- IV and -glucosidase, with no significant difference in treatment with Alcalase and Trypsin + Chymotrypsin suggesting that hazelnut meal protein can be a possible source of bioactive peptides and protein hydrolysates might be used as an alternative ingredient for functional foods.

Recently, valorisation applications of hazelnut meal have also focused on using hazelnut meal as a functional food ingredient. In this regard, Sen and Kahveci (2020) isolated protein from industrial hazelnut meal to assess its functional properties and potential utilisation of obtained protein in a functional drink. The functional beverage was prepared with two different concentrations of protein isolate (2% and 4%) and formulated beverages compared with a reference beverage. Study results suggested that untrained panellists favoured a beverage with 4% hazelnut protein as much as the reference drink. The potential use of hazelnut beverage obtained from defatted hazelnut meal for yoghurt production was evaluated in terms of microbiological, physicochemical, bioactive and rheological properties of the final product (Gul et al., 2022). Their findings revealed that, hazelnut beverage enriched yoghurt has higher

viscosity and lower syneresis than plain cow's milk yoghurt. Hazelnut enriched yoghurt had reduced acidity values during storage, which is important for extending shelf life. Sensory analysis results concluded that increasing the hazelnut beverage concentration reduced the sensory acceptability. However, for optimal yoghurt production in terms of sensory and physicochemical characteristics, a volume-based 3 (cow's milk) to 1 (hazelnut beverage) ratio is recommended. In another study, hazelnut meal was added as a partial replacer of milk-originated powders (whey and skimmed milk powders) and sugar in compound chocolate production (Bursa et al., 2021). The influence of hazelnut meal on the various rheological, physicochemical, sensory properties and bioaccessibility of phenolic compounds in compound chocolates was determined. The product with the highest bioactive and overall acceptability scores was targeted in the optimization study. Results suggested that the enrichment of compound chocolate with hazelnut meal could improve the functional properties of compound chocolate while reducing product costs. The same group also investigated the use of hazelnut meal as a partial replacer of sugar, whey and milk powder in the chocolate spread production (Acan et al., 2021). Similar results to the compound chocolate study were reported. On the other hand, Göksu et al. (2022b) investigated the addition of bioactive peptide fractions (1%) obtained from hazelnut meal in industrial hazelnut paste and evaluated the ACE-inhibitory activity after *in vitro* simulated digestion and effect of enzymatic proteolysis on allergenic characteristics of hazelnut paste. According to their results, the IC₅₀ values for ACE inhibitory fractions were around 2-27 $\mu\text{g/ml}$. After simulated digestion, several fractions showed significant bioactivity. The presence of intact and further hydrolysed peptides was predicted in the digested paste, and partial hydrolysis of the peptides might have increased ACE-inhibitory properties. Furthermore, allergic suppression was observed in some of the samples due to the allergenic activity test results. In other respects, the rheological, textural and rheological characteristics of final products need further investigation, while *in vivo* and clinical studies remain crucial. Same group conducted a similar study on the production of industrial cocoa cream with inclusion of hazelnut protein hydrolysates (1%) to evaluate stability of hydrolysates through processing and simulated digestion (Göksu et al., 2022a). Their results revealed that hazelnut protein allergenicity was

reduced by proteolysis up to around 20% in cocoa cream products. Regarding (ACE) inhibitory and antidiabetic action, partial degradation and mixing of degraded versus non-degraded peptides maintained and enhanced bioactive characteristics in digested cocoa cream products. However, antioxidant activity was not improved in most cases. Consequently, hazelnut meals are a valuable source of bioactive compounds' production and industrial utilisation, which could maintain their bioactivity beyond industrial production and gastrointestinal digestion.

Utilisation applications of hazelnut meal were further centred upon forming bioactive and edible films from hazelnut meal proteins. Aydemir et al. (2014) characterised the bioactive, functional and edible film-making attributes of hazelnut meal protein isolates. They applied hot extraction and acetone washing steps to meals before protein isolation. Both treatments improved the bioactive, gelling and solubility properties of protein isolates but got limited beneficial impact on the edible film making properties. On the other hand, the effects of ultrasound (US) treatment on nano-emulsion film-forming properties of hazelnut meal proteins and clove essential oil (CEO) were investigated by Gul et al. (2018). According to study results, US treatment significantly influenced the physical, optical, mechanical, barrier, and microstructural properties and the film's antibacterial and antioxidant activities due to altering particle characteristics of film-forming nano-emulsions. Enrichment with the CEO altered the mechanical properties of films by increasing the protein-oil contacts rather than the protein-protein interactions. At the same time, the US application enhanced the tensile strength and elongation at break due to a more homogenous dispersion of oil droplets in the protein matrix. The characteristics of hazelnut protein-based films can be further improved to fulfil criteria for commercial applications in the food industry by adjusting film-forming parameters such as ultrasound and dosages of plasticizers and emulsifiers.

2.4 Conclusions and Perspectives

Valorising waste products from the hazelnut industry is expected to have a positive impact on the environment and increase the sustainability of this important food system. Currently, hazelnut shells, roasted skin, and defatted meal are the most obvious waste streams to develop into value-added products. Increasing the value of these

products can create new commercial opportunities for farmers and hazelnut processors. Currently, most applications have been performed at lab-scale, and a considerable effort is needed to develop commodity-scale utilisation of these materials. Likewise, investments to develop the necessary infrastructure, transportation networks, storage, and commercially-viable applications are needed to fully realise the uses for these materials.

Finding new uses for hazelnut meal and roasted skin may have the lowest barrier to implementation, as hazelnut is already valued as an ingredient. Furthermore, the potential health benefits of nuts and their associated compounds are appealing to consumers. As skins and meal are used in new applications, careful attention is needed to maintain the proper allergen labelling. Furthermore, excessive consumption of phenolics can lead to anti-nutritional effects and toxicity. Overconsumption may not be a major concern, as the natural astringency of phenolics limit their intake. Importantly, these co-products are unlikely to bear current FDA-authorized health claims, as these are based on whole nut products, rather than isolated meal or skins. Further research is needed to validate the health-promoting mechanisms and amount of intake needed to improve human health.

Hazelnut skins and defatted meal could be used directly as food ingredients. However, further processing will increase their value as sources of bioactive peptides and phenolics. Additional research is needed to describe the specific benefits of these isolates. This may be a challenge given the bitter and astringent nature of these co-products. Thus, new technology and demonstration of consumer appeal and sensory acceptability are necessary to increase the desirability of these product that use these new ingredients.



3. COMBINED NEUTRASE-ALCALASE PROTEIN HYDROLYSATES FROM HAZELNUT MEAL, A POTENTIAL FUNCTIONAL FOOD INGREDIENT

3.1 Introduction

Hazelnut, widely cultivated in Turkey, constitute one of the most produced and consumed nuts worldwide (Ozdemir and Akinci, 2004). A big part of hazelnut production is processed industrially, mainly to produce hazelnut oil, leaving large quantities of hazelnut meal (Baldi, 2010). Hazelnut meal is very rich in portion of tea catechin with bovineoteins (38-54%) (Acan et al., 2021; Aydemir et al., 2014) and thus may be a cheap source of proteins that can be either introduced in food formulations or used as a base to produce bioactive peptides after enzymatic hydrolysis.

Plant-based proteins often have compact quaternary and tertiary structures, which may make them resistant to proteolysis (Hu et al., 2011). Microfluidization is a novel physical modification technique for processing food macromolecules with benefits such as continuous operation, low-temperature treatment, reduced nutrient component loss, and quick processing times (Zhang et al., 2021). In addition, microfluidization as a pretreatment may improve the functional properties of proteins and their enzymatic hydrolysis, with the protein structure becoming more loosened, exposing core groups hidden inside the folded structure (Hu et al., 2011; Zhang et al., 2021; Chen et al., 2016; Liu et al., 2017b).

Obesity and overweight are both major risk factors for several noncommunicable chronic diseases, including cardiovascular diseases, which are the leading causes of death worldwide; diabetes; musculoskeletal disorders; and even associated with some cancers, including liver, prostate, endometrial, breast, ovarian, gallbladder, colon, and kidney (WHO, 2021). According to the last statistics from the World Health Organization, 1.9 billion adults worldwide were overweight in 2016, with 650 million obese (WHO World Health Statistics, 2021). Pancreatic lipase (PL) is the primary

enzyme responsible for the hydrolysis of dietary fats (50–70%), which facilitates their absorption (Birari and Bhutani, 2007). This is why inhibiting PL is a good strategy to limit intestinal absorption of lipids and thus contribute to weight loss or prevent weight gain. In addition, plant-derived PL inhibitors are known resources that can lead to the selection of future drug candidates and thus enrich the current limited available anti-obesity drugs (Rajan et al., 2020; de la Garza et al., 2011). In recent years, bioactive peptides from edible plants emerged as very promising and safe candidates as PL inhibitors which may also be introduced in functional food formulations with anti-obesity potential (Coronado-Cáceres et al., 2020; Wang et al., 2022; Fan et al., 2018; Esfandi et al., 2022).

This study aimed to valorize hazelnut meal and explore the potential anti-obesity and antioxidant activities of its protein hydrolysates. In addition, the effect of the hydrolysis strategy (single or sequential hydrolysis) using Alcalase and Neutrase, as well as the application of microfluidization pretreatment on these activities and the functional properties of the protein isolates and hydrolysates, was investigated.

3.2 Materials and Methods

3.2.1 Enzymes and chemicals

Alcalase 2.4 L FG and Neutrase 0.8 L were obtained from Novozymes®(Bagsværd, Denmark), type II lipase from porcine pancreas (100-650 units/mg protein using olive oil and 30 min incubation) and bile salts (B8756-100G) sodium dodecyl sulfate (SDS), DPPH (2,2-Diphenyl-1-picrylhydrazyl), ABTS (2,2'-azino-di-(3-ethylbenzthiazoline sulfonic acid), were purchased from Sigma–Aldrich. (St.Louis, Missouri, USA). Other reagents were purchased from Merck, and only analytical-grade reagents were used for analysis.

3.2.2 Hazelnut meal characterization

Hazelnut meal from *Corylus avellana* L. species was kindly donated by a local company in Ordu, Turkey. The meal was obtained as a by-product of cold press oil extraction followed by hexane defatting. Proximate analysis of the meal was

characterized according to standard methods (AOAC, 1990). Total carbohydrate content was calculated by subtracting total protein, lipid, ash, and moisture percentages from a hundred. Protein, fat, ash, and total calculated carbohydrates of the hazelnut meal were 35.52 ± 1.72 , 3.64 ± 0.33 , 7.84 ± 0.09 , and $41.65 \pm 2.20\%$ (dry basis), respectively. Moisture represented $11.37 \pm 0.02\%$ of the meal.

3.2.3 Protein extraction from hazelnut meal

Crude hazelnut proteins were isolated from hazelnut meal by the conventional alkali extraction-isoelectric precipitation method as described in the literature with slight modifications (Saricaoglu et al., 2018; Tatar et al., 2015). The meal was first suspended in distilled water (1:12, meal:water), and the pH of the slurry was adjusted to 12 with 2 N NaOH. The mixture was then stirred for an hour at room temperature. After centrifugation at 14480 g for 10 minutes (25°C), the supernatant was collected and the pellets were subjected to two further extractions. After filtration of the supernatants (Whatman grade-4 filter paper to remove eventual low-density particles), proteins were precipitated upon pH adjustment to the isoelectric point (4.5) with 2 N HCl and further centrifugation for 5 minutes at the same centrifuge force. For easier solubilization of the dried protein isolates, the precipitate was redissolved in water, and the pH was adjusted to 7 before lyophilization. The protein content of the hazelnut meal and protein isolate was estimated using the Kjeldahl method (nitrogen content $\times 5.18$; AOAC 18: method 950.48). The protein recovery from hazelnut meal was calculated as the ratio of the proteins extracted from 100 g dry meal to the protein content of the meal, multiplied by a hundred. Crude proteins isolated were $22.75 \pm 1.18\%$ of the dry meal. Considering a purity of $62.12 \pm 0.22\%$ and the actual protein content in the meal ($35.52 \pm 1.72\%$), protein recovery was estimated at $39.87 \pm 3.99\%$. The purity of the isolates was considered in the calculation of the degree of hydrolysis of the proteins.

3.2.4 Preparation of hazelnut protein hydrolysates

Hazelnut protein isolates (PI) were hydrolyzed by Alcalase and Neutrase separately or sequentially combined in both orders. Microfluidization pretreatment was applied to improve the hydrolysis and functionality of the proteins tentatively. PI was solubilized

in distilled water at a concentration of 3% with pH adjusted to 8. Microfluidized samples were passed two times through the microfluidizer (LM10, Microfluidics, Westwood, MA, USA) at 120 MPa (Chen et al., 2016). The enzymatic hydrolysis conditions were set with respect to the manufacturer's recommendations. Briefly, hydrolysis by Neutrase (1%, enzyme/substrate) or Alcalase (0.15%) was performed at pH 8 (1N NaOH) and a temperature of 50 °C under continuous stirring (200 rpm). Upon the addition of the enzyme, the pH was maintained at 8 (1 N NaOH) every 15 minutes, and the volume of the added base was recorded each time for 120 min. The enzymes were inactivated by heating the mixture at 95 °C for 10 min. Combined enzymatic hydrolysis was performed by hydrolysis at halftime by one enzyme and the addition of the second enzyme after the inactivation of the first one. After cooling down, the hydrolysates were centrifuged at 5000 g for 30 min, and the supernatant was lyophilized and then stored at -80°C until further use (Cağlar et al., 2021a). The degree of hydrolysis was calculated according to the method proposed by Adler-Nissen et al. (1986) as given in Equation 3.1.

$$DH(\%) = \frac{B \times N_b}{\alpha \times MP \times h_{tot}} \times 100 \quad (3.1)$$

where B is the volume of NaOH consumption in L; N_b is the normality of the base; MP refers to the mass of protein in kg (nitrogen content $\times 5,18$ for hazelnut; 18); h_{tot} is the total number of peptide bonds in the protein substrate (meqv/g protein) (the average $h_{tot} = 8$ meqv/g for most of the proteins (Nielsen et al., 2001)); α is the average degree of dissociation of the α -amino groups released during hydrolysis expressed as:

$$\alpha = \frac{10^{(pH-pK)}}{1 + 10^{(pH-pK)}} \quad (3.2)$$

where pK is the average pK of the α -NH₂ groups liberated during hydrolysis, which was assumed to be 8 for hazelnut proteins (Thurlkill et al., 2006); the pH at which the proteolysis was conducted was 8, making $\alpha = 0.5$ and $1/\alpha = 2$.

The following obtained samples were characterized as described in the next sections: PI: hazelnut protein isolate; MFPI: microfluidized PI; NH: Neutrase hydrolysates of PI; MFNH: Neutrase hydrolysates of MFPI; AH: Alcalase hydrolysates of PI; MFAH: Alcalase hydrolysates of MFPI; MFNAH: Hydrolysates obtained with sequential

hydrolysis by respectively, Neutrased and Alcalase of MFPI; MFANH: Hydrolysates obtained with sequential hydrolysis by respectively, Alcalase and Neutrased of MFPI.

3.2.5 SDS-PAGE analysis

Mini-protean TGX 4-20% pre-cast gels (Bio-Rad Laboratories, USA) were used to perform SDS-PAGE in accordance with Laemmli's (Laemmli, 1970) methodology. The range of the protein molecular standard for this gel was 5-250 kDa. For the range of 5-50 kDa, Mini-protean Tris-Tricine 10-20% pre-cast gels (Bio-Rad Laboratories, USA) were also employed. Briefly, 20 μg of protein were loaded into each well after the loading dye and SBW samples were mixed 1:1 (v/v). Coomassie Brilliant blue G-250 was used to stain protein bands.

3.2.6 Molecular Weight (MW) distribution

A high-performance size-exclusion chromatograph (HP-SEC) (Dionex HPLC, Dionex GmbH) outfitted with two serially connected Agilent columns, Agilent Bio SEC-5 (5 m particle size, 100 pore size) and Agilent Bio SEC-5 (5 m particle size and 300 pore size), as well as a UV-detector was used to analyse the hazelnut protein isolates and hydrolysates. A calibration curve of known molecular weights as a function of retention time was made using a commercial protein standard mix with a molecular weight range of 1 to 670 kDa. Three independent injections ($n = 3$) were used, and the average area of each peak was calculated and displayed in relation to the overall peak area.

3.2.7 Amino acid profile

After mixing a known quantity of freeze-dried and powdered samples with 4 ml of 6 N HCl, then flushing with nitrogen gas for 30 s, the process of hydrolysis involved maintaining tubes at 110 C for 24 hours, and were filtered (using a syringe filter made of PES, 0.2 m). Samples were diluted before being determined to contain AA using LC/APCI-MS. A 250 m 4.6 m 3 m C18 Phenomenex column connected to an Agilent 6120 quadrupole operating in SIM positive mode was used to inject a 2 μL sample into an LC-MS system (Agilent 1100 HPLC, Waldbron, Germany) for mass spectrometry

(Agilent Technologies, Germany). Agilent Mass Hunter, Qualitative software was used to quantify the peak area and compare it to an AA standard mix (Ref# NCI0180.20,088, Thermo Scientific Pierce, Rockford, IL, USA).

3.2.8 Fourier-Transform Infrared spectroscopy (FTIR)

An FTIR tensor II spectrophotometer was used to determine the secondary structure of the materials (Bruker Optics Inc., Billerica, USA). Lyophilized materials at room temperature were used to determine the spectra as absorbance at wavelengths between 400–4000 cm^{-1} in every four scans. After baseline correction, the amide I region (1600–1700 cm^{-1}) was smoothed by the Savitzky-Golay algorithm. The peak was deconvoluted using a Gaussian peak-fit model, and the limit of error (R^2) was converged between 0.99-1 by using Origin Pro 2022b software (Origin Lab Corporation, USA). Relative percentages of the peaks corresponding to β -sheet (1610-1645 and 1680-1700 cm^{-1}), random coil ($1648 \pm 2 \text{ cm}^{-1}$), α -helix ($1652 \pm 2 \text{ cm}^{-1}$), and β -turn (1660-1680 cm^{-1}), were calculated by the area of the deconvoluted peaks (Hu et al., 2011).

3.2.9 Scanning Electron Microscopy (SEM)

The surface morphologies of lyophilized protein samples were examined by SEM (Thermofisher ChemiSEM Axia). A thin layer of platinum was sputter coated onto the samples before being photographed at a 7.5 kV acceleration voltage and a 100 μm scale with low vacuum mode (Low Vacuum Detector, LVD).

3.2.10 Dynamic light scattering analysis

Average protein particle size, their polydispersity and ζ -potential were measured by the mean of dynamic light scattering analyser (Nano-ZS, Malvern Instruments, Worcestershire, UK). Samples were dissolved or diluted to a final concentration of 0.1% in PBS (pH 7.4). The following constants were set: sample refractive index: 1.33 and sample absorption: 0.1 (Bernat et al., 2015).

3.2.11 Determination of emulsifying properties

Emulsifying properties were determined according to the method by Pearce and Kinsella (Pearce and Kinsella, 1978). For each sample, 10 ml olive oil was mixed with 30 ml of protein in PBS solution (3.2 mg/ml). The mixture was homogenized using an Ultra Turrax homogenizer (T18 digital, IKA, Germany) at a speed of 20,000 rpm for 1 min. An aliquot of the emulsion (50 μ l) was pipetted from the bottom of the container at 0 and 10 min after homogenization and mixed with 5 ml of sodium dodecyl sulphate (SDS, 0.1%) solution. The absorbance of the diluted solution was measured at 500 nm using a UV-Vis spectrophotometer (Optima SP-3000 nano spectrophotometer, Tokyo, Japan). The absorbances measured immediately (A_0) and 10 min (A_{10}) after emulsion formation were used to calculate the emulsifying activity index (EAI) and the emulsion stability index (ESI), as shown in Equation 3.3 and Equation 3.4, respectively (Zarai et al., 2016).

$$\text{EAI (m}^2/\text{g)} = \frac{(2 \times 2.303 \times A_0 \times N)}{(c \times \phi \times 10000)} \quad (3.3)$$

$$\text{ESI(min)} = \frac{A_0 \times 10}{A_0 - A_{10}} \times 10 \quad (3.4)$$

where N refers to the dilution factor, c refers to the concentration of the proteins (g/ml), and ϕ refers to the volumetric fraction of the oil (0.25).

3.2.12 Assessment of FFA Release Inhibition

Potential anti-obesity activity of hazelnut protein peptides (hydrolysates) was assessed through their ability to inhibit pancreatic lipase (PL), by measuring the amount of free fatty acids (FFA) released from triglycerides by this later. The experimental procedure was performed according to Zhang et al. (2022) with slight modifications. Briefly, a volume of olive oil was homogenized with three volumes of bile salt (1.0 mg/ml) using the Ultra Turrax homogenizer (T18 digital, IKA, Germany). The emulsified substrate (4 ml) was mixed with 1 ml of each peptide solution at different concentrations (4, 8, 16, and 32 mg/ml) or PBS as control (pH 7.4) and homogenized at 15,000 rpm for 2 min. PL (1 ml, 1,6 mg/ml) (Liu et al., 2019) previously preincubated at 37 $^{\circ}$ C for 5 min was added to the mixture to undergo the lipolysis for 30 minutes. The

reaction was terminated by the addition of 15 ml of ethanol (95%) and vortex. The FFA produced was calculated after titration with 0.05 M NaOH to neutralization (pH 7). The inhibition of FFA release (%) was estimated using Equation 3.5 and Equation 3.6 (Aguilera-Angel et al., 2018).

$$\text{FFA}(\%w/w) = \frac{V_{\text{NaOH}} \times C_{\text{NaOH}} \times \text{MW}_{\text{Lipid}}}{2 \times W_{\text{Lipid}}} \quad (3.5)$$

$$\text{FFA release inhibition} (\%) = \frac{\text{FFA}_{\text{control}} - \text{FFA}_{\text{sample}}}{\text{FFA}_{\text{control}}} \times 100 \quad (3.6)$$

where FFA (%w/w) corresponds to the amount of free fatty acids released after the digestion process, V_{NaOH} is the volume of NaOH (in L) used to neutralize the FFAs released after hydrolysis (assuming that all triacylglycerides are hydrolyzed into two molecules of FFAs and one molecule of monoacylglyceride), C_{NaOH} is the molarity of NaOH, MW_{Lipid} is the average molecular weight of olive oil (885,4 g/mol) which was deduced from olive oil composition (99% triglycerides with 80% oleic acid, which refers to glyceryl trioleate) (Boskou et al., 2006), and W_{Lipid} is the weight of 1 ml olive oil (0.917 g), $\text{FFA}_{\text{control}}$ is the amount of FFA released in the control group, and $\text{FFA}_{\text{sample}}$ is the amount of FFA released in the sample group.

3.2.13 In-vitro Antioxidant Activity

Two different methods assessed the total antioxidant capacity; DPPH and ABTS analyses were performed. The DPPH radical scavenging activity was determined using a modified version of the method described by Wang et al. (2021b) Each sample was mixed with 2 ml of 0.1 mM DPPH in a 95% ethanol solution. The mixture was mixed and left for 30 minutes at room temperature in the dark before its absorbance was measured at 517 nm. The 50% inhibitory concentration values (IC_{50}) were calculated using a nonlinear fit to the experimental data and used to evaluate the scavenging activity. The DPPH radical scavenging rate was calculated using Equation 3.7.

$$\text{DPPH radical scavenging activity} (\%) = \left(\frac{A_1 - A_s + A_0}{A_1} \right) \times 100 \quad (3.7)$$

where A_0 represents the absorbance of ethanol and the sample solution at 517 nm, A_1 represents the absorbance of ethanol and DPPH at 517 nm, and A_s represents the absorbance of the sample solution and DPPH at 517 nm.

ABTS radical scavenging activity was determined following the method of Liu et al. (2016) with slight modifications. First, ABTS and potassium persulfate were combined after being dissolved in distilled water to final concentrations of 7 and 2.6 mmol/L, respectively. Allow the mixture to remain dark at room temperature for 12 hours before using. It was then diluted by combining 1 ml of ABTS solution with 60 ml of phosphate-buffered saline (PBS) to get an absorbance of around 1.00 at 734 nm using a spectrophotometer. PBS was used to dissolve all analyzed samples. 5 ml of fresh ABTS solution was mixed with 500 L of analyzed materials for 2 hours in the dark. A spectrophotometer was then used to measure the absorbance at 734 nm. As a blank control, PBS was used.

The ABTS radical scavenging activity was calculated according to the following formula Equation 3.8.

$$\text{ABTS scavenging activity (\%)} = \frac{A_{\text{blank}} - A_{\text{sample}}}{A_{\text{blank}}} \times 100 \quad (3.8)$$

3.2.14 Statistical Analysis

All analyses were performed in triplicate, and the data were presented as mean \pm standard deviation (SDSD One-way analysis of variance (ANOVA) followed by Duncan's post hoc multiple comparison test using GraphPad Prism 8.0 (San Diego, California, USA) and the SPSS statistic program (Version 28.0) for IOS (SPSS Inc. Chicago, IL).

3.3 Results and Discussion

3.3.1 Protein Hydrolysis Efficiency

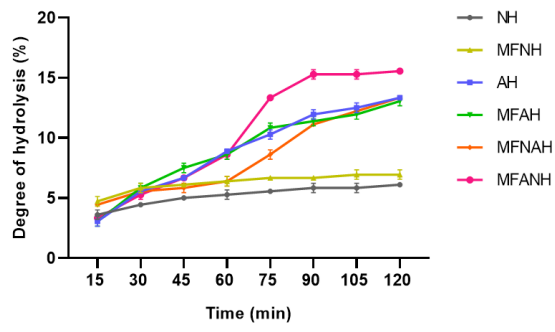
3.3.1.1 Degree of protein hydrolysis and SDS-PAGE patterns

Combined enzymatic hydrolysis showed sigmoidal curves, while individual enzymes showed the usual asymptotic curves (Figure 3.1a). The highest degree of hydrolysis (DH) was achieved by Alcalase-Neutrase combined enzymatic treatment (MFANH) with a maximum of $15.57 \pm 0.0\%$. When the order of the enzyme treatment was inverted (MFNAH), the DH dropped to $13.34 \pm 0.0\%$, which was not significantly

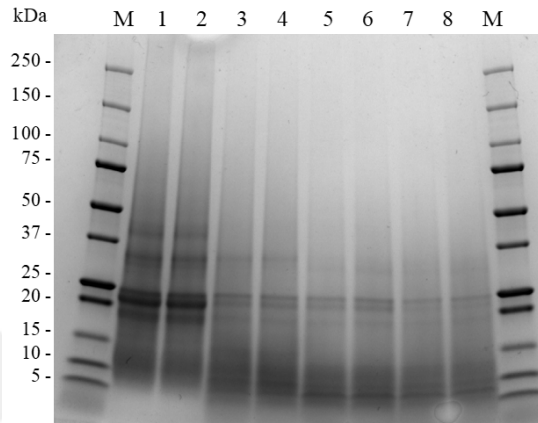
different from Alcalase single enzymatic treatment (AH: $13.34\pm 0.0\%$; MFAH: $13.06\pm 0.39\%$). Neutrase showed the lowest DH with values of $6.12\pm 0.0\%$ (NH) and $6.95\pm 0.39\%$ (MFNH). Differences between microfluidized and non-microfluidized samples were not significant.

The SDS-PAGE profiles confirm the different hydrolysis rates achieved by each sample (Figure 3.1b and Figure 3.1c). Protein isolates (PI and MFPI) exhibited five distinct protein patterns, 1: 37-50 kDa; 2: 25-37 kDa; 3: 25 kDa; 4: 20-25 kDa (the most intense protein); and 5: 15-20 kDa (Figure 3.1b). The intensity of these protein bands was significantly reduced upon enzymatic hydrolysis, with the most reduction shown by each combination of Alcalase and Neutrase (MFNAH and MFANH).

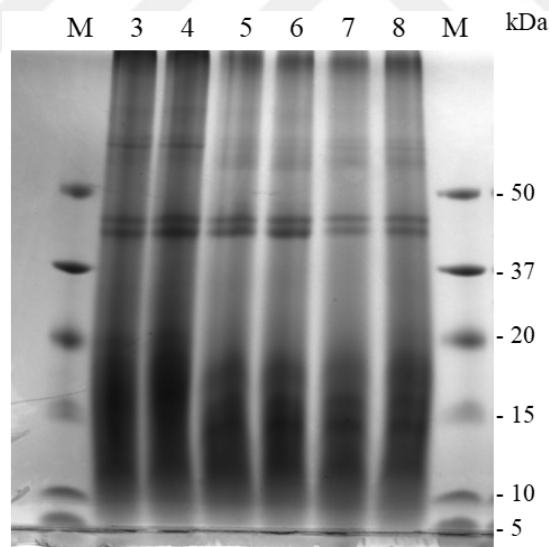
Literature reported that microfluidization pretreatment might enhance the hydrolysis of specific proteins by different enzymes, e.g., soy protein by pancreatin (Chen et al., 2016) and papain (Lin et al., 2015), and oyster protein by trypsin (Cha et al., 2018). The non-significant effect of microfluidization on the degree of hydrolysis of hazelnut protein in our study could be due to an insignificant change in the total available cleavage sites for Alcalase and Neutrase, despite the observed morphological and functional changes described in the following sections. The literature lacks sufficient information on the effect of microfluidization on the hydrolysis of proteins by these two enzymes. Zhang et al. (2021) studied the effect of microfluidization on the functional properties of rice dreg protein before hydrolysis by Alcalase and Neutrase, but the authors did not provide details on the changes in the degree of hydrolysis. Combined enzyme hydrolysis of proteins may result in a synergistic effect on both the degree of hydrolysis and the biological activities of the hydrolysates (Wang et al., 2010; Zheng et al., 2018; Hunsakul et al., 2022; Stressler et al., 2019). Nevertheless, research on this promising strategy is still very limited and can be further explored. Alcalase and Neutrase are bacterial endoproteases produced by *Bacillus licheniformis* and *Bacillus amyloliquefaciens*, respectively. The first is a relatively aggressive but stereoselective serine protease, while the latter is a mild metalloprotease (Novozymes®catalogs). Wang et al. (2010) found that the sequential hydrolysis of whey protein with Alcalase and Neutrase was more efficient and effective in inhibiting ACE activity than single-enzyme hydrolysis or Alcalase-trypsin combination.



(a)



(b)



(c)

Figure 3.1 : Degree of hydrolysis (A) and changes in SDS-PAGE profiles of microfluidized and non-microfluidized hazelnut protein isolates and their hydrolysates, prepared with Alcalase, Neutrase, or the combination of both (B, C). M: Marker, 1:PI, 2: MFPI, 3:NH, 4:MFNH, 5:AH 6:MFAH, 7:MFNAH, 8:MFANH.

3.3.2 Molecular Weight (MW) Distribution of Protein Isolates and Hydrolysates

The molecular weight profiles of microfluidized and non-microfluidized hazelnut protein isolates and their hydrolysates, prepared with Alcalase, Neutrase, or the combination of both, are displayed in Figure 3.2.

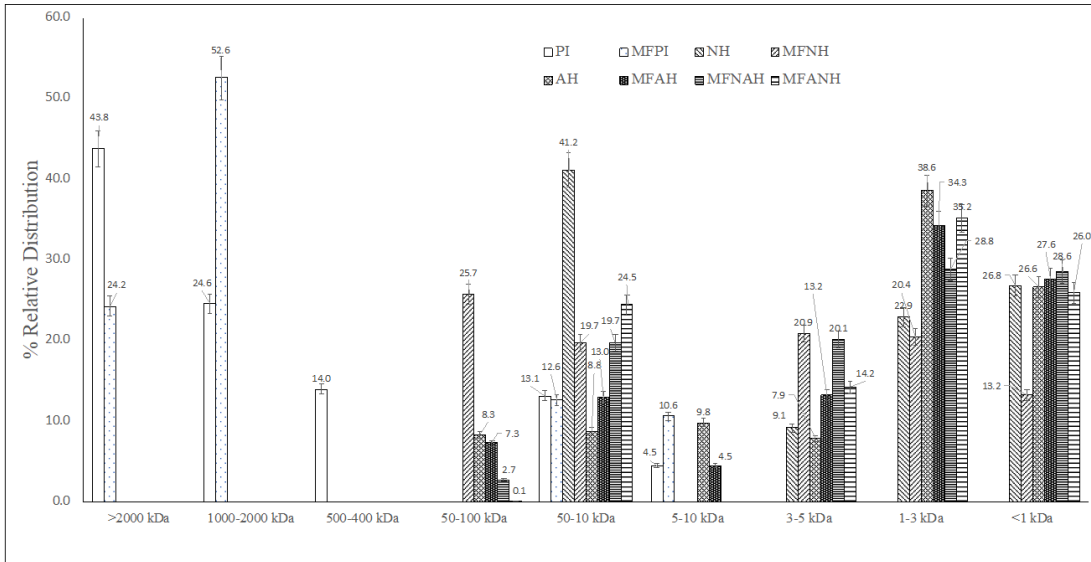


Figure 3.2 : Molecular weight distribution of hazelnut protein isolates and their hydrolysates, prepared with Alcalase, Neutrase, or the combination of both.

The pattern of the MW distribution of PI was of >2000 kDa (43.8%), 1000-2000 kDa (24.6%), 400-500 kDa (14.0%), 10-50 kDa (13.1%) and 5-10 kDa (4.5%). The MW distribution increased 52.6% at 1000-2000 kDa, while more (10.6%) peptides were obtained at 5-10 kDa with the microfluidization pretreatment. On the contrary, microfluidization pretreatment negatively affected Neutrase hydrolysates. Peptide fractions obtained by Neutrase hydrolysis were distributed <50 kDa; however, larger size peptide fractions (50-100 kDa) were obtained by Neutrase hydrolysis with microfluidization pretreatment. There was no significant effect of microfluidization on Alcalase hydrolysates. On the other hand, peptide fractions were extensively obtained at <3 kDa with the combined enzyme treatments (MFNAH and MFANH).

Molecular weight is a crucial factor that reflects protein hydrolysis and corresponds with the bioactivity of protein hydrolysates (Li et al., 2008). AH and MFAH had high

percentages of <3 kDa fraction, while lower percentages of this fraction were found in NH and MFNH. This revealed that this fraction was a significant substrate for Alcalase.

3.3.3 Amino Acid Profile of Hazelnut Protein Isolates and Hydrolysates

The amino acid composition of hazelnut meal protein isolate was analyzed in order to assess its potential as a functional food component. The results are shown in Table 3.1.

Table 3.1 : Amino acid profile of hazelnut meal protein isolates (mg/g protein).

Amino acids	Content	Amino acids	Content
LYS	11.04±0.7	MET	6.44±0.7
ARG	83.22±3.5	TYR	21.4±0
HIS	17.12±1.4	ILE	51.18±1.7
GLY	28.81±0.7	LEU	51.02±3.4
SER	33.92±0.3	PHE	34.03±1.8
ALA	32.24±0.9	ΣEAA	216.81±11.7
THR	23.42±0.9	$\Sigma BCAA$	131.21±6.8
GLU	80.34±0.3	$\Sigma NEAA$	298.26±2.3
ASP	151.75±0.7		
PRO	25.92±0.5		
VAL	29±1.7		

The data are presented as the mean± standard deviation of three replicates. LYS: Lysine, ARG: Arginine, HIS: Histidine, GLY: Glycine, SER: Serine, ALA: Alanine, THR: Threonine, GLU: Glutamic acid, ASP: Aspartic acid, PRO: Proline, VAL: Valine, MET: Methionine, TYR: Tyrosine, ILE: Isoleucine, LEU: Leucine, PHE: Phenylalanine, EAA: Essential amino acids, BCAA: Branched chain amino acids, NEAA: Non-essential amino acids

Aspartic acid (151.75±0.7 mg/g), arginine (83.22±3.5 mg/g) and glutamic acid (80.34±0.3 mg/g) were the major amino acids found in PI. The essential amino acid (EAA) contents of PI that are used as functional food ingredients are crucial, especially in terms of sports nutrition (Kato et al., 2018), since these amino acids act as substrates in muscle protein synthesis (Gorissen et al., 2018; Sen and Kahveci, 2020). EAA content of PI was determined as 32.79% of total amino acids, and leucine and isoleucine were the major EAA. This result was similar to the result of Sen and Kahveci (2020) and was substantially higher than many different plant-based proteins such as lupin (21%), oat (21%), wheat (22%), hemp (23%), soy (27%) and brown rice (28%) (Gorissen et al., 2018). On the other hand, branched-chain amino acids (BCAA) have also been reported to be potent stimulators of skeletal and liver protein synthesis

in addition to serving as substrates (Kato et al., 2018). Thus, BCAA content (sum of leucine, isoleucine and valine) of PI was also determined and found to be 19.27% of total protein in PI, which was higher than the results of Sen and Kahveci (2020) and other plant-based proteins mentioned above. Moreover, non-essential amino acid (NEAA) content was found 67.21% of the total protein in PI.

3.3.4 Fourier-Transform Infrared (FTIR) Spectroscopy

FTIR is a spectrophotometric method that provides information about the structures of proteins and measures the wavelength and strength of IR radiation's absorption (Kong and Yu, 2007). FTIR measures the vibrational transitions of functional groups, generally between the ground state and the first excited state ($4000\text{-}500\text{ cm}^{-1}$). Covalent bonds in atoms exhibit distinctive vibrations known as stretching (changes in bond lengths) and bending (changes in bond angles) (Arrondo et al., 1993). To make assumptions about the presence of a specific functional group of the molecule, the FTIR spectrum is divided into four distinct regions according to their binding type: single bond (O-H, C-H, N-H: $2500\text{-}4000\text{ cm}^{-1}$), triple bond ($\text{C}\equiv\text{C}$, $\text{C}\equiv\text{N}$, $\text{X}=\text{C}=\text{Y}$: $2000\text{-}2500\text{ cm}^{-1}$), double bond ($\text{C}=\text{O}$, $\text{C}=\text{N}$, $\text{C}=\text{C}$: $1500\text{-}2000\text{ cm}^{-1}$), fingerprint region ($500\text{-}1500\text{ cm}^{-1}$) (Mohamed et al., 2017).

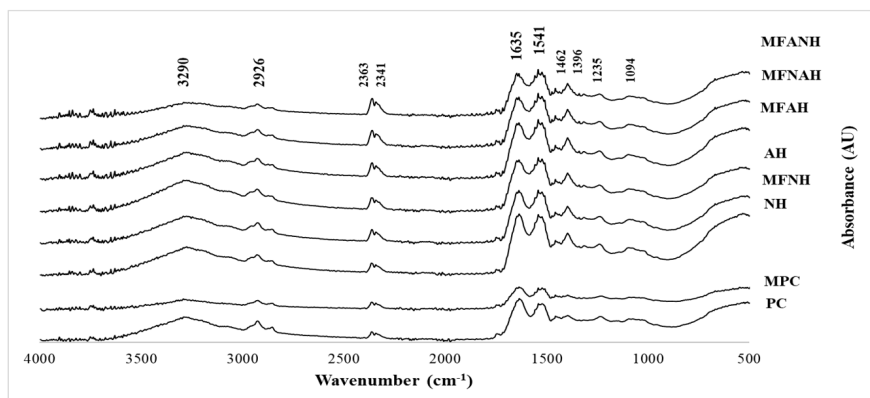
FTIR spectra of all protein samples are given in Figure 3.3. Nine distinct IR peaks of protein concentrate were observed by the various functional groups from lipids, proteins, and other substances. These are Amide A, Amide B, Amide I, Amide II, and fingerprint region bands (Amide III-VII). The maximum intensity points of PI or these bands were indicated in Figure 3.3. Microfluidization and enzyme treatment changes the conformational properties of proteins. Although there was a change in the intensity of the peaks after different treatments, no new peak was observed in any sample. The most prominent peaks were observed between $1200\text{-}1800\text{ cm}^{-1}$ and $2800\text{-}3500\text{ cm}^{-1}$. Two peaks determined in the fingerprint region of the native protein PI originated from bending vibrations of aliphatic CH_2 at 1462 cm^{-1} (asymmetric) and at 1396 cm^{-1} (symmetric) (Dogan et al., 2007). The bands at 1233 cm^{-1} and 1094 cm^{-1} are antisymmetric and symmetric double-bond stretching vibrations of the phosphate

moiety (PO_2^-), respectively (Arrondo and Goñi, 1998). All the bands in the fingerprint region are specific to the molecule and are often used to describe the molecules.

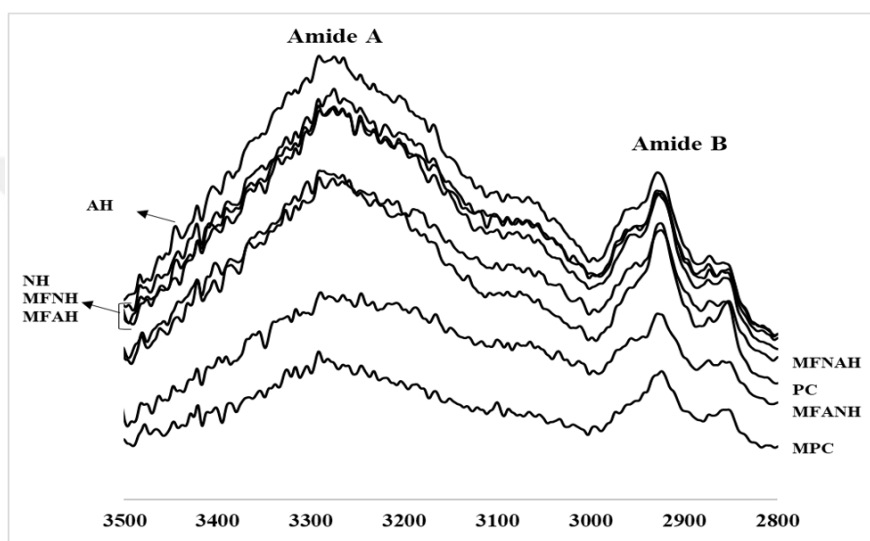
Moreover, Kavipriya and Ravitchandirane (2021) stated that the peaks in 2363 cm^{-1} and 2341 cm^{-1} in the triple bond region were related to CO_2 symmetric axial deformation, and these peaks in this region were ignored in this study.

The peaks between $1200\text{-}1800\text{ cm}^{-1}$ and between $2800\text{-}3500\text{ cm}^{-1}$ were the most significant ones. The spectrum of PI had characteristic amide A band at 3290 cm^{-1} (tensile vibration of intermolecular hydrogen bonding between O-H and N-H stretching occurring in the hydrogen bonds and intermolecular H bonding), amide B band at 2926 (asymmetric stretching of aliphatic CH_2) and 2854 (symmetric stretch of aliphatic CH_2), amide I band at 1635 cm^{-1} (C=O stretching vibrations of peptide linkages), and amide II at 1541 cm^{-1} (C-N stretching, 40%, and N-H bending, 60% of amino acids) (Dogan et al., 2007). The changes of the spectra in the range of $2800\text{-}3500\text{ cm}^{-1}$ were indicated in Figure 3.3b. The increase in the intensity of the amide A band indicates the formation of hydrogen bonds and the decrease in the hydrogen bonds indicates that the hydrogen bonds are partially broken down (Liu et al., 2022). MFANH and MFPI had lower peak intensity while the other protein samples had higher. However, the Amide B band ($2800\text{-}3000\text{ cm}^{-1}$) of MFANH and MFPI was lower than PI and blue shifted to 2924 and 2852 cm^{-1} , which means that the hydrophobic regions of the protein (aliphatic groups) are destroyed (Liu et al., 2022). The increase in the intensity of the peaks in this region is related to the fragmentation of the proteins into smaller pieces as a result of the enzyme application and the exposure of their hydrophobic regions.

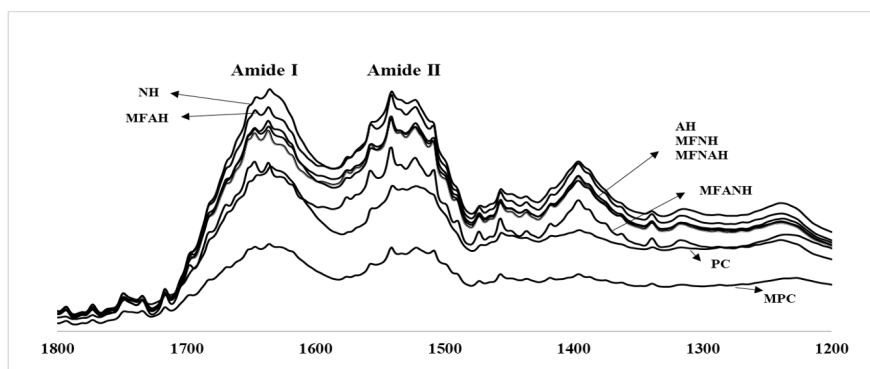
The two major peaks, (Amide I and II) are clearly related to the structure of the peptide bond (OC-NH). Since the peak intensities in the protein backbone region ($800\text{-}1800\text{ cm}^{-1}$) are related to the vibrations of the peptides in the sample, they vary linearly with the decomposition products of protein. Therefore, the area under these bands was calculated in Table 3.2 to see the difference in treatments in contrast to the control (PI) (Andrade et al., 2019). The secondary structure of the proteins was calculated by the deconvoluted amide I band in Table 3.2.



(a)



(b)



(c)

Figure 3.3 : FTIR spectra of hazelnut protein isolates and their hydrolysates, prepared with Alcalase, Neutrase, or the combination of both in the range of 500-4000 cm^{-1} (A), 2800-3500 cm^{-1} (B) and 1200-1800 cm^{-1} (C).

Table 3.2 : Secondary structure content (%) of protein samples from FTIR data.

	PI	MPI	NH	MFNH
Integrated Areas				
Amide I (1712-1579 cm ⁻¹)	5.28±0.5	2.82±0.9	7.37±0.6	6.32±0.1
Amide II (1579-1477 cm ⁻¹)	2.67±0.3	1.56±0.08	4.33±0.2	3.69±0.3
Amide A (3700-3000 cm ⁻¹)	16.69±0.2	7.87±0.6	20.31±0.06	18.91±0.5
Amide B (3000-2815 cm ⁻¹)	2.26±0.1	1.30±0.5	1.84±0.1	2.09±0.2
Secondary Structure (%)				
α -helix	0.86	0	26.21	57.51
β -sheet	55.98	47.46	34.8	22.98
β -turn	20.35	19.76	19.29	15.81
Random Coil	22.81	32.78	19.71	3.69
α -helix+ β -sheet	56.83	47.46	61.01	80.49
	AH	MFAH	MFNAH	MFANH
Integrated Areas				
Amide I (1712-1579 cm ⁻¹)	5.95±0.6	6.49±0.9	5.70±0.7	4.80±0.4
Amide II (1579-1477 cm ⁻¹)	3.52±0.08	4.03±0.4	3.60±0.7	3.10±0.03
Amide A (3700-3000 cm ⁻¹)	22.72±0.2	17.98±0.7	15.43±0.2	9.29±0.1
Amide B (3000-2815 cm ⁻¹)	2.18±0.3	1.97±0.7	1.83±0.1	1.27±0.3
Secondary Structure (%)				
α -helix	39.13	65.56	83.08	50.99
β -sheet	25.22	17.45	14.31	34.53
β -turn	27.2	15.63	0.15	0.22
Random Coil	8.45	1.36	2.46	14.26
α -helix+ β -sheet	64.35	83.01	97.39	85.52

The data are presented as the mean± standard deviation of three replicates.

After the microfluidization process (MFPI), a significant decrease in the intensity of the amide A, I, and II bands and even the disappearance of the peaks were observed. It was stated that after the microfluidization process, the amide I band density of rice dreg protein 6 and peanut protein 5 decreased and unfolded in the structures of the proteins, especially due to the increase in the random coil structure. Microfluidization is an efficient pretreatment technique that aids in enzymatic hydrolysis. Pressure changes the protein structure and affects the enzyme's cleavage sites, changing the rate of hydrolysis and the properties of the protein 6.

Since the sum of α -helix and β -sheet gives the total intermolecular hydrogen bonds (degree of compactness) (Liu et al., 2022), they are also indicated in Table 3.2. The β -sheet structure in all protein samples compared to PI was decreased and the α -helix structure was increased especially after enzyme treatments, similar to

the Alcalase hydrolysis of potato protein isolate reported by Akbari et al. (2020). β -Sheet structures, which preserve hydrophobic amino acids, are in the interior regions of folded proteins, while α -helix typically resides on the exterior of protein molecules. As a result of the protein unfolding during hydrolysis, (1) β -sheet structure disassembles and decreases by the revealing of hidden hydrophobic residues, and (2) an improvement in the α -helix structure of the protein was observed (Akbari et al., 2020).

A significant increase was observed in the amide A band (hydrogen bonding was intense) and amide B (aliphatic groups were exposed) in the enzyme application alone (AH and NH) while a decrease in the amide A and B was observed with the microfluidization application beforehand (MFAH and MFNH).

For MFNAH and MFANH, there was less intensity in the Amide A, B, and I and II bands compared to the enzyme treatments alone (MFNH and MFAH). Since Neutrase is more selective than Alcalase, the first use of Alcalase may have increased the number of free amino acids transferred to the water phase and increased the availability of amino acids for the more selective Neutrase (MFANH). Consequently, applying microfluidization before enzyme application or using firstly Alcalase and then Neutrase enzyme caused a decrease in these amide bands.

3.3.5 Scanning Electron Microscopy (SEM)

Microfluidization or enzyme treatment caused a reduction in the particle size (Figure 3.4) of the proteins. The microstructure of native protein (PI) is in the form of heterogeneous large clumps with a flake-like and smooth structure. This was probably due to the removal of water during the lyophilization process (Ghanghas et al., 2021). The absence of forces necessary to break up the frozen liquid into droplets or significantly modify their surface topology during the freezing evaporation process may be the cause of the bigger particles and flake-like shape 58. A significant change in the surface structure of the protein was observed with the deformation of the proteins by the microfluidization treatment. Massive, irregular protein clumps were broken up into smaller sizes, in line with the results obtained by particle size analysis. Similarly, large clumps of rice dreg protein (Zhang et al., 2021), fenugreek

(Ghanghas et al., 2021), and peanut protein (Hu et al., 2011) protein were reported to be fragmented into smaller clumps after the microfluidization as well as a decrease in particle size. Enzyme treatment alone (Alcalase or Neutrase) supported the formation of low-sized clumps on the one hand, and large clumps were formed on the other. More platy, fragile and angular structures were observed in AH than in NH. The enzyme treatment together with microfluidization supported the formation of small clumps in the samples. A similar result was obtained by Hu et al. (2011) with the application of microfluidization and trans-glutaminase enzyme of peanut proteins. Proteins with a lower molecular structure may come into contact with more water, causing the structure to become more porous when the water sublimes. This is evident in MFANH, which has a significantly smaller pore structure.

3.3.6 Particle Size, Size Distribution and ζ -potential

Both microfluidization and enzymatic hydrolysis treatments significantly reduced the average particle size of hazelnut protein isolate, from 374.3 ± 20.65 (PI) to 182.6 ± 2.26 (MFPI); 241.97 ± 7.75 (NH); and 261.13 ± 0.96 nm (AH). The lowest size was observed in proteins that have undergone both microfluidization and proteolysis, with no significant differences between these samples, 159.9 ± 4.23 (MFNH); 145.90 ± 0.85 (MFAH); 151.97 ± 2.07 (MFNAH); and 157.1 ± 0.44 nm (MFANH) (Figure 3.5a).

Likewise, microfluidization reduced the size dispersity of the protein particles, from a PDI of 0.45 ± 0.02 (PI) to ≈ 0.21 for all microfluidized samples, regardless of the enzymatic hydrolysis (Figure 3.5b). However, non-microfluidized hydrolysates showed a slight increase in their PDI, 0.53 ± 0.03 (NH) and 0.55 ± 0.02 (AH). Hazelnut protein isolates and hydrolysates were negatively charged with ζ -potential comprised between -12.47 ± 0.59 and -17.7 ± 1.61 mV (Figure 3.5b). Particle size and size polydispersity reduction is a common consequence of protein microfluidization (Ge et al., 2021; Wang et al., 2021a). Generally, enzymatic hydrolysis also reduces the size of protein particles (Wang et al., 2021b; Du et al., 2022).

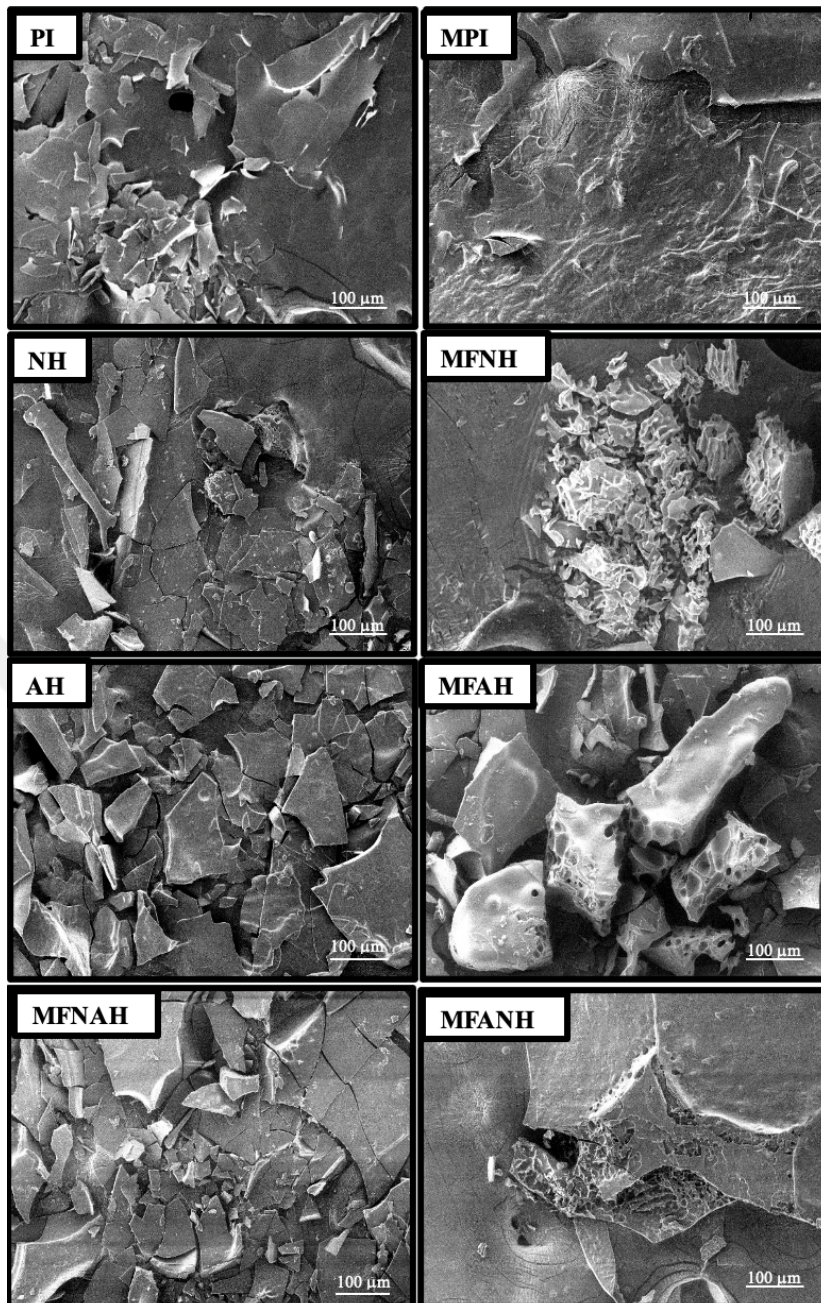
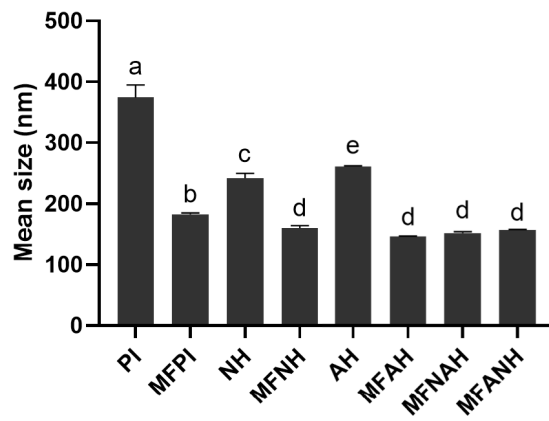


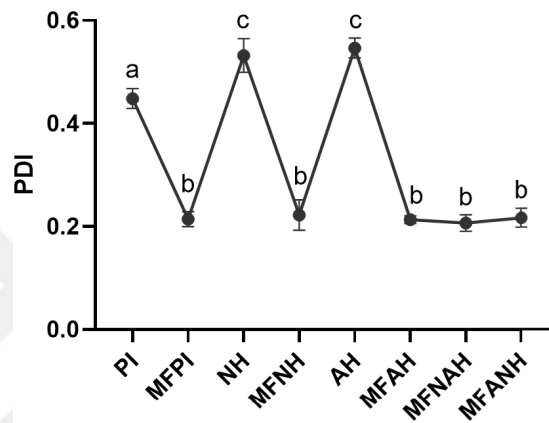
Figure 3.4 : Morphologies of microfluidized and non-microfluidized hazelnut protein isolates and their hydrolysates, prepared with Alcalase, Neutrase, or the combination of both.

3.3.7 Emulsifying Properties

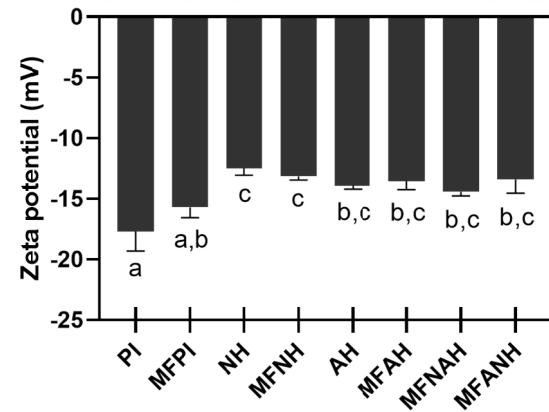
Emulsifying properties of microfluidized and non-microfluidized hazelnut protein isolates and their hydrolysates, prepared with Alcalase, Neutrase, or the combination



(a)



(b)



(c)

Figure 3.5 : Average particle size (a), size distribution (b) and (c) surface charge of microfluidized and non-microfluidized hazelnut protein isolates and their hydrolysates, prepared with Alcalase, Neutrase, or the combination of both. Different letters (a-d) indicate statistically significant differences ($P < 0.05$).

of both are expressed as emulsifying activity index (EAI) and emulsion stability index (ESI) (Figure 3.6). Emulsifying activity index was expressed as the area of oil/water interface stabilized per unit weight of protein. Emulsion stability index stability was expressed as the time needed to achieve a turbidity of the emulsion that is one-half of its original value. Microfluidization treatment allowed a significant increase in terms of EAI, from 58.76 ± 1.34 (PI) to 71.80 ± 0.9 m²/g (MFPI). Hydrolysates obtained by Neutrase showed the best emulsifying activity with EAI of 84.32 ± 1.43 (NH) and 88.04 ± 2.22 m²/g (MFNH). On the contrary, Alcalase hydrolysis did not significantly improve the EAI of the protein isolates, 55.36 ± 1.77 (AH) and 61.24 ± 1.63 m²/g (MFAH), even though EAI in MFAH was significantly higher than AH. Interestingly, the combined enzymatic treatment reduced the EAI of the proteins to 40.35 ± 0.94 (MFNAH) and 41.65 ± 0.65 m²/g (MFANH), which again correlates with the highest degree of hydrolysis achieved by these samples. Unlike EAI, the best ESI was achieved by the most hydrolyzed proteins, 46.96 ± 1.58 (MFNAH) and 60.03 ± 1.28 min (MFANH).

Alcalase hydrolysates showed better ESI than Neutrase, which also positively correlates with their respective degrees of hydrolysis. Microfluidization had an additional positive impact on the stability of emulsions in hydrolyzed proteins, 23.70 ± 0.81 (MFNH) vs 16.71 ± 0.64 min (NH) and 34.42 ± 0.91 (MFAH) vs 24.02 ± 1.12 min (AH). Protein isolates showed the least ESI with 14.04 ± 0.94 for PI and 14.00 ± 0.75 min for MFPI, with no significant differences from the control, 10.69 ± 0.21 min.

Similarly to our results, Imura et al. (2015) obtained the best emulsifying properties with soybean hydrolysates with the lowest degree of hydrolysis and the worst with the most hydrolyzed proteins, even lower than protein isolates. Increased degree of hydrolysis of proteins was associated with low emulsifying capacity by many other researchers (Linarès et al., 2000; Quaglia and Orban, 1990; Leni et al., 2020; Ahmed et al., 2019a; Avramenko et al., 2013). Inversely, the stability index of emulsions was reported to be higher in hydrolysates with most degree of hydrolysis by Baharuddin et al. (2016), which is in agreement with our present data. However, protein hydrolyzation can also independently increase EAI, decrease ESI, or have

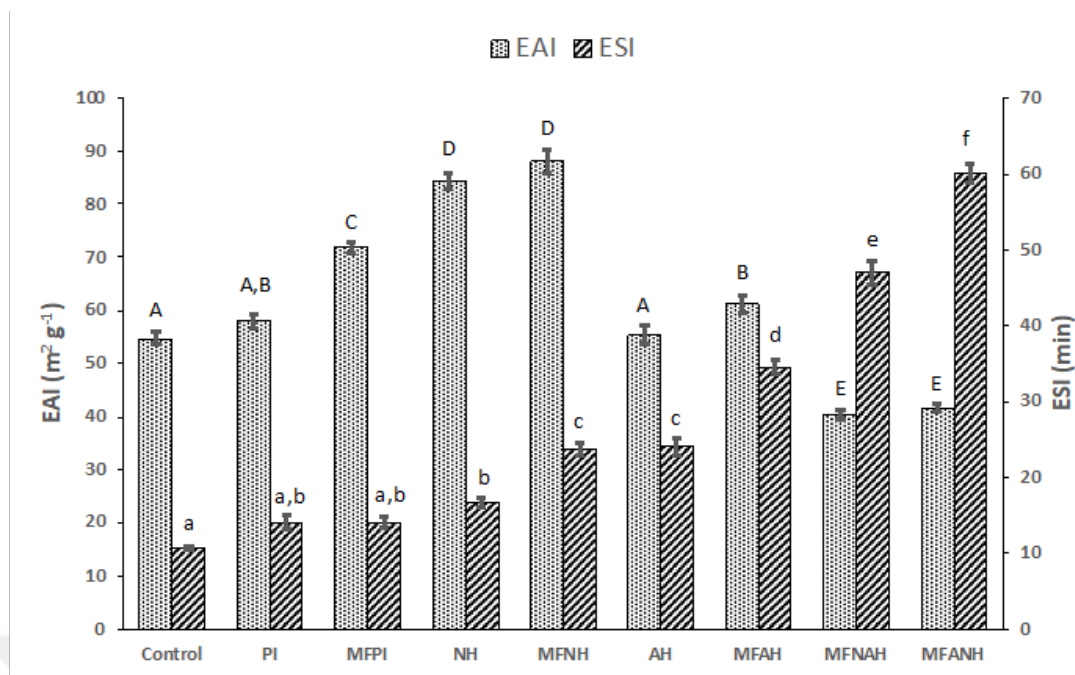


Figure 3.6 : Emulsifying properties of microfluidized and non-microfluidized hazelnut protein isolates and their hydrolysates, prepared with Alcalase, Neutrase, or the combination of both. Results are expressed as emulsifying activity index (EAI) and emulsion stability index (ESI). Small letters (a-f) indicate significant differences between ESI groups ($p < 0.05$). Capital letters (A-D) indicate significant differences between EAI groups ($p < 0.05$).

no significant effect on the emulsifying properties of proteins (Ghribi et al., 2015; Arteaga et al., 2020; Konieczny et al., 2020; Betancur-Ancona et al., 2009; Barac et al., 2012). This was reported to be dependent on other factors including the pH, protein source, processing steps, and the enzyme type being used for the hydrolysis process (Vogelsang-O'Dwyer et al., 2022). For instance, Tamm et al. (2016) have found that a higher degree of hydrolysis by Alcalase on pea protein had a negative effect on their emulsifying properties while trypsin had improved emulsions with the increase of the degree of hydrolysis of the same protein source. Thus, further studies sibling directly the effects of structural and surface properties of protein hydrolysates on their functional properties would be very useful (Vogelsang-O'Dwyer et al., 2022). Recently, Zhang et al. (2021) had reported a negative effect of microfluidization (120 MPa) on rice dreg protein isolate on EAI and no effect on ESI, which differs from our findings for hazelnut isolates. This, once again shows that the impact of a single parameter can drastically differ when the other parameters are different. Nevertheless,

in this study emulsification conditions were identical between all samples thus, the differences between the samples may only be ascribed to their respective functional properties.

3.3.8 Inhibition of FFA Release

Hazelnut protein isolates and hydrolysates showed a dose-dependent inhibition of FFA release by the action of pancreatic lipase on olive oil triglycerides (Figure 3.7). The best FFA inhibition was achieved by the most hydrolyzed proteins which were obtained by combining Alcalase and Neutrase, i.e., MFNAH and MFANH, with respectively a maximum inhibition of 38.56 ± 0.66 and $36.15 \pm 0.62\%$ at the concentration of 32 mg/ml and a minimum of 15.65 ± 1.44 and $12.05 \pm 0.21\%$ at the concentration of 4 mg/ml. There were no significant differences between these two samples. Among Alcalase hydrolysates, microfluidization had a significant positive effect on the inhibition of FFA release in comparison with non-microfluidized samples at all test concentrations (at 32mg/ml: $25.29 \pm 1.27\%$ (MFAH) vs $20.47 \pm 1.36\%$ (AH)), except for the lowest concentration which had no significant difference between these two samples (7.23 ± 0.12 and $6.01 \pm 1.6\%$, respectively). Neutrase hydrolysates had lower FFA release inhibition with maximums of 8.45 ± 1.85 (MFNH) and $8.42 \pm 1.56\%$ (MH), which correspond to the lowest degrees of hydrolysis. Protein isolates had the lowest inhibition with 4.82 ± 0.08 (MFPI) and $2.41 \pm 0.04\%$ at their highest concentrations.

Plant-based bioactive peptides may inhibit pancreatic lipase through different mechanisms. They may bind directly to the active site of the enzyme, alter its conformation, or destroy bile salts/oil emulsions, on which lipase relies for effective hydrolysis, by altering the lipophilic/hydrophilic balance of bile salts (Zhang et al., 2022). This last mechanism concords with the low emulsifying activity shown by MFNAH and MFANH in the present study. Wang et al. (2020) identified a bioactive peptide (RLLPH) isolated from *Corylus heterophylla* Fisch with, in addition to the inhibition of pancreatic lipase, had an adipogenesis inhibition in 3T3-L1 adipocytes by the regulation of adipogenic transcription factors and adenosine monophosphate-activated protein kinase (AMPK) activation. This makes hazelnut

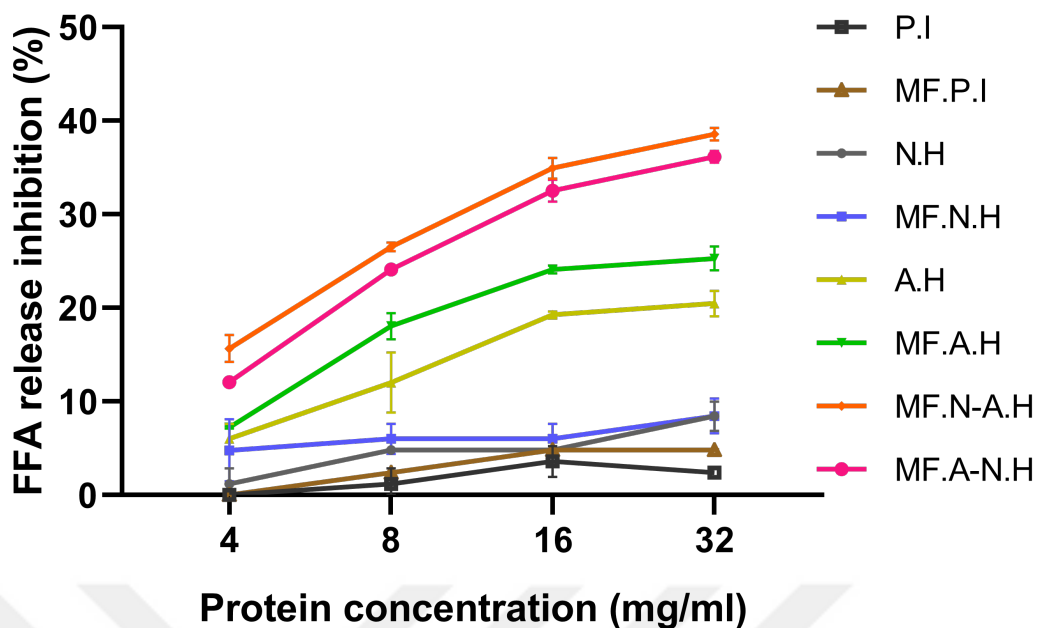


Figure 3.7 : Inhibition of FFA (%) of microfluidized and non-microfluidized hazelnut protein isolates and their hydrolysates, prepared with Alcalase, Neutrase, or the combination of both.

protein hydrolysates a good candidate as a functional food ingredient with anti-obesity potential.

3.3.9 In-vitro Antioxidant Activity of Protein Isolates and Hydrolysates

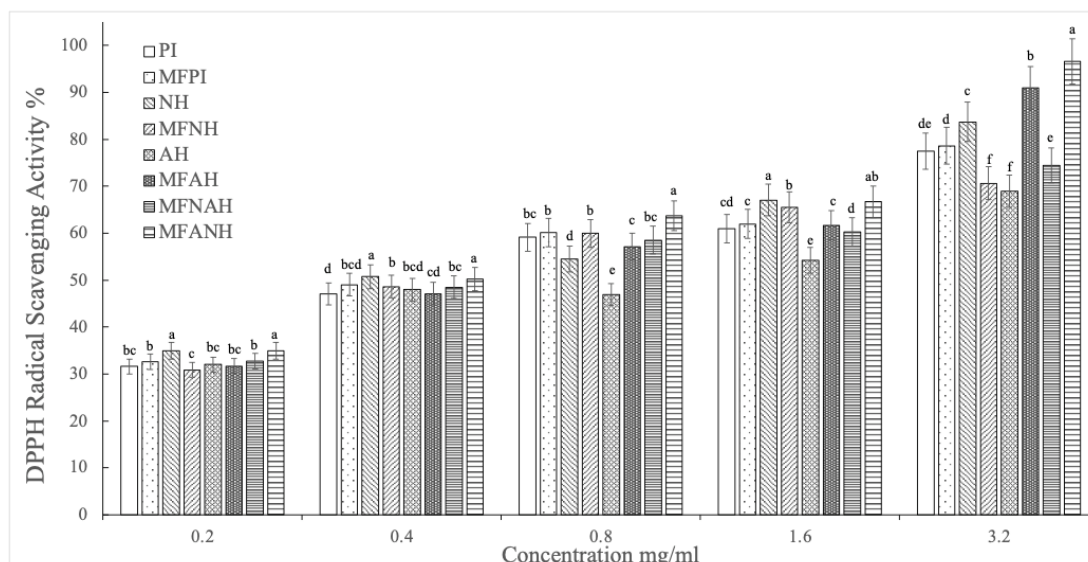
3.3.9.1 DPPH Radical Scavenging Activity

The DPPH radical is frequently used to measure antioxidant activity of numerous natural bioactive compounds due to its stability and potential to behave as a free radical scavenger (JAO and KO, 2002). A concentration-dependent analysis was performed on hazelnut PI and hydrolysates prepared with Neutrase and Alcalase with or without microfluidization pretreatment and their combinations. Figure 3.8a shows the DPPH radical scavenging activity of hazelnut PI and its hydrolysates at various concentrations (0.2-3.2 mg/ml). As shown in Figure 3.8, the effect of combined enzyme application and microfluidization pretreatment on DPPH radical scavenging activity becomes increasingly significant as concentration increases ($p < 0.05$). The DPPH radical scavenging activities of MFNAH and MFANH at highest concentration

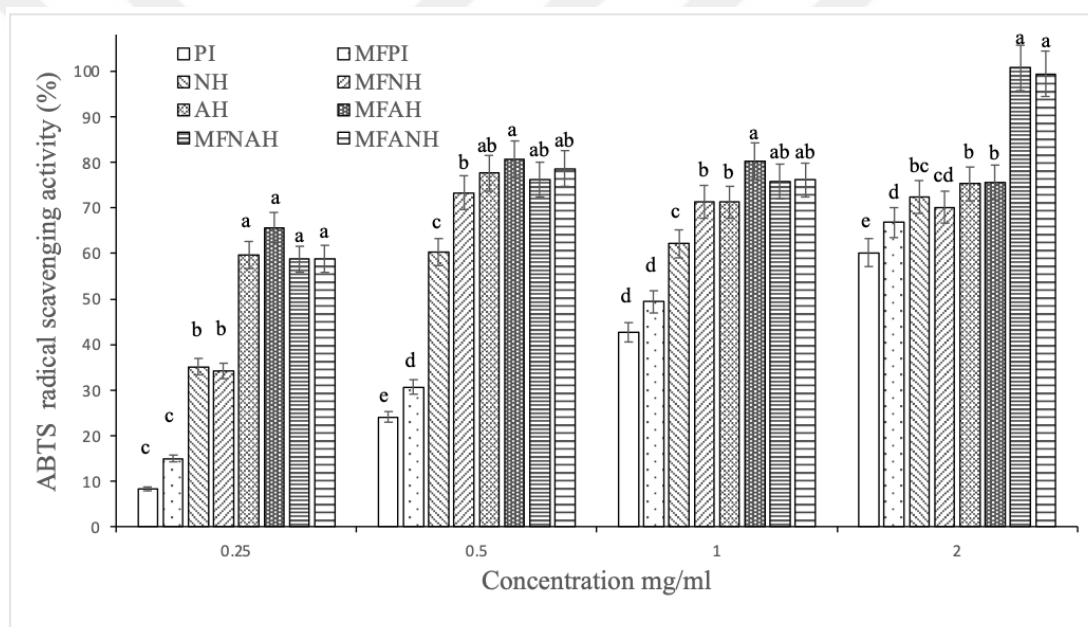
(3.2 mg/ml) were $74.45 \pm 1.94\%$ and $96.63 \pm 1.06\%$, respectively. Microfluidization pretreatment had no statistically significant difference in DPPH radical scavenging activity of PI as the concentration increased. In contrast, it negatively affected hydrolysates prepared using Neutrase and positively on hydrolysates prepared using Alcalase. ($p < 0.05$). The DPPH radical scavenging activities of combined Alcalase-Neutrase hydrolysates with microfluidization pretreatment were higher than that of combined Neutrase-Alcalase hydrolysates with microfluidization pretreatment at all concentrations ($p < 0.05$), which indicates the order of the enzyme is critical in combined enzyme application. These results are in accordance with the findings of Zhang et al. (2021) on rice dreg protein isolates. For the hazelnut PI and hydrolysates, the lowest IC₅₀ value (the highest radical scavenging activity) of MFANH was 0.86 mg/ml, followed by 0.91, 0.97, 0.98, 1.18, 1.24, 1.25 and 1.53 mg/ml for the MFAH, MFNH, NH, MFPI, MFNAH, PI and AH respectively. The differences in DPPH radical scavenging capacities across hydrolysates may be linked to free amino acid compositions, molecular distribution, peptide structures and sequencing (Sarmadi and Ismail, 2010; Li et al., 2015).

3.3.9.2 ABTS Radical Scavenging Activity

The peroxidase substrate ABTS has become a useful substrate for assessing total antioxidant capacity since it forms a relatively stable radical (ABTS) on one electron oxidation (Liu et al., 2016; Apak et al., 2007). The ABTS radical scavenging activity of the hazelnut PI and hydrolysates were measured at 0.25-2 mg/ml to further confirm the antioxidant activities and the results are shown in Figure 3.8b. Increasing trends were monitored on ABTS radical scavenging activities of PI and MHPI in a concentration-dependent manner. No significant difference was observed in the radical scavenging activities of individual enzyme hydrolysates with or without microfluidization pretreatment (NH, MFNH, AH, MFAH) after 0.5 mg/ml concentration. Unlike the DPPH analysis, it was observed that the antioxidant activities of Alcalase hydrolysates at low concentrations were higher than other hydrolysates ($p < 0.05$).



(a)



(b)

Figure 3.8 : DPPH (A) and ABTS (B) radical scavenging activities of microfluidized and non-microfluidized hazelnut protein isolates and their hydrolysates, prepared with Alcalase, Neutrase, or the combination of both. Different letters (a-d) indicate statistically significant differences ($P < 0.05$).

On the other hand, again different from the DPPH analysis, no significant difference was observed between combined enzyme treatments (MFNAH and MFANH) at all concentrations ($p < 0.05$). The highest ABTS radical scavenging activities of MFANH and MFNAH were $99.37 \pm 0.13\%$ and $100.73 \pm 0.63\%$, respectively at the concentration

of 2 mg/ml. The lowest IC₅₀ value (the highest radical scavenging activity) of MFNH was 0.33 mg/ml among the hazelnut PI and hydrolysates, followed by 0.55, 0.55, 0.75, 0.96, 1.04, 1.37 and 1.67 mg/ml for the MFNAH, MFANH, NH, AH, MFAH, MFPI and PI respectively.

3.4 Conclusion

In this study, hazelnut meal, a by-product of the hazelnut oil industry was valorized and used as a source of bioactive peptides with a special focus on their potential anti-obesity and antioxidant activities. Sequential or individual hydrolysis by Neutrase and Alcalase was performed to prepare the protein hydrolysates. Microfluidization was applied to tentatively improve the hydrolysis and the functional properties of the hydrolysates. Combined Alcalase-Neutrase hydrolysis resulted in the best records regarding the DH the inhibition of FFA release by pancreatic lipase, and free radical scavenging activities. The DH correlated positively with the ESI of the hydrolysates but negatively correlated with their EAI. Microfluidization caused the unfolding of protein structure which resulted in the enhancement of the EAI of protein isolates and hydrolysates and the FFA release inhibition for Alcalase hydrolysates. Hazelnut protein hydrolysates from hazelnut meal may be a good candidate as a functional food ingredient with potential anti-obesity and antioxidant properties. Protein processing (pretreatment, degree of hydrolysis, etc.) should be mastered according to the desired application of the protein hydrolysates.

4. INTERACTIONS BETWEEN HAZELNUT (*CORYLUS AVELLANA L.*) PROTEIN AND PHENOLICS AND IN VITRO GASTROINTESTINAL DIGESTIBILITY

4.1 Introduction

Hazelnuts are grown in countries with temperate climates around the world. In 2020, Turkey (approximately 63%) met most of the world's requirements in hazelnut production, followed by Italy (about 13%) (FAOSTAT, 2022a). After cracking their hard shells, they are processed as hazelnut oil, hazelnut paste, or direct use as natural or roasted fine particles. The hazelnut oil and protein contents are approximately 60% and 15%, respectively (USDA, 2022). On the other hand, the protein content of defatted hazelnut meal after cold press oil extraction was in the range of 35-41% (Saricaoglu et al., 2018). Thus, the high protein amount of hazelnut meal makes it possible to evaluate it as a potential plant-based protein source.

Protein-phenolic interactions occur with the proteins found in the plant, during food processing, or after consumption together with phenolic sources (Rohn, 2014). These interactions are covalent or non-covalent and are affected by parameters such as temperature, pH, types and concentrations of proteins or phenolics (Ozdal et al., 2013). Although it has been a widely investigated subject in recent years, studies on the interaction of plant-based proteins with phenolics are limited. To the best of authors' knowledge, studies on the interaction of proteins obtained from nuts are also limited to walnuts or peanuts. Therefore, interactions of walnut protein isolate walnut hull phenolics (Su et al., 2018) and walnut flour phenolics from walnut flour/hull (Labuckas et al., 2008) were investigated in addition to the investigations on the effect of walnut phenolics in walnut protein edible coating (Grosso et al., 2020).

Fluorescence spectroscopy and Fourier-transform infrared spectroscopy (FTIR) are productive techniques for understanding ligand binding with protein molecules. Changes in the microenvironments of tryptophane (Trp) and tyrosine (Tyr) amino

acids in proteins can be observed, and tips on how proteins can interact with phenols by fluorescence spectroscopy. FTIR is one of the spectroscopic methods that provide information about the secondary structures of proteins. Moreover, dynamic light scattering (DLS) and ζ -potential are practical complementary techniques for determining the changes in proteins with the formation of the protein-phenolic complex by monitoring the alteration in hydrodynamic radius and charge distribution of the proteins, respectively.

It has been stated that protein-phenolic complexes formed as a result of interaction suppress the antioxidant effects of phenolic compounds during gastrointestinal digestion and form indigestible complexes (Ozdal et al., 2013; Rawel and Rohn, 2010). However, phenols interacting with proteins during gastrointestinal digestion are thought to be protected from oxidation (Jakobek, 2015). Therefore, as the gastric chyme waits for a certain time, the appearance of phenolic compounds in the blood may be delayed as a result of protein-phenolic interaction during digestion, and phenolics can be separated from the complexes in the gastrointestinal tract without any change in the total amount of phenolic substances (Zhang et al., 2014).

In this study, protein isolate was prepared with hazelnut meal obtained from a cold press oil extraction after removing its remaining oil (defatting) and phenolics (dephenolisation). Phenolic compounds were obtained from the hazelnut skin. Protein-phenolic complexes were examined by fluorescence quenching, FTIR analyses, and dynamic light scattering (DLS). Moreover, the bioaccessibility of phenolics after protein-polyphenol complexation was also monitored after in-vitro gastrointestinal digestion, and thus changes in the degree of hydrolysis of proteins by pancreatin were also determined.

4.2 Materials and Methods

4.2.1 Materials

Hazelnut (*Corylus avellana* L.) meal (Tombul variety), obtained after cold press oil extraction, was kindly donated by Hazelnut Research Institute, Giresun, Turkiye. The meal was first characterised for fat, protein, moisture, and ash content by

standard methods (AOAC, 1990). Then, total carbohydrate content was calculated by subtracting percentages of total fat, protein, ash, and moisture contents from a hundred. Protein, fat, ash, moisture, and total calculated carbohydrates of the hazelnut meal were 32.08 ± 1.66 , 26.72 ± 1.33 , 5.31 ± 0.01 , 4.08 ± 0.04 , and $31.81 \pm 0.37\%$, respectively.

Hazelnut skin was obtained from the roasting process of hazelnut destined for direct consumption. α -amylase (A1031, 1500 U/L), pepsin from porcine gastric mucosa (P7012, ≥ 25000 U/mL), bile extract porcine (B8631, 160 mM), pancreatin from porcine pancreas (P7545, 8 \times USP), Trolox ((\pm)-6-Hydroxy-2,5,7,8-tetramethylchromane-2-carboxylic acid), DPPH (2,2-Diphenyl-1-picrylhydrazyl) and HPLC grade standards (catechin (C), gallic acid (GA), protocatechuic acid (PCA), gallic acid gallate (GCG), (-)-epigallocatechin (EGC), epicatechin (EC), (-)-epigallocatechin gallate (EGCG), phlorizin, quercetin 3-O-rhamnoside (Q3R), quercetin (QUE)) were purchased from Sigma-Aldrich (St. Louis, Missouri, USA). Other reagents were purchased from Merck (Darmstadt, Germany). The chemicals used in this study were from a commercial source and were either from analytical or HPLC grade.

4.2.2 Preparation of hazelnut skin extracts (HSE)

200 ml of 70% aqueous ethanol was added to 30 ± 0.01 g of hazelnut skins, vortexed for 1 min, and then sonicated in a cooled ultrasonic bath for 15 min. After that, the treated samples were centrifuged for 10 min at 4000 rpm at 4 °C (Heidolph, Schwabach, Germany)), and the supernatant was collected. Then 200 ml 70% aqueous-ethanol was added to the pellet, and this procedure was repeated two more times. Ethanol was evaporated using a rotary evaporator (IKA RV 10 auto pro V, Staufen, Germany), and the aqueous extract was freeze-dried (Christ Alpha 1-2 LD plus, Osterode am Harz, Germany) and kept at -20°C until further analyses.

4.2.3 Preparation of protein isolate from hazelnut meal)

Before protein extraction, hazelnut meal was first defatted and then dephenolyzed. Meal defatting was performed by stirring the meal in n-hexane overnight with a solid/solvent ratio of 1:4, followed by decantation and drying under a fuming hood

(Norazalina et al., 2011). Dephenolisation of the defatted meal was performed using the same extraction method with hazelnut skin explained in section 2.2. According to the literature, total proteins were isolated from defatted and dephenolyzed hazelnut meal by the mean of the alkali extraction-isoelectric precipitation method, with slight modifications (Saricaoglu et al., 2018; Tatar et al., 2015). A non-dephenolyzed sample was also extracted. Hazelnut meals were dissolved in distilled water at a solid/water ratio of 1:12. After pH adjustment to 12 (5 M NaOH), the mixture was stirred for 1 hour at room temperature. After centrifugation at full speed (14 480 g) for 10 min, the supernatant was collected, and the pellets were subjected to two further extractions under the same conditions, with a reduction of the volume of water to 2/3 of the initial. The supernatants were mixed and filtered through Whatman grade-4 filter paper to remove present low-density particles. Protein precipitation accrued upon pH adjustment to 4.5 with HCl 5M. The heterogeneous solution was then centrifuged for 5 minutes at the same speed. The precipitate was dispersed in water, and the pH was readjusted to 7 before freeze-drying the proteins. This last step has permitted better solubilization of the lyophilized proteins in the following analysis. The protein contents of the hazelnut meals and protein isolates were estimated using the Kjeldahl method (nitrogen content $\times 5,18$; AOAC method 950.48 (AOCS, 1990)). The protein recovery from hazelnut meal was calculated as the ratio of the proteins extracted from 100 g dry meal (with consideration of the purity) to the meal's protein content, multiplied by 100.

4.2.4 Amino acid profile of the hazelnut protein isolate

A known amount of freeze-dried and powdered samples was mixed with 4 mL of 6 N HCl, followed by 30 s of nitrogen gas flushing; hydrolysis was carried out by keeping tubes at 110°C for 24 h, after which hydrolyzed samples were filtered (syringe filter, PES, 0.2 m) and diluted before AA determination using LC/APCI-MS. A 2 μ L sample was injected into an LC-MS system (Agilent 1100 HPLC, Waldbron, Germany) through a C18 Phenomenex column (250 m 4.6 m 3 m), which was linked to an Agilent 6120 quadrupole in SIM positive mode (Agilent Technologies, Germany). The peak area was compared to an AA standard mix (Ref# NCI0180.

20,088, Thermo ScientificPierce, Rockford, IL, USA) and quantified using Agilent MassHunter, Qualitative software (Harrysson et al., 2018).

4.2.5 Preparation of protein-phenolic complex solutions

The total phenolic content of the phenolic extract was calculated as mM catechin equivalent per g with the calibration graph of catechin solutions between 0.10-1 mM.

The mixture of protein and phenolic solutions were prepared according to Günal-Köroğlu et al. (Günal-Köroğlu et al., 2022). The stock protein solution was at 10 mg/ml concentration, and dilution series of phenolic extract or catechin between 0-0.5 mM concentrations was prepared.

4.2.5.1 Particle size, size distribution, and ζ -potential determination

Mean particle size, size distribution, and ζ -potential of protein-polyphenol complexes were measured using a dynamic light scattering analyzer (Nano-ZS, Malvern Instruments, Worcestershire, UK). Samples were diluted to a final concentration of 0.1% solid matter in 1X PBS (pH 7.4) to avoid multiple scattering effects (Adrar et al., 2021). In addition, constant values of the samples concerning refractive index and absorption of 1.33 and 0.1 were considered, respectively (Bernat et al., 2015).

4.2.5.2 Fluorescence quenching

Phosphate buffered saline (10 x PBS) at pH 7, and 25% ethanol solution with PBS were used to dissolve protein and phenolic compound, respectively. Stock solutions of dHPI and HSE were freshly prepared and mixed at 1:1 (v/v) shortly before analysis. The change in fluorescence emission intensity was measured after 2 min of adding HSE to dHPI. The addition of a constant volume of quencher to the protein solution avoided complications due to dilution effects within titration-type experiments.

The FS5 Spectrofluorometer (Edinburgh Instruments, Livingston, UK) with a 150 W Xenon lamp and a single photon counting photomultiplier (PMT) detector was used for all intrinsic fluorescence measurements (Hamamatsu, R928P). The excitation wavelength range (λ_{ex}) was 280/295 nm, while the emission wavelength range (em)

was 290/310 to 420 nm (measured every 2 nm). Other instrument parameters were a slit width of 2 nm (for excitation and emission) and a photomultiplier (PMT) detector voltage of 1245 V.

The phenolic extracts did not absorb significant energy at the established emission wavelength. However, a blank was still prepared for each phenolic concentration, where the protein solution was replaced by phosphate-buffered saline (PBS). The respective spectrum of each phenolic extract was then subtracted from the emission spectrum of the corresponding mixture. Finally, each measurement was repeated in triplicate, and the mean and standard deviations were calculated.

4.2.5.3 Stern-Volmer equation

Stern-Volmer Equation at different temperatures (298, 308, 318 K) was used to determine the fluorescence quenching in Equation 4.1 (Papadopoulou et al., 2005).

$$F_0/F = 1 + K_{sv}[Q] = 1 + K_q\tau_0[Q] \quad (4.1)$$

where F_0 is the fluorescence intensity of dHPI solution, F is the fluorescence intensity of dHPI- HSE solutions, $[Q]$ is the concentration of phenolic extract in dHPI solution (mM), τ_0 is the lifetime of the fluorophore in the absence of quencher (10^{-8} s), K_{sv} is the Stern-Volmer constant, defining the quenching efficiency (M^{-1}), K_q is equal to K_{sv}/τ_0 the bimolecular quenching constant ($M^{-1} s^{-1}$). The Stern-Volmer quenching constant K_{sv} for dHPI-HSE system was obtained by the slope of the regression curves of (F_0/F) against $[Q]$.

The fluorescence quenching includes both static and dynamic quenching, and the maximum dynamic constant is $2.0 \times 10^{10} M^{-1} S^{-1}$ in an aqueous solution (Lakowicz, 2006). In the case where K_q is greater than the maximum dynamic constant, static quenching is dominant. The static quenching constants were also calculated in Equation 4.2 according to the double-logarithmic Equation (Zhang et al., 2018).

$$\log \left[\frac{F_0 - F}{F} \right] = \log K_A + n \log [Q] \quad (4.2)$$

where K_A is the intercept of the plot (binding constant), and n is the slope of the plot (the number of the binding sides).

4.2.5.4 Thermodynamic parameters

Van't Hoff equations were used to calculate the thermodynamic parameters at 298, 308, and 318 K (Equation 4.3, Equation 4.4, and Equation 4.5) (Jia et al., 2017; Seedher and Agarwal, 2010).

$$\ln K_A = -\Delta H/RT + \Delta S/R \quad (4.3)$$

$$\Delta G = -RT \ln K_A \quad (4.4)$$

$$\Delta G = \Delta H - T\Delta S \quad (4.5)$$

where K_A represents the binding constant, R represents the universal gas constant ($8.134 \text{ J mol}^{-1} \text{ K}^{-1}$), and T is the experimental temperature (K). ΔH , ΔS , and ΔG represent the changes in the enthalpy (kJ mol^{-1}), entropy ($\text{kJ K}^{-1} \text{ mol}^{-1}$), and Gibbs free energy (kJ mol^{-1}), respectively.

The following data (enthalpy change (ΔH) and entropy change (ΔS)) were used to assess the results: (a) hydrophobic forces when $\Delta H > 0$ and $\Delta S > 0$, (b) electrostatic interactions when $\Delta H < 0$ and $\Delta S > 0$, (c) electrostatic and hydrophobic interactions when $\Delta H > 0$ and $\Delta S < 0$, (d) H-bonding and van der Waals forces when $\Delta H < 0$ and $\Delta S < 0$ (Ross and Subramanian, 1981).

4.2.5.5 Fourier Transform Infrared (FTIR) spectroscopy

The secondary structure of dHPI-HSE complexes was determined using an FTIR tensor II spectrophotometer (Bruker Optics Inc., Billerica, USA). The materials in powder form were measured as absorbance at room temperature at wavelengths of $400\text{--}4000 \text{ cm}^{-1}$. Signals were captured in every four scans. The second derivative of the amide I region ($1600\text{--}1700 \text{ cm}^{-1}$) was smoothed by the Savitzky-Golay algorithm and was deconvoluted using a Gaussian peak-fit model by using OriginPro 2022b software (Origin Lab Corporation, USA). Relative percentages of the peaks corresponding to intermolecular β -sheet ($161\text{--}1645$ and $1680\text{--}1700 \text{ cm}^{-1}$), random coil ($1641\text{--}1648 \text{ cm}^{-1}$), α -helix ($1648\text{--}1656 \text{ cm}^{-1}$), and β -turn ($1660\text{--}1680 \text{ cm}^{-1}$), were calculated by the area of the deconvoluted peaks (Shi et al., 2017).

4.2.6 Assessment of hazelnut protein digestibility by pancreatin

According to the literature, hazelnut protein isolates were hydrolyzed by pancreatin (Berdutina et al., 2000; Karamać et al., 2016; Moreno et al., 2020). As the protein concentrations should be significant for proteolysis (protein/water ratio of 1:20), the concentrations of HSE and catechin were made to meet the protein/polyphenols ratios used in the fluorescence quenching study. Before pancreatin addition (enzyme/substrate 1:20, w/w) under a continuous stirring (400 rpm), the pH and the temperature of the protein-phenolic solutions were adjusted to 8 with 0.5 N NaOH and 40°C. The pH was maintained at 8 (0.5 N NaOH) every 15 minutes, and the volume of added NaOH was recorded for 2 h. The enzyme was inactivated by heating the mixture at 95°C for 15 minutes (Daliri et al., 2021). After cooling down, the solutions were centrifuged at 5000 g for 30 min to remove the insoluble matter. The supernatant containing the hydrolysates was freeze-dried and then stored at -80°C until further use (Cağlar et al., 2021a). The degree of hydrolysis was calculated according to Adler-Nissen (1979) in Equation 4.6:

$$\text{DH}(\%) = \frac{\mathbf{B} \times \mathbf{N}_b}{\alpha \times \mathbf{M}_P \times \mathbf{h}_{tot}} \times 100 \quad (4.6)$$

where B is the base consumption in litres; N_b is the normality of the base; M_P refers to the mass of protein in kg (nitrogen content $\times 5,18$; (AOAC, 1990)); h_{tot} is the total number of peptide bonds in the protein substrate (meqv/g protein) (the average $h_{tot} = 8$ meqv/g for most of the proteins (Nielsen et al., 2001)); α is the average degree of dissociation of the α -NH₂ groups released during hydrolysis expressed in Equation 4.7:

$$\alpha = \frac{10^{(\text{pH}-\text{pK})}}{1 + 10^{(\text{pH}-\text{pK})}} \quad (4.7)$$

where pK is the average pK of the α -NH₂ groups liberated during hydrolysis, it was assumed to be 8 for hazelnut proteins (Thurlkill et al., 2006); the pH at which the proteolysis was conducted is 8, making $\alpha = 0.5$, $1/\alpha = 2$.

4.2.7 Simulated in-vitro gastrointestinal digestion for HSE bioaccessibility

In-vitro gastrointestinal digestion conditions were applied, and the salivary, gastric, or intestinal fluids were prepared according to Minekus et al. (2014). The flow diagram of the protocol is given in Table 4.1. Considering the detectability of compounds after digestion, 0.5 mM catechin and HSE were used for in-vitro gastrointestinal digestion analysis. Digests from the gastric and intestinal phases were centrifuged (Hettich, Tuttlingen, Germany) at 14 000 rpm and 4 °C for 5 min, and the supernatants were kept at 20 °C until further analyses.

4.2.7.1 Spectrophotometric analyses

The total phenolic content was determined using the Folin-Ciocalteu reagent according to the method modified from Turkmen et al. (2006) using gallic acid as a standard.

TPCs in the samples were calculated via the recovery index values of the samples as mg gallic acid equivalent (GAE) per gram extract (R1). TPC of the HSE or catechin solutions (HSE or C) at the initial phase was assumed as reference (R0) and the recovery index of the phenolic compounds (RI) in the samples was calculated according to Equation 4.8.

$$RI(\%) = \frac{R_1}{R_0} \times 100 \quad (4.8)$$

The total antioxidant capacity was assessed by two different assays, cupric ion reducing antioxidant capacity (CUPRAC) and DPPH (2,2-diphenyl-1-picrylhydrazyl) analyses were performed according to Apak et al. (2004) and Kumaran and karunakaran (2006), respectively. In all assays, Trolox (6-hydroxy-2,5,7,8-tetramethylchroman-2-carboxylic acid) was used as a standard, and the results were expressed in terms of mg Trolox equivalent (TE) per 100 g of sample.

4.2.7.2 HPLC-DAD analysis of phenolic compounds

The polyphenolic profiles of samples were identified using the method of Capanoglu et al. (2008). Sample extracts were filtered via a 0.45 μm membrane filter and analyzed

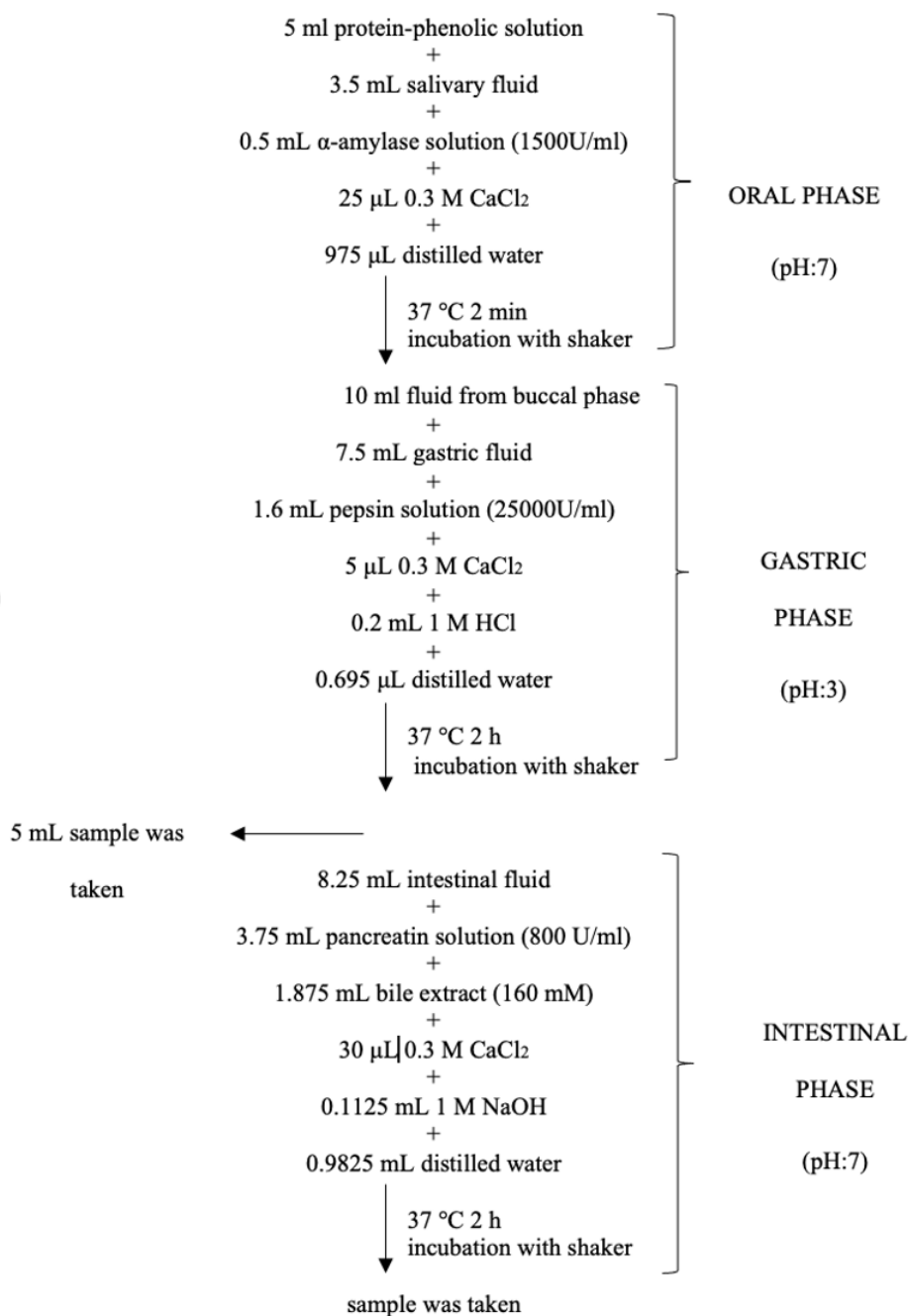


Figure 4.1 : Flow diagram of simulated in vitro gastrointestinal digestion. pH adjustment was made with 0.1 M HCL or 1 M NaOH for each phase.

using a Waters 2695 HPLC system equipped with a PDA (Waters 2996) detector. A Supelcosil LC-18 (25 cm \times 4.60 mm, 5 μ m column Sigma-Aldrich, Steinheim, Germany) was used. The mobile phases were composed of Milli-Q water with 0.1 per cent (v/v) Trifluoroacetic acid (TFA) (Mobile A) and acetonitrile with 0.1 per cent (v/v)

TFA (Mobile B). A linear gradient was utilized, with 95% solvent A and 5% solvent B at 0 minutes, 65% solvent A and 35% solvent B at 45 minutes, 25% solvent A and 75% solvent B at 47 minutes, and returning to original conditions at 54 minutes. The flow rate was 1 ml/min. Detection was carried out at 280 and 360 nm. Identification was based on the retention times and distinctive UV spectra. External standards were used for quantification.

4.2.8 Statistical analysis

All the experiments were replicated three times, and the data were represented as mean \pm SD. Data were statistically analyzed for multiple comparisons using SPSS software (version 28, IBM SPSS inc, Armonk, NY, USA) for analysis of variance (ANOVA). Duncan's novel multiple-range test was applied to compare different samples ($p < 0.05$). For size results, values with four digits were analyzed separately from the two and three-digit groups (due to their extremely high size, all two/three-digit numbers would not seem significantly different).

4.3 Results and Discussion

4.3.1 Effect of dephenolisation on protein purity and protein recovery and amino acid profile

Dephenolisation of hazelnut meal before protein isolation affected both protein recovery and the purity of the protein isolates. Indeed, dephenolisation treatment permitted the achievement of a much higher purity of the isolates (98.38 ± 1.04 %) than the non-dephenolised sample (78.73 ± 1.33 %). However, the protein recovery was significantly lower in the dephenolised sample than the non-dephenolised one (45.57 ± 4.48 vs 76.65 ± 6.13 %), which is assumed due to protein loss during dephenolisation treatment (there was a significant decrease in protein content after dephenolisation) (Table 4.1). The amino acid profile of hazelnut meal protein isolate is shown in Table 4.2.

Table 4.1 : Protein content and protein recovery from defatted hazelnut meal (dry basis).

	Defatted meal	Dephenolised meal
Protein content (%)	46.87 ± 1.04	28.06 ± 0.59
Crude proteins isolated (%)	39.52 ± 1.08	12.98 ± 1.00
Purity of isolates (%)	78.73 ± 1.33	98.38 ± 1.04
Recovery (% , pure basis)	76.65 ± 6.13	45.57 ± 4.48

Table 4.2 : Amino acid profile of hazelnut meal protein isolate (mg/g protein).

GLYCINE	38.86±0.81	ASPARGINE	88.22±0.67
ALANINE	35.81±1.09	LYSINE	18.89±0.48
SERINE	41.83±0.4	GLUTAMINE	184.81±3.42
PROLINE	28.36±0.99	METHIONINE	4.68±5.32
VALIN	27.54±1.4	HISTIDINE	17.31±3.2
THREONINE	25.31±0.32	PHENYLALANINE	38.79±1.65
CYSTEINE	nd	ARGININE	94.33±11.46
ISOLEUCINE	53.88±2.17	TYROSINE	19.92±0.08
LEUCINE	54.56±3.04		

4.3.2 Average particle size, size distribution, and ζ -charge

The average particle size, polydispersity index (PDI), and ζ -potential of the protein isolates with or without the complexation/presence with/of polyphenols are shown in Figure 4.2. The dephenolisation of the protein isolates reduced their average size from 164.23±2.85 nm (HPI) to 73.86±5.56 nm (dHPI). The addition of HSE to dHPI at 0.05 mM resulted in particles of similar size to HPI (190.37±2.89 nm, P-value= 0.8911). Interestingly, the size increased tremendously with the increase of HSE concentrations (1840.67±102.3; 2908.33±45.61 and 7807.33±570.62 nm for dHPI+HSE: 0.125;0.25; and 0.5 mM, respectively). dHPI+C resulted in complexes with a size similar to HPI at all tested concentrations (p < 0.05). HPI showed a PDI of 0.40±0.01 which increased upon dephenolisation (dHPI) 0.64±0.06) and then decreased to the initial PDI after the addition of catechin (dHPI+C) at all concentrations (p < 0.05) (Figure 4.2a). The lowest PDI was reached by dHPI+HSE at the concentration of 0.25 and 0.5 mM of HSE, respectively: 0.18±0.04 and 0.21±0.00).

All samples showed net negative surface charges at pH 7.4, as indicated by their ζ -potentials, with no significant differences (avg. \approx -9.84 mV) except for dHPI+HSE (0.5) which showed higher absolute charge than the other samples (-12.56 ± 1.23 mV) (Figure 4.2b).

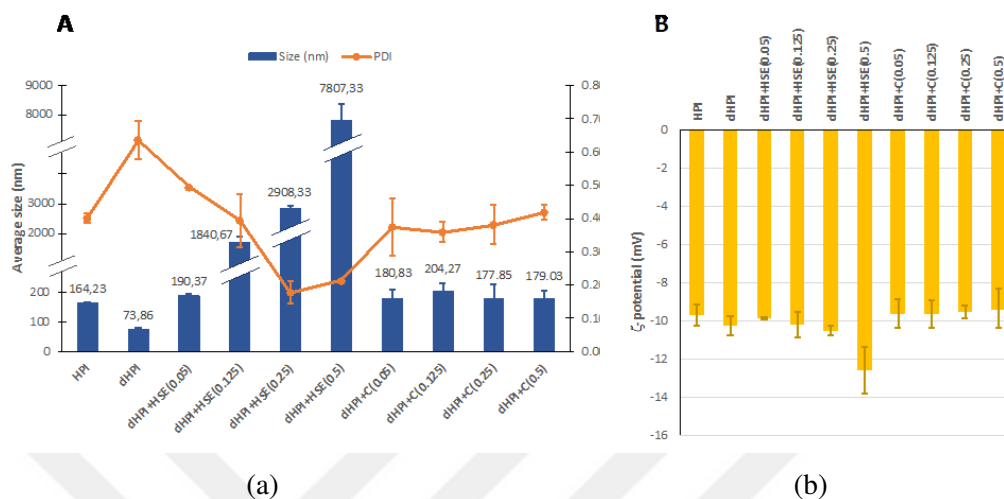


Figure 4.2 : DLS results of hazelnut protein isolates (HPI), dephenolized HPI (dHPI), and dHPI-HSE/Catechin complexes at different concentrations of polyphenols (mM). A: Average size and polydispersity index (PDI). B: ζ -potential.

With the increase in HSE concentration, polyphenols may function as bridging agents between protein molecules, leading to the creation of greater protein-polyphenol complexes (Su et al., 2018; He et al., 2009). However, catechin did not increase the size of HPI with the same significance as HSE even though it was the main component later. This could be ascribed to the presence of other polyphenols with larger molecular sizes than catechin in the extract (e.g. GCG, EGC, EGCG, phlorizin, Q3R, QUE shown in Table 4.6). Indeed, it has been reported that only phenolic compounds with sufficient size are able to interact with more than one site on the proteins, which may form cross-links between distant proteins, in what is called the “multidentate” mechanism of polyphenol-protein interaction leading to the aggregation of the proteins (Bin Bao, 2018). In contrast, catechin, a relatively small molecule, would form a layer around the proteins without being able to link between them in the “monodentate” mechanism. Similarly, Dai et al. (2022) reported that the saturating level of SPI and catechin binding occurred when the catechin concentration rose over a specific point. Since

there was more catechin than SPI's binding sites could accommodate, the complex's particle size was no longer raised.

The precipitation of these samples evidenced the aggregation of HPI+HSE samples after storage (supplementary data 1). It is quite predictable for proteins to have a negative net charge in a solution with pH (7.4) above their isoelectric point (pI = 4.5) (Ghribi et al., 2015). The slight increase in the surface charge of dHPI+HSE at the highest concentration of skin extracts could be conferred by these later due to the eventual saturation of protein particles with polyphenols (Ghribi et al., 2015). Proteins and peptides need to have relatively high absolute ζ -potential in order to avoid their natural tendency to aggregate in the aqueous environment (Mohan et al., 2015). This, together with the DLS results of the dHPI alone, strengthens the assumption that dHPI+HSE aggregated because of the presence of polyphenols, not due to the pH of the medium or an eventual low net charge of the proteins. Bulkier phenolics in the extract have more bonding points (-OH groups) and are more flexible forms (gallolated), resulting in more intense interactions (Jakobek, 2015). Bulkier phenolics in the extract have more bonding points (-OH groups) and are more flexible forms (gallolated), resulting in more intense interactions (Jakobek, 2015), which may cause some charged groups (amino acids) buried inside the protein, and these groups couldn't contribute surface charge anymore.

4.3.3 Fluorescence quenching

Changes in the intrinsic fluorescence intensities (FI) of dHPI in the presence of an increasing concentration of HSE are shown in Table 4.3.

A broad and slightly shouldered peak was observed in the hazelnut protein itself, independent of phenol. This type of fluorescence intensity peak means the presence of a high amount of tyrosine (Tyr) amino acid in addition to the tryptophan (Trp). When the amino acid composition of the HPI was controlled, the concentration of Tyr and Trp were calculated as around 19.9 mg/g-protein and 25.3 mg/g-protein, respectively.

The fluorescence emission of the proteins is dominated by Trp, which absorbs at the longest wavelength. In the presence of Trp, although there are phenylalanine (Phen)

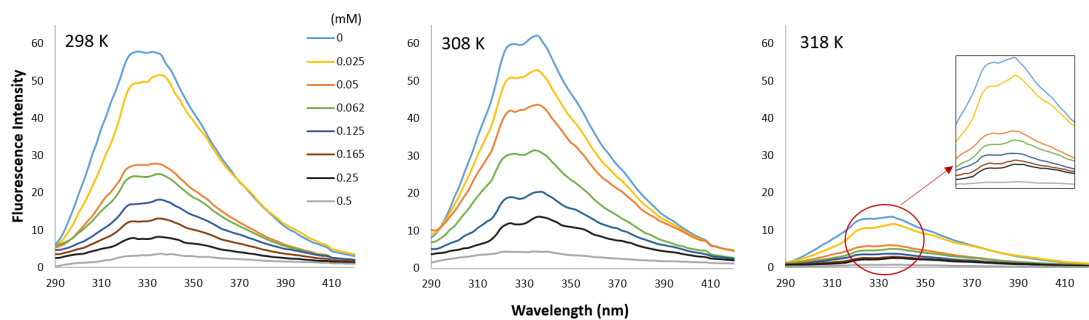


Figure 4.3 : Fluorescence emission spectra (at λ_{ex} 280 nm) of dHPI HSE.complex at 298 (a), 308 (b), and 318 K (c) in phosphate buffer solution at pH 7 with an increase in HSE concentration (0-0.5 mM). Each curve represents a triplicate assay after correction for phenol extract fluorescence.

and Tyr amino acids in the protein, the energy they absorb is mainly transferred to Trp. Protein fluorescence is generally excited at 280 nm, but Phen displays a structured emission with a maximum near 282 nm. Therefore, Phen, having a very small quantum yield, was not excited as in this present study. The emission maximum of Tyr and Trp in water occurs at 303 nm and 350 nm, respectively. Thus, in Figure 4.3, the observed emission peaks were due to the absorption of both Tyr and Trp at 280 nm. On the other hand, resonance energy transfers repeatedly occur from Tyr to Trp, so only a minor contribution of Try to the emission of most proteins can be observed.

In order to display the emission of Trp alone, the fluorescence intensity of the same samples was also excited at 295 nm, where the absorption is primarily due to Trp, and no excitation of Tyr exists. In Figure 4.4, the fluorescence intensity of dHPI obtained at $\lambda_{ex} = 295 \text{ nm}$ was much lower than 280 because only the Trp residues were excited at this wavelength with a lower quantum yield. This decreased fluorescence intensity at 295 nm was another indicator of the presence of Tyr in terms of the contribution of Tyr to the higher fluorescence intensity at 280 nm.

There was a continuous decrease in the fluorescence intensity of HPI when the phenol concentration increased from zero to 0.5 mM at all temperature conditions. This means that a fluorescence quenching of hazelnut proteins is induced by phenolic extracts. Fluorescence quenching is the decrease of the quantum yield of fluorescence from a fluorophore induced by a variety of molecular interactions with quencher molecules (Papadopoulou et al., 2005). For quenching, molecular contact is required between

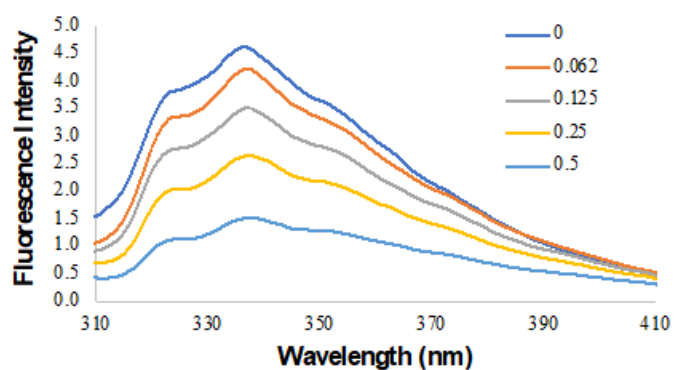


Figure 4.4 : Fluorescence intensity results of dHPI at the excitation wavelength of 295 nm with an increase in HSE concentration (0-0.5 mM) in PBS at pH 7 and room temperature.

the fluorophore and the quencher. Due to molecular interaction or the change in the solvent composition, the excitation and emission behaviour of fluorophore can be changed. For instance, Tyr is relatively insensitive to solvent polarity, while Trp is highly dependent upon polarity and/or the local environment (Lakowicz, 2006). The reason is the uniquely complex fluorophore of Trp with two nearby isoenergetic transitions; however, emission from tyrosine appears to occur from a single electronic state.

The quenching ability of HSE (0-0.5 mM) on the fluorescence emission of native hazelnut protein was investigated at different temperatures (298, 308, 318 K) (Table 4.3). The intensity of the fluorescence dropped considerably as the HSE concentration was increased at all temperatures.

When the effect of temperature on the changes in fluorescence intensity was compared in the presence of phenol extracts, no significant change was observed between 298 and 308 K (Figure 4.3). However, the further increase in temperature to 318 K resulted in a rapid decrease in protein fluorescence intensity indicating the hazelnut protein is thermally unstable at this temperature.

Although the phenol induced a decrease in fluorescence intensity, λ_{max} for HPI was measured at 340 nm, which is the expected λ_{max} for the indole group of Trp alone (Figure 4.4). Moreover, linear Stern-Volmer curves were observed at all temperature

conditions (Figure 4.5a). This usually has a meaning that all the main fluorescing residues of the protein are equally accessible to the solvent. If two fluorophore populations are present, and one class is not accessible to the quencher, then the Stern-Volmer plots deviate from linearity toward the x-axis.

The fraction of accessible fluorescence was also calculated from the Equation (9):

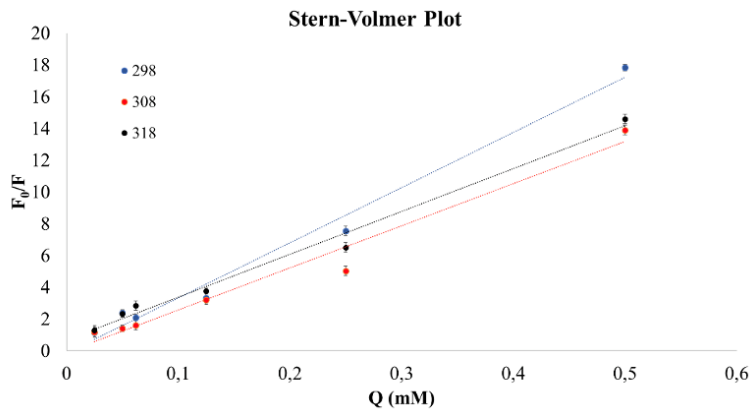
$$\frac{F_0}{\Delta F} = \frac{F_0}{F_0 - F} = \frac{1}{f_a K_a} \frac{1}{[Q]} + \frac{1}{f_a} \quad (4.9)$$

$F_0/\Delta F$ was found linear to $1/[Q]$ so that the slope gave the $1/(f_a K_a)$, and from the intercept to ordinate, $1/f_a$ was found. Then the effective quenching constant for the accessible fluorophore (K_a) was calculated as the ratio of $1/f_a$ to $1/(f_a K_a)$. The linear lines intersect the y-axis at a value of around 1, meaning that all the fluorescence is due to quenchable Trp. This data, therefore, conforms to the assumptions from the Stern-Volmer curves that all the main fluorescing tryptophan residues are quenchable and no others buried within the protein or unavailable to the quencher are expected.

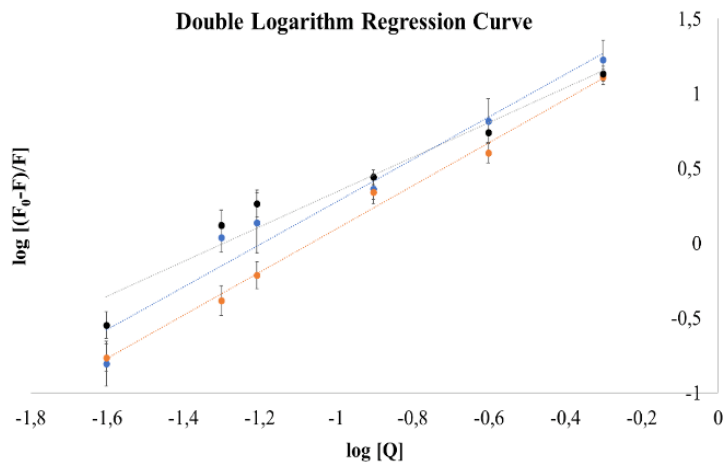
4.3.3.1 Stern-Volmer plot

Stern-Volmer plots were obtained in Figure 4.5a by plotting the F and F_0 values versus the phenolic extract concentration $[Q]$ at different temperatures. The linearity of the Stern-Volmer plot indicates that there is only one quenching mechanism, which can be static or dynamic. The maximum dynamic bimolecular quenching constant (K_q) is $2 \times 10^{10} \text{ M}^{-1} \text{ s}^{-1}$, and the major quenching process is static if the K_q values are higher than this value (Cao and Xiong, 2017; Chen et al., 2019). K_q values of dHPI+HSE complexes were calculated as 34.716, 26.548, and 27.001 at 298, 308, and 318 K, respectively, which indicated the major quenching mechanism was static.

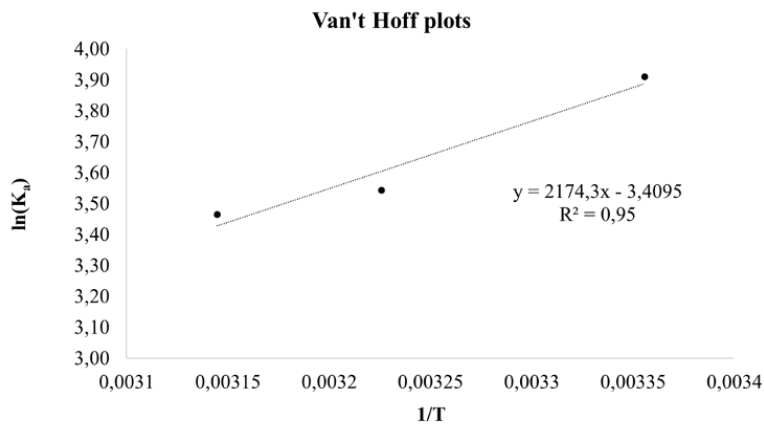
A non-fluorescent ground-state complex is formed between the fluorophore and quencher via static quenching (Lakowicz, 2006). The Stern-Volmer constant (K_{sv}) was lower at higher temperatures. The decrease in K_{sv} values as the temperature increases is observed in the case of the static quenching mechanism (Zhang et al., 2018; Al-Shabib et al., 2020) due to its negative effect on the stability of complex formation (Jia et al., 2017; Liu et al., 2017a; Wu et al., 2011).



(a)



(b)



(c)

Figure 4.5 : Stern-Volmer plots (a). the double logarithm regression curves (b). and Van't Hoff plots (c) for dHPI-HSE mixtures at different temperatures (blue: 298 K; red: 308 K; black: 318 K) to calculate the number of binding sites (n). binding constant (K_A). and thermodynamic parameters.

Relatively high values were obtained from the K_{sv} values determined for β -lactoglobulin/ α -casein/ β -casein catechin/derivatives complexes in the literature (Hasni et al., 2011; Kanakis et al., 2011). A fluorophore buried in a macromolecule is usually inaccessible to water-soluble quenchers, so the value of K is low. Larger values of K are found if the fluorophore is free in solution or on the surface of a biomolecule (Lakowicz, 2006). It is known that β -lactoglobulin has one Trp residue on the surface of the protein molecule and is accessible to the solvent (Yilmaz et al., 2021). Moreover, it has been reported in some studies that gallolated forms have higher binding affinity compared to catechin (Hasni et al., 2011; Kanakis et al., 2011). Relatively larger phenolic compounds provide two or more aromatic rings and hydroxyl groups for interactions. It was also reported that phenols with gallolated monomers (epigallocatechin gallate-EGCG) have a higher affinity for whey protein or β -lactoglobulin binding than non-gallate ones (Gallic acid, chlorogenic acid, ferulic acid) (Jia et al., 2017; Cao and Xiong, 2017). The molecular weight of phenols, their structural flexibility, and the number of OH groups in their structures have greatly affected the formation of multiple bonds, as well as an increase in hydrophobicity with size (Jakobek, 2015). Many of the phenolics found in HSE were in gallolated or glycosylated form, as well as a mixture of these. This explains the high binding affinity in this study.

The number of binding sites (n) was calculated from the double-logarithm regression curve (Figure 4.5b). The n values at all temperature conditions were greater than 1 as a result of intermolecular cross-linking between proteins at all temperatures indicating that at least one phenol molecule independently interacted with the protein and while the other phenolic compound may have formed a bridge between the proteins. In addition, The decrease in K_a values with temperature indicates that the protein-phenolic interaction is exothermic, and the stability of the complex decreases (Acharya et al., 2013).

4.3.3.2 Thermodynamic parameters

Thermodynamic parameters were calculated from Van't Hoff plot (Figure 4.5c) and shown in Table 4.3. Since $\Delta H < 0$ and $\Delta S < 0$, hydrogen bonding and van der

Waals forces were the main interaction mechanism between the dHPI and HSE. Since $\Delta H > \Delta S$, dHPI+HSE interaction was induced primarily by enthalpy (Tang et al., 2016). Negative entropy (ΔS) resulted in an unfavourable increase in molecular order upon complex formation. The decrease in conformational mobility in the protein, as well as the exposure of hydrophobic surfaces to the solvent, can both contribute to unfavourable entropy (Petrucci et al., 2011). Negative enthalpy (ΔH) implies that the enthalpy of the protein-phenolic complex is lower than that of the reactants (protein and phenolics), which relates to (1) the increase in bond enthalpy, the number of the bonds, and bond strength, and (2) immobilization of the sufficiently counteracted ligand by liberation of bound water (Li and Wang, 2015). Besides, hydrogen bonding is an exothermic event (Petrucci et al., 2011).

Table 4.3 : Stern-Volmer constants and thermodynamic parameters of dHPI-HSE complex at different temperatures.

Temperature (K)	Stern-Volmer Constants			Double-Log Plot			ΔG (kJ mol ⁻¹)	ΔH (J mol ⁻¹)	ΔS (J K ⁻¹ mol ⁻¹)
	K _{sv} (1014 L mol ⁻¹)	K _q (106 L mol ⁻¹)	R ²	K _A (105 L mol ⁻¹)	n	R ²			
298	34.696	34.696	0.986	49.9114	1.422	0.952	-9671.72	-18944.28	-31.12
308	26.548	26.548	0.973	345,939	1.443	0.993	-9298.33		
318	27.001	27.001	0.988	319,890	1.162	0.949	-9049.4		

Favourable enthalpy contributions overcome unfavorable entropic contributions, and the reaction depends on temperature. Eventually, molecular interactions must have been strong enough as a result of complex formation to cover the loss of entropy. As temperature rises, hydrophobic interactions grow more powerful, and hydrogen bonds become weaker. A reduction in the binding constant with rising temperature points to H-bonding as the main force (Acharya et al., 2013).

ΔG of all dHPI+HSE complexation was negative, and the interaction was spontaneous. Generally, protein-phenolic interactions were reported as spontaneous reactions ($\Delta G < 0$). On the other hand, mainly hydrogen bonding and van der Waals forces were responsible for human serum albumin (Li and Wang, 2015) and bovine serum albumin (Li and Hao, 2015) catechin interaction in the literature.

4.3.4 Fourier Transform Infrared (FTIR) spectroscopy

To investigate further whether any structural change of dHPI was associated with the interaction with phenolic extracts, FTIR spectra of dHPIs were recorded with and without the addition of HSE (0.05, 0.125, and 0.25 mM) and catechin (0.125 mM). There are basic FTIR spectrum regions specific to each sample: (1) the functional group region between 1500 and 4000 cm^{-1} , and (2) the fingerprint region between 400 and 1500 cm^{-1} . The fingerprint region is unique for each protein. The characteristics of the side chains, the force field's specifics, and hydrogen bonding all play a role in the complexity of the fingerprint region bands. As a result, structural information from these bands is limited. In this region (Table 4.3), a peak was observed at 1462 cm^{-1} originating from CH_2 bending vibrations and 1396 cm^{-1} originating from CH_3 bending vibrations (Dogan et al., 2007).

Nine distinctive IR bands are produced by the amide groups of the protein backbone (Amides A and B and amides I–VII) and provide important information about the secondary structure and conformation of the protein backbone. The two most noticeable vibrational bands of the protein backbone are amides I and II (Ferraro et al., 2015). The absorbance of dHPI had characteristic amide I band at 1631 cm^{-1} (C=O stretching vibrations of peptide linkages), amide II at 1522 cm^{-1} (C-N stretching, 40% and N-H bending, 60% of amino acids), and a wide amide A band at 3273 cm^{-1} (tensile vibration of intermolecular hydrogen bonding between O-H and N-H stretching occurring in the hydrogen bonds and intermolecular H bonding) and amide B at 2922 cm^{-1} (CH_2 asymmetric stretch) and 2855 cm^{-1} (CH_2 symmetric stretch) (Dai et al., 2022; Dogan et al., 2007) (Figure 4.6).

No new bands were formed with dHPI HSE or catechin complex formation. Thus, the protein-phenolic complex formation was mostly a physical process, and no covalent

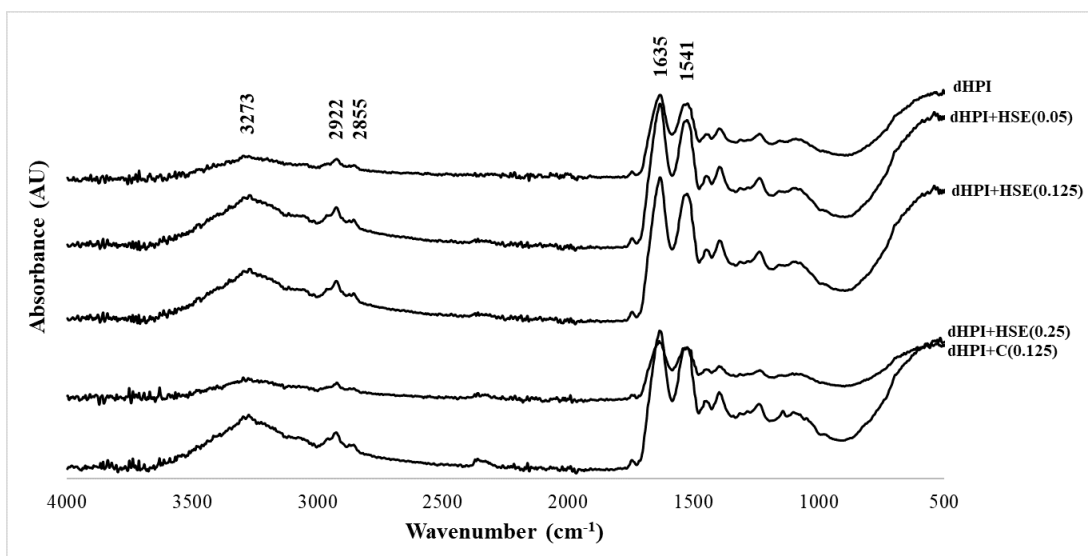


Figure 4.6 : FTIR spectra of dHPI. dHPI-HSE complex and dHPI-catechin complex. dHPI: dephenolyzed protein isolate; dHPI+C: hazelnut meal protein isolate-catechin solution; dHPI+HSE: hazelnut meal protein isolate-hazelnut skin extract solution.

bonds were created between the matrix and the core as a result (Han et al., 2021). Any change in spectral peak intensity and position implies a constitutive change in the protein (Yan et al., 2021). dHPI HSE or catechin complexes caused differences in all amide bands of native hazelnut protein. The amide A band of dHPI HSE complexes was slightly shifted to 3276 cm^{-1} , suggesting that the hydrogen bonds were increased, while dHPI catechin complex had any shifts.

The amide B band is attributed to the C–H tensile vibration of the CH_3 and CH_2 groups of protein (Dai et al., 2022). The amide B band of all dHPI-phenolic complexes was shifted to 2925 cm^{-1} , suggesting that hydrophobic interactions took place.

Any change in the amide I band ($1600\text{--}1700\text{ cm}^{-1}$) and amide II bands ($1500\text{--}1600\text{ cm}^{-1}$) relates to the secondary structure of the protein (Jiang et al., 2018). Amide I and II band was red-shifted from $1631/1522$ to $1634/1525$, $1637/1524$, $1637/1524$ and $1635/1525\text{ cm}^{-1}$ for dHPI+HSE(0.05), dHPI+HSE (0.125), dHPI+ HSE(0.25) or dHPI+C(0.125) complexes, respectively. Hence, the secondary structure of hazelnut proteins was altered upon extract or catechin complexation (Figure 4.6). The reason for the increase in the intensity of the amide I and amide II bands was related to the increase of the protein C=O, C-N, and N-H groups with hydrogen and hydrophobic interactions (Hasni et al., 2011).

The secondary structure content of hazelnut protein is given in Table 4.4. In the presence of the lowest concentration of phenolic extract (0.05 mM), the distinct decrease in β -turn was supported by transition to α -helix as with the dHPI catechin (0.125) complex. A significant increase was observed in the number of the random coil as the phenolic concentration increased compared to the native dHPI. At the highest phenolic concentration (0.25 mM), there was a slight decrease in the α -helix and β -sheet structure, although the number of random coil increased. The effect of phenolic concentration was observed by the regular or irregular structure (Table 4.4). In the presence of phenolic at the lowest concentration (0.25 mM), regular structures (α -helix and β -sheet) increase, and the protein became more stable and rigid. The sum of the regular structures of the native protein was interrupted, and a more unfolded protein was formed via protein-phenolic interaction at medium at higher phenolic extract concentration. Similarly, Hasni et al. (2011) emphasized that the secondary structure of α - and β -casein tea polyphenol (catechin, epicatechin, epigallocatechin, and epigallocatechin gallate) complexes changed depending on the phenolic concentration. At the same time, polyphenols at higher concentrations caused a decrease in the α -helix structure, while it increased at lower concentrations.

Table 4.4 : Intensity values of major FTIR bands and Secondary structure content (%) of dHPI-phenolic complexes from FTIR data.

	dHPI	dHPI+HSE (0.05)	dHPI+HSE (0.125)	dHPI+HSE (0.25)	dHPI+Catechin (0.125)
α -helix	17.92	32.88	28.78	26.76	36.88
β -sheet	60.78	54.10	49.29	28.23	54.62
β -turn	17.38	1.78	24.10	11.79	1.63
Random Coil	3.92	11.23	11.44	33.22	6.87
Regular Structure	78.70	86.99	78.07	55.00	91.50
Irregular Structure	21.30	13.01	35.54	45.00	8.50

dHPI: dephenolyzed protein isolate; dHPI+C: dephenolyzed hazelnut meal protein isolate-catechin solution; dHPI+HSE: dephenolyzed hazelnut meal protein isolate-hazelnut skin extract solution.

The protein/phenol concentration in the medium is of great importance for the protein-phenolic interaction. At low phenolic concentration, the interaction regions of the proteins do not reach saturation, and intermolecular interactions occur due to the interaction of phenolics (multisite ligand) with several regions of the protein

(multidentate mechanism). For this mechanism, phenolics must be large enough to form bridges between proteins. Thence, the irregular structure gradually increased in the presence of phenolic extract at 0.05 and 0.125 mM concentration via multidentate mechanism. When the phenolic ratio increases, several phenolics interact with one protein (monodentate mechanism) (Bin Bao, 2018). Especially most likely the monodentate mechanism is seen more intensely at higher phenolic extract concentrations because it was very close to the saturation point of the protein-phenolic interaction. Eventually, the more irregular structure of the protein was altered upon phenolic binding, so the protein was more flexible. Similar to this study, changes in the amide I band density of α -/ β -casein or β -lactoglobulin tea phenolic (catechin, epicatechin, epigallocatechin, and epigallocatechin gallate) complexes (Hasni et al., 2011; Kanakis et al., 2011) and rice bran protein catechin complexes (Li et al., 2020) were observed depending on the phenolic concentration, and the amide I band intensity increased at low phenol concentration and decreased as the concentration increased. Moreover, it was also reported that conformational changes were more noticeable for epigallocatechin and epigallocatechin gallate compared to catechin and epicatechin since the bulkier and larger phenolics provide more perturbation (Hasni et al., 2011; Kanakis et al., 2011). As a result, phenolics in the HSE at a lower concentration (0.05 mM) showed a similar effect to catechin (0.25 mM) since they contain glycosylated or gallolated forms of catechin.

4.3.5 Effect of polyphenols on hazelnut protein digestibility

The rate of hydrolysis of hazelnut proteins by pancreatin was fast during the first 1 h, then gradually decreased to become almost stagnant between 105 and 120 minutes, a typical proteolysis trend (Figure 4.7). Non-dephenolised proteins showed a higher digestibility in comparison with all dephenolised samples during all the reaction times ($p < 0.05$) and reached a maximum of 32.55 ± 1.12 % after 2 h. Within the dephenolised samples, the degree of hydrolysis was slightly reduced by the presence of HSE or catechin but progressively retrieved with time till no significant difference was observed after 120 min ($DH \approx 25\%$). Interestingly, the addition of HSE or catechin

to the dephenolised hazelnut proteins did not restore the degree of hydrolysis achieved by non-dephenolised proteins.

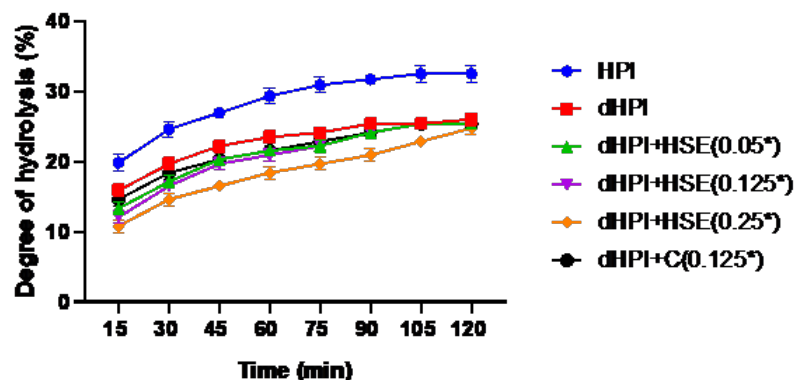


Figure 4.7 : Degree of hydrolysis of hazelnut protein isolates (HPI), dephenolized HPI (dHPI), and dHPI-HSE/Catechin (C) complexes at different concentrations of polyphenols (mM). *The actual concentrations are 16.67 times higher but protein/polyphenol ratios are kept the same as what was used in the other parts of the study.

Although polyphenols may have mostly a negative effect on the digestibility of proteins, literature data showed a quite unpredictable effect of polyphenols on the enzymatic digestibility of proteins (Velickovic and Stanic-Vucinic, 2018). Ni et al. (2020) have shown a positive impact of salal fruit phenolic extracts on the degree of hydrolysis of whey protein by Flavourzyme®. On the contrary, Wang and Tang (2012) reported an enhancement in the degree of hydrolysis, by trypsin, of buckwheat protein isolates upon dephenolisation. The enhancement of hydrolysis by the presence of polyphenols may be ascribed to an eventual partial unfolding of the proteins caused by polyphenols, facilitating the access of the protease to catalytic sites in non-dephenolised hazelnut protein isolates and thus may have enhanced their hydrolysis (Ni et al., 2020). This hypothesis is also supported by the decrease in the size of the dHP sample (Figure 4.2), which could be due to an eventual folding upon dephenolisation, making some catalytic sites inaccessible inside the three-dimensional structure of the protein. The fact that the addition of polyphenols did not improve the digestibility of the proteins implies that what may be happened upon dephenolisation was irreversible. Finally, the recovery of the degree of hydrolysis in the dHPI+HSE and dHPI+C after 120 min in comparison with dHPI supports the fact that the interactions

between dHPI and polyphenols were non-covalent and thus reversible, which is in total correlation with the fluorescence quenching study (section 3.2).

4.3.6 Simulated in vitro gastrointestinal digestion

In order to determine the effect of in vitro gastrointestinal digestion on the phenolic extract and protein-phenolic solutions, total phenolic content and total antioxidant capacities were measured, and individual phenolic compounds were identified for each gastrointestinal digestion phase. The results vary in both extract and protein-phenolic solutions at each stage of in vitro gastrointestinal digestion due to their solubility at acidic or alkaline pH and interactions with enzymes.

4.3.6.1 Spectrophotometric analyses

The changes in the total phenolic contents (TPC) of samples and recovery indexes (RI) of phenolic compounds at each digestion phase are shown in Table 4.5. At the initial phase, the TPC of phenolic solution systems was determined in the following order: extract solutions > protein-phenolic solutions. The HSE solutions followed a similar trend as the initial phase in the gastric phase, whereas the TPCs of the c solutions were found as protein-phenolic solution extract solutions. The TPCs of the extract solutions were higher in the intestinal phase than the TPCs of the protein-phenolic solutions, as they were in the initial phase.

TPCs of C and dHPI+C showed a significant increase in the intestinal phase compared with the initial phase, following a decreasing trend after gastric digestion. Similar trends were observed in the gastric and intestinal phases of HSE and dHPI+HSE samples, apart from the intestinal phase of HSE. After intestinal digestion, 136.1% and 78.2% of the phenolic compounds were present in the intestinal fraction for C and HSE extract solutions, respectively. However, 98.4% and 68.4% of these compounds were available in the dHPI+C and dHPI+HSE solutions, respectively.

In order to determine the effect of in vitro gastrointestinal digestion on total antioxidant capacity, DPPH and CUPRAC assays were performed. The total antioxidant capacities of initial solutions and gastric and intestinal phases are given in Table 4.5. The total antioxidant capacities of C and HSE extract solutions throughout the digestive

tract varied between 94.04 ± 5.9 to 143 ± 0.5 mg TE/g extract and 128.71 ± 0.4 to 181.01 ± 11.9 mg TE/g extract, respectively, whereas the total antioxidant capacities of dHPI+C and dHPI+HSE protein-phenolic solutions ranged from 128.71 ± 0.4 to 181.01 ± 11.9 mg TE/g extract and 62.85 ± 7 and 106.75 ± 10.6 mg TE/g extract, respectively throughout the gastrointestinal tract according to the DPPH method. The DPPH values of the extract solutions decreased from the initial phase to the intestinal phase. In contrast, the DPPH values of the protein-phenolic solutions increased in the intestinal phase following the decrease in the gastric phase.

The total antioxidant capacities of C and HSE extract solutions across the gastrointestinal system changed from 1067.58 ± 23 to 2285.63 ± 90.5 mg TE/g extract and 321.2 ± 22.7 to 705.01 ± 8.9 mg TE/g extract, respectively, on the other hand, the total antioxidant capacities of dHPI+C and dHPI+HSE protein-phenolic solutions varied between 1849.34 ± 35.7 to 2174.95 ± 195.2 mg TE/g extract and 364.46 ± 19.4 and 763.34 ± 8.1 mg TE/g extract, respectively throughout the digestive tract according to the CUPRAC method. The CUPRAC values of the extract solutions decreased from the initial phase to the intestinal phase ($p < 0.05$). In contrast, the DPPH values of the protein-phenolic solutions increased in the intestinal phase following the reduction in the gastric phase ($p < 0.05$). In addition, the CUPRAC values of the extract solutions showed a significant increase in the intestinal phase compared with the initial phase, following a decreasing trend after gastric digestion ($p < 0.05$). Similar trends were found in the dHPI+HSE protein-phenolic solution ($p < 0.05$).

4.3.6.2 HPLC-DAD analysis of phenolic compounds

The major phenolic compounds of initial and digested extract solutions and protein-phenolic solutions were detected by HPLC-DAD analysis. Comparisons of the phenolic profiles of samples are shown in Table 4.6. Up to 10 individual phenolic compounds were identified in the samples. Since the phenolic compounds identified in the HSE are mainly composed of catechins, the catechin standard was used as the control group in this study.

In the analyzed HSE initial extract solutions, gallic acid (GA) and protocatechuic acid (PCA) were detected as the hydroxybenzoic acids; gallic acid gallate (GAG),

Table 4.5 : Total phenolic content (TPC), recovery index of phenolic compounds (RI) and antioxidant capacities (DPPH and CUPRAC methods) in gastrointestinal digestion phases.

		Initial Phase			
		TPC	RI	DPPH	CUPRAC
Exact Solution	C	1040.37±61.5 ^{ab}	100.0	143±0.5 ^{aA}	1221.99±66.5 ^{bB}
	HSE	714.39±54.3 ^{cA}	100.0	142.61±0.1 ^{aA}	705.01±8.9 ^{cA}
Protein-Phenolic Solution	HPI+C	982.11±66.6 ^{bA}	94.4	130.6±2.1 ^{bB}	1945.56±54.5 ^{aB}
	HSE+dHPI	317.88±26.4 ^{dB}	44.5	104.61±12.4 ^{cA}	522.54±4.4 ^{dB}
		Gastric Phase			
		TPC	RI	DPPH	CUPRAC
Exact Solution	C	760.68±3.3 ^{bC}	73.1	131.38±0.9 ^{aB}	1067.58±23.2 ^{bC}
	HSE	357.78±22.4 ^{cC}	50.1	128.52±1.3 ^{aB}	321.2±22.7 ^{cC}
Protein-Phenolic Solution	HPI+C	891.77±32.1 ^{aB}	85.7	128.71±0.4 ^{aB}	2174.95±195.2 ^{aA}
	HSE+dHPI	256.5±16.7 ^{dC}	35.9	62.85±7 ^{bB}	364.46±19.4 ^{cC}
		Intestinal Phase			
		TPC	RI	DPPH	CUPRAC
Exact Solution	C	1416.09±6.8 ^{aA}	136.1	94.04±5.9 ^{bC}	2285.63±90.5 ^{aA}
	HSE	559±33.5 ^{cB}	78.2	105.84±7.7 ^{bC}	638.84±26.1 ^{cB}
Protein-Phenolic Solution	HPI+C	1024.03±63.9 ^{bA}	98.4	181.01±11.9 ^{aA}	1849.34±35.7 ^{bB}
	HSE+dHPI	488.64±29.4 ^{dA}	68.4	106.75±10.6 ^{bA}	763.34±8.1 ^{cA}

a-d Small letters show the variation among initial, gastric, and intestinal phases of the same sample ($p < 0.05$). A-C Capital letters show the variation between samples at the same phase ($p < 0.05$). TPC: total phenolic compounds, mg GAE/g extract; RI: recovery index of phenolic compounds, %; DPPH: antioxidant capacity by DPPH, mg trolox equivalent/g extract; CUPRAC: antioxidant capacity by CUPRAC, mg trolox equivalent/g extract. C: catechin solution; HSE: hazelnut skin extract solution; DHPI+C: hazelnut meal protein-catechin solution; HSE+dHPI: hazelnut meal protein-hazelnut skin extract solution. The analyses were performed in triplicate. The results are given as mean \pm standard deviation.

(-)-epigallocatechin (EGC), catechin (C), epicatechin (EC) and (-)-epigallocatechin gallate (EGCG) were identified as the flavanols; quercetin 3-O-rhamnoside (Q3R) and quercetin (QUE) were detected as flavonols, and phlorizin was identified as chalcone. On the other hand, no phenolic compounds were detected in the initial phases of protein-phenolic solutions of both dHPI+C and dHPI+HSE. A lower amount of catechin was observed in the C solution's gastric phase compared to the initial amount ($p < 0.05$). Besides, the amount of C that reappeared in the gastric phase of the dHPI+C solution was significantly lower than the amount determined in the gastric phase of the C solution ($p < 0.05$). The amounts of detected phenolic compounds other than GA and GCG decreased in the HSE solutions' gastric phase compared to their initial levels ($p < 0.05$).

Table 4.6 : Phenolic profiles of initial gastric and intestinal phases of solutions after in vitro GI digestion.

Compounds mg/g	C			dHPI+C		
	Initial	Gastric	Intestinal	Initial	Gastric	Intestinal
Galic acid	nd	nd	nd	nd	nd	nd
Protocatechuic acid	nd	nd	nd	nd	nd	nd
Gallocatechin	nd	nd	10.43±0.6	nd	nd	32.1±2.6
(-)-Epigallocatechin gallate	nd	nd	18.45±1.6	nd	nd	14.22±1.2
Catechin	2417.25±102.4	2144.43±87.3	917.82±23.9	nd	1837.46±64.9	885.8±17.4
Epicatechin	nd	nd	22.94±2.5	nd	nd	151.54±8.4
(-)-Epigallocatechin gallate	nd	nd	11.11±0.2	nd	nd	nd
Phlorizin	nd	nd	nd	nd	nd	nd
quercetin 3-O-rhamnoside	nd	nd	nd	nd	nd	nd
Quercetin	nd	nd	nd	nd	nd	nd
Compounds mg/g	HSE			dHPI+HSE		
	Initial	Gastric	Intestinal	Initial	Gastric	Intestinal
Galic acid	1.02±0.3	1.05±0.2	1.12±0.1	nd	0.88±0.0	1.5±0.1
Protocatechuic acid	1.04±0.7	0.8±0.0	1.01±0.1	nd	0.84±0.0	0.62±0.0
Gallocatechin	0.23±0.0	0.87±0.0	9.9±0.6	nd	0.32±0.0	29.65±2.8
(-)-Epigallocatechin gallate	2.42±0.2	2.2±0.1	0.58±0.0	nd	1.52±0.1	4.46±0.3
Catechin	4.01±0.8	2.56±0.2	4.85±0.3	nd	2.8±0.3	1.94±0.1
Epicatechin	2.03±0.1	1.31±0.1	2.39±0.2	nd	0.98±0.0	3.2±0.2
(-)-Epigallocatechin gallate	2.08±0.3	0.63±0.0	8.27±0.6	nd	0.45±0.0	41.81±2.6
Phlorizin	0.44±0.0	0.33±0.0	nd	nd	0.27±0.0	0.64±0.0
quercetin 3-O-rhamnoside	0.98±0.0	0.78±0.0	0.67±0.0	nd	0.51±0.0	0.85±0.0
Quercetin	0.1±0.0	nd	nd	nd	nd	nd

a-c Small letters show the variation of the same phenolic compound among initial, gastric, and intestinal phase of the same sample ($p < 0.05$).

Furthermore, QUE was found to be below the limit of detection for the gastric and intestinal phases of HSE solutions. The phenolic compounds identified in the HSE solution, except for QUE, were re-detected in the gastric phase of the dHPI+HSE solution. There were significant reductions in the quantities of the phenolic compounds, except for PCA and C, between the gastric phases of HSE and dHPI+HSE ($p < 0.05$). C was metabolized with digestion, and GCG, EGC, C, and EC were detected in the intestinal phases of C and C + dHPI solutions, whereas EGCG was only determined in the C solution. GC and EC were found to be significantly higher amounts in the intestinal phases of dHPI+C solution than in C solution ($p < 0.05$). On the other hand, GA, GCG, EGC, EC and EGCG, and Q3R had better accessibility in the intestinal phase of the dHPI+HSE solution than in the intestinal phase of the HSE solution after digestion ($p < 0.05$).

To the best of our knowledge, there is no study investigating the changes of phenolic compounds of hazelnut skin during in-vitro gastrointestinal digestion, while there is many research in the literature examining their phenolic profile and antioxidant activities. However, since tea and green tea principally contain high amounts of

catechins, the bioaccessibility of tea catechins and the effect of protein-catechins interactions on their digestibility is trend topic research areas.

It is reasonable to conclude from the fact that the inability to detect phenolic compounds from the initial phases of dHPI+C and dHPI+HSE complexes might be explained that the lower (or non) the recovery, the more catechins and other polyphenols bind to proteins. These findings are in accordance with prior research on tea polyphenols and milk proteins (Green et al., 2007; Hasni et al., 2011). However, during the simulated gastric digestion, these bound polyphenols and catechins were released from polyphenol-protein complexes. The addition of hazelnut meal protein did not affect PCA and C recovery after gastric digestion. GA, GCG, and EGC might be more stable in acidic conditions compared to C, EC, and EGCG, but also acid-catalyzed epimerization of EGCG might occur (Xie et al., 2013).

GCG and EC were more stable after intestinal digestion in dHPI+C complex, while EGC, C, and EGCG were more accessible in C solution. Some studies have also reported that EGC and EGCG are unstable, while EC and ECG are relatively stable (Chen et al., 1998; Zhu et al., 1999). The difference in intestinal stability of these catechins might be attributed to the fact that three adjacent hydroxyl groups in EGC and EGCG at positions 3', 4', and 5' are more susceptible to the formation of semiquinone free radicals at near neutral pH when a proton was donated (Shim et al., 2012). Additionally, strong protein-flavonoid interactions are mediated by the hydrophobic binding of flavonoids with proline-rich regions of intact proteins and peptide fragments. According to the literature, larger polyphenols with a higher number of aromatic rings and hydroxyl groups are more effective in forming complexes with proline-rich peptides. Gallate catechins ECG, GCG, and EGCG have more aromatic and hydroxyl groups than non-gallolated catechins EC and EGC resulting in higher binding activity with proteins. As a result, they become more stable during in-vitro digestion, which explains GCG and EGCG's increased bioaccessibility in HSE when complexed with hazelnut protein (Green et al., 2007; Xie et al., 2013).

4.4 Conclusions

In the presence of hazelnut skin phenolics, quite large complexes were formed depending on the HSE concentration, and catechin formed relatively smaller complexes. This was related to the fact that the phenolics found in hazelnut skin were bulkier and more flexible. Moreover, it was found that the dominant forces in dHPI HSE complex formation were hydrogen bonding and van der Waals forces. The reaction depends on temperature and spontaneous ($\Delta H < 0$; $\Delta S < 0$; $\Delta G < 0$). The interaction of dHPI and HSE caused significant changes in the secondary structure of proteins, which was mainly affected by the phenolic concentration. With the increase of phenolic concentration, the secondary structure of the protein became loosened and protein disordered. This situation most likely increased the flexibility of the protein, especially improving its functional properties. The protein-polyphenol interactions principally had a positive effect on the bioaccessibility of hazelnut skin polyphenols, mainly on the gallolated form of the catechins such as GCG and EGCG. Phenolics and plant based-proteins isolated from natural sources are among the subjects that have been researched in recent years. It is especially important in vegan formulations such as foam-like products (mousse) or emulsions (mayonnaise), where the functional properties of proteins are essential. Furthermore, there is no definite opinion on whether the effects of protein-phenolic interactions on the bioavailability of phenols are positive or negative in their consumption. Therefore, more research on this subject needs to be done and brought to the literature.



5. CONCLUSIONS

5.1 Status and Main Outcomes of This Thesis

5.1.1 Valorisation of hazelnut by-products: current applications and future potential

The valorisation of waste products from the hazelnut industry is expected to have a positive impact on the environment and contribute to the sustainability of this important food sector. The most obvious waste streams to develop into value-added products are hazelnut shells, roasted skins, and defatted meal. It may be possible to increase the value of these products, which may open up new commercial opportunities for farmers and hazelnut processors. There is a considerable amount of work that needs to be done to develop commodity-scale applications of these materials; most applications are currently conducted at the lab-scale. To fully exploit the possibilities of these materials, investments will also be necessary to develop the necessary infrastructure, transportation networks, storage, and commercially-viable applications.

Developing new uses for hazelnut meal and roasted skin might be the easiest to implement since hazelnut is already regarded as a valuable ingredient. The potential health benefits of nuts and their associated compounds are also attractive to consumers. A careful attention to allergen labeling is required as skins and meal are utilized in new applications. A high intake of phenolics may also cause toxicity and antinutritional effects. Due to the natural astringency of phenolics, overconsumption may not be a serious concern. Importantly, as these co-products are derived from whole nuts, rather than isolated meals and skins, they are unlikely to bear FDA-authorized health claims. Further research is needed to validate the health-promoting mechanisms and amount of intake needed to improve human health.

Defatted hazelnut meal and skins of hazelnuts can be used directly as ingredients in foods. However, further processing will make them more valuable as sources of bioactive peptides and phenolics. In order to describe the specific benefits of these isolates, further research is required. Considering the bitter and astringent nature of these co-products, this may be a challenge. Therefore, it is necessary to demonstrate the consumer appeal and sensory acceptability of products containing these new ingredients in order to increase their desirability.

5.1.2 Combined Neutralse-Alcalase protein hydrolysates from hazelnut meal, a potential functional food ingredient

A by-product of the hazelnut oil industry, hazelnut meal, was valorised and used as a source of bioactive peptides with a special focus on their potential anti-obesity and antioxidant properties. Protein hydrolysates were prepared by sequential or individual hydrolysis by Neutralse and Alcalase. In order to improve the hydrolysis and the functional properties of the hydrolysates, microfluidization was applied. The combination of Alcalase-Neutralse hydrolysis achieved the highest DH, inhibited the release of FFA by pancreatic lipase, and free radical scavenging activities. A positive relationship was found between the DH and the ESI of the hydrolysates, while a negative relationship was found between the DH and their EAI. As a result of microfluidization, protein structures became unfolded, resulting in enhanced EAI and FFA inhibition in Alcalase hydrolysates. Protein hydrolysates from hazelnut meal may be a potential anti-obesity and antioxidant food ingredient. Pretreatment of proteins (degree of hydrolysis, etc.) should be optimized according to the intended application of the protein hydrolysates.

5.1.3 Interactions between hazelnut (*Corylus Avellana L.*) protein and phenolics and in vitro gastrointestinal digestibility

The presence of hazelnut skin phenolics led to relatively large protein complexes depending on the HSE concentration, whereas catechin formed relatively smaller complexes. There was a link between this and the fact that the phenolic compounds found in hazelnut skin were bulkier and more flexible. Moreover, it was found that

the dominant forces in dHPI HSE complex formation were hydrogen bonding and van der Waals forces. The reaction depends on temperature and it is spontaneous ($\Delta H < 0$; $\Delta S < 0$; $\Delta G < 0$). Protein secondary structure was significantly altered by the interaction of dHPI and HSE, mainly due to the concentration of phenolics in the mixture. The secondary structure of the protein became loosened and disordered with an increase in phenolic concentration. Due to this situation, the protein is more likely to have a greater degree of flexibility, thereby improving its functional properties. In this study, protein-polyphenol interactions mainly influenced the bioavailability of hazelnut skin polyphenols, especially GCG and EGCG, which are galloylated types of catechins. Recently, several studies have been conducted on phytochemicals and plant proteins isolated from natural sources. The function of proteins is particularly important in vegan formulations such as foam-like products (mousse) and emulsions (mayonnaise). Further, there is no consensus regarding whether protein-phenolic interactions affect the bioavailability of phenols positively or negatively. Thus, it is necessary to conduct further research and bring it to the attention of the literature on this topic.



REFERENCES

- AACCI Report** (2001). The definition of dietary fiber. *Cereal Foods World*, 46:112–126.
- Acan, B. G., Toker, O. S., Palabiyik, I., Pirouzian, H. R., Bursa, K., Kilicli, M., ...Konar, N.** (2021). Physicochemical properties of chocolate spread with hazelnut cake: Comparative study and optimization. *LWT*, 147:111548.
- Acharya, D. P., Sanguansri, L., Augustin, M. A.** (2013). Binding of resveratrol with sodium caseinate in aqueous solutions. *Food Chemistry*, 141:1050–1054.
- Adler-Nissen, J.** (1979). Determination of the degree of hydrolysis of food protein hydrolysates by trinitrobenzenesulfonic acid. *Journal of Agricultural and Food Chemistry*, 27:1256–1262.
- Adler-Nissen, J. others** (1986). *Enzymic hydrolysis of food proteins*. Elsevier applied science publishers.
- Adrar, N., Bahadori, F., Ceylan, F. D., Topçu, G., Bedjou, F., Capanoglu, E.** (2021). Stability evaluation of interdigitated liposomes prepared with a combination of 1,2-distearoyl-sn-glycero-3-phosphocholine and 1,2-dilauroyl-sn-glycero-3-phosphocholine. *Journal of Chemical Technology & Biotechnology*, 96:2537–2546.
- Aguilera-Angel, E.-Y., Espinal-Ruiz, M., Narváez-Cuenca, C.-E.** (2018). Pectic polysaccharides with different structural characteristics as inhibitors of pancreatic lipase. *Food Hydrocolloids*, 83:229–238.
- Agyei, D. Danquah, M. K.** (2011). Industrial-scale manufacturing of pharmaceutical-grade bioactive peptides. *Biotechnology Advances*, 29:272–277.
- Ahmed, J., Mulla, M., Al-Ruwaih, N., Arfat, Y. A.** (2019a). Effect of high-pressure treatment prior to enzymatic hydrolysis on rheological, thermal, and antioxidant properties of lentil protein isolate. *Legume Science*, 1.
- Ahmed, S. B., Stoica-Guzun, A., Kamar, F. H., Dobre, T., Gudovan, D., ...Jipa, I.** (2019b). Ultrasound enhanced removal of lead from wastewater by hazelnut shell: an experimental design methodology. *International Journal of Environmental Science and Technology*, 16:1249–1260.

- Akbari, N., Milani, J. M., Biparva, P.** (2020). Functional and conformational properties of proteolytic enzyme-modified potato protein isolate. *Journal of the Science of Food and Agriculture*, 100:1320–1327.
- Aksoz, E., Korkut, O., Aksit, D., Gokbulut, C.** (2020). Vitamin e (-, + - and -tocopherol) levels in plant oils. *Flavour and Fragrance Journal*, 35:504–510.
- Al-Shabib, N. A., Khan, J. M., Malik, A., Rehman, M. T., AlAjmi, M. F., Husain, F. M., Hisamuddin, M., Altwaijry, N.** (2020). Molecular interaction of tea catechin with bovine β -lactoglobulin: A spectroscopic and in silico studies. *Saudi Pharmaceutical Journal*, 28:238–245.
- Alasalvar, C., Karamać, M., Kosińska, A., Rybarczyk, A., Shahidi, F., Amarowicz, R.** (2009). Antioxidant activity of hazelnut skin phenolics. *Journal of Agricultural and Food Chemistry*, 57:4645–4650.
- Alasalvar, C., Odabasi, A. Z., Demir, N., Balaban, M. O., Shahidi, F., Cadwallader, K. R.** (2006). Volatiles and flavor of five turkish hazelnut varieties as evaluated by descriptive sensory analysis, electronic nose, and dynamic headspace analysis/gas chromatography-mass spectrometry. *Journal of Food Science*, 69:SNQ99–SNQ106.
- Alasalvar, C. Shahidi, F.** (2008). Compositional characteristics and health effects of hazelnut (*corylus avellana* l.): an overview. In *Tree Nuts*, page 30. CRC Press.
- Amaral, J. S., Casal, S., Citová, I., Santos, A., Seabra, R. M., Oliveira, B. P. P.** (2006). Characterization of several hazelnut (*corylus avellana* l.) cultivars based in chemical, fatty acid and sterol composition. *European Food Research and Technology*, 222:274–280.
- Anderson, J. W., Baird, P., Jr, R. H. D., Ferreri, S., Knudtson, M., Koraym, A., ... Williams, C.** (2009). Health benefits of dietary fiber. *Nutrition Reviews*, 67:188–205.
- Andrade, J., Pereira, C. G., de Almeida Junior, J. C., Viana, C. C. R., ... de Carvalho dos Anjos, V.** (2019). Ftir-atr determination of protein content to evaluate whey protein concentrate adulteration. *LWT*, 99:166–172.
- Anil, M.** (2007). Using of hazelnut testa as a source of dietary fiber in breadmaking. *Journal of Food Engineering*, 80:61–67.
- AOAC** (1990). *Official Methods of Analysis of the Association of Official Analytical Chemists*, volume 2.
- AOCS** (1990). *Official Methods and Recommended Practices of the American Oil Chemists' Society*. AOCS Press: Arlington, Virginia.

- Apak, R., Güçlü, K., Demirata, B., Özyürek, M., Çelik, S., Bektaşoğlu, B., Berker, K., Özyurt, D.** (2007). Comparative evaluation of various total antioxidant capacity assays applied to phenolic compounds with the cuprac assay. *Molecules*, 12:1496–1547.
- Apak, R., Güçlü, K., Özyürek, M., Karademir, S. E.** (2004). Novel total antioxidant capacity index for dietary polyphenols and vitamins c and e, using their cupric ion reducing capability in the presence of neocuproine: Cuprac method. *Journal of Agricultural and Food Chemistry*, 52:7970–7981.
- Arrondo, J. L. R. Goñi, F. M.** (1998). Infrared studies of protein-induced perturbation of lipids in lipoproteins and membranes. *Chemistry and Physics of Lipids*, 96:53–68.
- Arrondo, J. L. R., Muga, A., Castresana, J., Goñi, F. M.** (1993). Quantitative studies of the structure of proteins in solution by fourier-transform infrared spectroscopy. *Progress in Biophysics and Molecular Biology*, 59:23–56.
- Arslan, Y. Eken-Saraçoğlu, N.** (2010). Effects of pretreatment methods for hazelnut shell hydrolysate fermentation with pichia stipitis to ethanol. *Bioresource Technology*, 101:8664–8670.
- Arslan, Y., Takaç, S., Eken-Saraçoğlu, N.** (2012). Kinetic study of hemicellulosic sugar production from hazelnut shells. *Chemical Engineering Journal*, 185-186:23–28.
- Arteaga, V. G., Guardia, M. A., Muranyi, I., Eisner, P., Schweiggert-Weisz, U.** (2020). Effect of enzymatic hydrolysis on molecular weight distribution, techno-functional properties and sensory perception of pea protein isolates. *Innovative Food Science & Emerging Technologies*, 65:102449.
- Atalar, I.** (2019). Functional kefir production from high pressure homogenized hazelnut milk. *LWT*, 107:256–263.
- Avramenko, N. A., Low, N. H., Nickerson, M. T.** (2013). The effects of limited enzymatic hydrolysis on the physicochemical and emulsifying properties of a lentil protein isolate. *Food Research International*, 51:162–169.
- Aydemir, L. Y., Gökbulut, A. A., Baran, Y., Yemenicioğlu, A.** (2014). Bioactive, functional and edible film-forming properties of isolated hazelnut (*corylus avellana* l.) meal proteins. *Food Hydrocolloids*, 36:130–142.
- Baharuddin, N., Halim, N., Sarbon, N.** (2016). Effect of degree of hydrolysis (dh) on the functional properties and angiotensin i-converting enzyme (ace) inhibitory activity of eel (*monopterus* sp.) protein hydrolysate. *International Food Research Journal*, 23(4):1424.

- Balci, S., Dođru, T., Yücel, H.** (1994). Characterization of activated carbon produced from almond shell and hazelnut shell. *Journal of Chemical Technology AND Biotechnology*, 60:419–426.
- Baldi, S.** (2010). Italian Tree Nuts 2010 (*Technical Report IT1040*). USDA's Global Agricultural Information Network (GAIN) Report.
- Barac, M., Cabrilo, S., Stanojevic, S., Pesic, M., Pavlicevic, M., Zlatkovic, B., Jankovic, M.** (2012). Functional properties of protein hydrolysates from pea (*pisum sativum*,l) seeds. *International Journal of Food Science & Technology*, 47:1457–1467.
- Battegazzore, D., Bocchini, S., Alongi, J., Frache, A.** (2014). Plasticizers, antioxidants and reinforcement fillers from hazelnut skin and cocoa by-products: Extraction and use in pla and pp. *Polymer Degradation and Stability*, 108:297–306.
- Bayrak, Y., Yesiloglu, Y., Gecgel, U.** (2006). Adsorption behavior of cr(vi) on activated hazelnut shell ash and activated bentonite. *Microporous and Mesoporous Materials*, 91:107–110.
- Beisl, S., Friedl, A., Miltner, A.** (2017). Lignin from micro- to nanosize: Applications. *International Journal of Molecular Sciences*, 18:2367.
- Bener, M., Şen, F. B., Önem, A. N., Bekdeşer, B., Çelik, S. E., Lalikoglu, M., ...Apak, R.** (2022). Microwave-assisted extraction of antioxidant compounds from by-products of turkish hazelnut (*corylus avellana* l.) using natural deep eutectic solvents: Modeling, optimization and phenolic characterization. *Food Chemistry*, 385:132633.
- Berdutina, A., Neklyudov, A., Ivankin, A., Karpo, B., Mitaleva, S.** (2000). Comparison of proteolytic activities of the enzyme complex from mammalian pancreas and pancreatin. *Applied Biochemistry and Microbiology*, 36:363–367.
- Bernat, N., Cháfer, M., Rodríguez-García, J., Chiralt, A., González-Martínez, C.** (2015). Effect of high pressure homogenisation and heat treatment on physical properties and stability of almond and hazelnut milks. *LWT - Food Science and Technology*, 62:488–496.
- Bertolino, M., Belviso, S., Bello, B. D., Ghirardello, D., Giordano, M., Rolle, L., Gerbi, V., Zeppa, G.** (2015). Influence of the addition of different hazelnut skins on the physicochemical, antioxidant, polyphenol and sensory properties of yogurt. *LWT - Food Science and Technology*, 63:1145–1154.
- Betancur-Ancona, D., Martínez-Rosado, R., Corona-Cruz, A., ...Chel-Guerrero, L.** (2009). Functional properties of hydrolysates from phaseolus lunatus seeds. *International Journal of Food Science & Technology*, 44:128–137.

- Bin Bao, Qianqian Chu, W. W.** (2018). Mechanism of interaction between phenolic compounds and proteins based on non-covalent and covalent interactions. *Medicine Research*, 2(3):180014–.
- Birari, R. B. Bhutani, K. K.** (2007). Pancreatic lipase inhibitors from natural sources: unexplored potential. *Drug Discovery Today*, 12:879–889.
- Bjelić, A., Hočevár, B., Grilc, M., Novak, U., Likozar, B.** (2022). A review of sustainable lignocellulose biorefining applying (natural) deep eutectic solvents (dess) for separations, catalysis and enzymatic biotransformation processes. *Reviews in Chemical Engineering*, 38:243–272.
- Boskou, D., Blekas, G., Tsimidou, M.** (2006). 4 - olive oil composition. In Boskou, D., editor, *Olive Oil*, pages 41–72. AOCS Press, second edition.
- Brown, R., Ware, L., Tey, S. L.** (2022). Effects of hazelnut consumption on cardiometabolic risk factors and acceptance: A systematic review. *International Journal of Environmental Research and Public Health*, 19:2880.
- Bursa, K., Toker, O. S., Palabiyik, I., Yaman, M., Kian-Pour, N., Konar, N., Kilicli, M.** (2021). Valorization of hazelnut cake in compound chocolate: The effect of formulation on rheological and physical properties. *LWT*, 139:110609.
- Buyukcapar, H. Kamalak, A.** (2007). Partial replacement of fish and soyabean meal protein in mirror carp (*cyprinus carpio*) diets by protein in hazelnut meal. *South African Journal of Animal Science*, 37(1):35–44.
- Caccamo, M., Valenti, B., Luciano, G., Priolo, A., Rapisarda, T., Belvedere, G., ... Pauselli, M.** (2019). Hazelnut as ingredient in dairy sheep diet: Effect on sensory and volatile profile of cheese. *Frontiers in Nutrition*, 6.
- Campione, A., Natalello, A., Valenti, B., Luciano, G., Rufino-Moya, P. J., Avondo, M., ... Pauselli, M.** (2020). Effect of feeding hazelnut skin on animal performance, milk quality, and rumen fatty acids in lactating ewes. *Animals*, 10:588.
- Cao, Y. Xiong, Y. L.** (2017). Interaction of whey proteins with phenolic derivatives under neutral and acidic ph conditions. *Journal of Food Science*, 82:409–419.
- Capanoglu, E., Beekwilder, J., Boyacioglu, D., Hall, R., de Vos, R.** (2008). Changes in antioxidant and metabolite profiles during production of tomato paste. *Journal of Agricultural and Food Chemistry*, 56:964–973.
- Cağlar, A. F., Göksu, A. G., Çakır, B., Gülseren, I.** (2021a). Tombul hazelnut (*corylus avellana* l.) peptides with dpp-iv inhibitory activity: In vitro and in silico studies. *Food Chemistry: X*, 12:100151.

- Cağlar, A. F., Çakır, B., Gülseren, I.** (2021b). Lc-q-tof/ms based identification and in silico verification of ace-inhibitory peptides in giresun (turkey) hazelnut cakes. *European Food Research and Technology*, 247:1189–1198.
- Cha, Y., Wu, F., Zou, H., Shi, X., Zhao, Y., Bao, J., Du, M., Yu, C.** (2018). High-pressure homogenization pre-treatment improved functional properties of oyster protein isolate hydrolysates. *Molecules*, 23:3344.
- Chen, L., Chen, J., Yu, L., Wu, K.** (2016). Improved emulsifying capabilities of hydrolysates of soy protein isolate pretreated with high pressure microfluidization. *LWT - Food Science and Technology*, 69:1–8.
- Chen, Y., Sharma-Shivappa, R. R., Keshwani, D., Chen, C.** (2007). Potential of agricultural residues and hay for bioethanol production. *Applied Biochemistry and Biotechnology*, 142:276–290.
- Chen, Z., Wang, C., Gao, X., Chen, Y., Santhanam, R. K., Wang, C., Xu, L., Chen, H.** (2019). Interaction characterization of preheated soy protein isolate with cyanidin-3-o-glucoside and their effects on the stability of black soybean seed coat anthocyanins extracts. *Food Chemistry*, 271:266–273.
- Chen, Z.-Y., Zhu, Q. Y., Wong, Y. F., Zhang, Z., Chung, H. Y.** (1998). Stabilizing effect of ascorbic acid on green tea catechins. *Journal of Agricultural and Food Chemistry*, 46:2512–2516.
- Ciemniewska-Żytkiewicz, H., Verardo, V., Pasini, F., Bryś, J., Koczoń, P., Caboni, M. F.** (2015). Determination of lipid and phenolic fraction in two hazelnut (*corylus avellana* l.) cultivars grown in poland. *Food Chemistry*, 168:615–622.
- Cikrikci, S., Demirkesen, I., Mert, B.** (2016). Production of hazelnut skin fibres and utilisation in a model bakery product. *Quality Assurance and Safety of Crops Foods*, 8:195–206.
- Cimino, G.** (2000). Removal of toxic cations and cr(vi) from aqueous solution by hazelnut shell. *Water Research*, 34:2955–2962.
- Contini, M., Baccelloni, S., Frangipane, M. T., Merendino, N., Massantini, R.** (2012). Increasing espresso coffee brew antioxidant capacity using phenolic extract recovered from hazelnut skin waste. *Journal of Functional Foods*, 4:137–146.
- Contini, M., Baccelloni, S., Massantini, R., Anelli, G.** (2008). Extraction of natural antioxidants from hazelnut (*corylus avellana* l.) shell and skin wastes by long maceration at room temperature. *Food Chemistry*, 110:659–669.

- Coronado-Cáceres, L. J., Rabadán-Chávez, G., Mojica, L., Hernández-Ledesma, B., Quevedo-Corona, L., Cervantes, E. L.** (2020). Cocoa (theobroma cacao l.) seed proteins' anti-obesity potential through lipase inhibition using in silico, in vitro and in vivo models. *Foods*, 9:1359.
- Cuhadar, C.** (2005). Production and Characterization of Activated Carbon from Hazelnut Shell and Hazelnut Husk. *M.Sc. Thesis, Middle East Technical University*.
- Cummings, J. H.** (2001). The effect of dietary fiber on fecal weight and composition. *CRC handbook of dietary fiber in human nutrition*, 3:183–252.
- Dai, S., Lian, Z., Qi, W., Chen, Y., Tong, X., Tian, T., Lyu, B., Wang, M., Wang, H., Jiang, L.** (2022). Non-covalent interaction of soy protein isolate and catechin: Mechanism and effects on protein conformation. *Food Chemistry*, 384:132507.
- Daliri, H., Ahmadi, R., Pezeshki, A., Hamishehkar, H., Mohammadi, M., ...Ghorbani, M.** (2021). Quinoa bioactive protein hydrolysate produced by pancreatin enzyme- functional and antioxidant properties. *LWT*, 150:111853.
- de la Garza, A., Milagro, F., Boque, N., Campión, J., Martínez, J.** (2011). Natural inhibitors of pancreatic lipase as new players in obesity treatment. *Planta Medica*, 77:773–785.
- Demirbas, E.** (2002). Removal of ni(ii) from aqueous solution by adsorption onto hazelnut shell activated carbon: equilibrium studies. *Bioresource Technology*, 84:291–293.
- Demirbas, E., Dizge, N., Sulak, M., Kobya, M.** (2009). Adsorption kinetics and equilibrium of copper from aqueous solutions using hazelnut shell activated carbon. *Chemical Engineering Journal*, 148:480–487.
- Demirbaş, Ö., Karadağ, A., Alkan, M., Doğan, M.** (2008). Removal of copper ions from aqueous solutions by hazelnut shell. *Journal of Hazardous Materials*, 153:677–684.
- Demirbaş, A.** (2005). Estimating of structural composition of wood and non-wood biomass samples. *Energy Sources*, 27:761–767.
- Dervisoglu, M.** (2006). Influence of hazelnut flour and skin addition on the physical, chemical and sensory properties of vanilla ice cream. *International Journal of Food Science and Technology*, 41:657–661.
- Dinkçi, N., Aktaş, M., Akdeniz, V., Sirbu, A.** (2021). The influence of hazelnut skin addition on quality properties and antioxidant activity of functional yogurt. *Foods*, 10:2855.

- Dogan, A., Siyakus, G., Severcan, F.** (2007). Ftir spectroscopic characterization of irradiated hazelnut (*corylus avellana* l.). *Food Chemistry*, 100:1106–1114.
- Du, X., Jing, H., Wang, L., Huang, X., Wang, X., Wang, H.** (2022). Characterization of structure, physicochemical properties, and hypoglycemic activity of goat milk whey protein hydrolysate processed with different proteases. *LWT*, 159:113257.
- Emre, Y., Sevgili, H., Şanlı, M.** (2008). A preliminary study on the utilization of hazelnut meal as a substitute for fish meal in diets of european sea bass (*dicentrarchus labrax* l.). *Aquaculture Research*, 39:324–328.
- Erdogan, V. Mehlenbacher, S. A.** (2000). Interspecific hybridization in hazelnut (*corylus*). *Journal of the American Society for Horticultural Science*, 125:489–497.
- Esfandi, R., Seidu, I., Willmore, W., Tsopmo, A.** (2022). Antioxidant, pancreatic lipase, and -amylase inhibitory properties of oat bran hydrolyzed proteins and peptides. *Journal of Food Biochemistry*, 46.
- Esposito, T., Sansone, F., Franceschelli, S., Gaudio, P. D., Picerno, P., Aquino, R., Mencherini, T.** (2017). Hazelnut (*corylus avellana* l.) shells extract: Phenolic composition, antioxidant effect and cytotoxic activity on human cancer cell lines. *International Journal of Molecular Sciences*, 18:392.
- Esposito, T., Silva, N. H., Almeida, A., Silvestre, A. J., Piccinelli, A., Aquino, R. P., ...Freire, C.** (2020). Valorisation of chestnut spiny burs and roasted hazelnut skins extracts as bioactive additives for packaging films. *Industrial Crops and Products*, 151:112491.
- Fan, X., Cui, Y., Zhang, R., Zhang, X.** (2018). Purification and identification of anti-obesity peptides derived from spirulina platensis. *Journal of Functional Foods*, 47:350–360.
- Fanali, C., Gallo, V., Posta, S. D., Dugo, L., Mazzeo, L., Cocchi, M., Piemonte, V., Gara, L. D.** (2021). Choline chloride–lactic acid-based nades as an extraction medium in a response surface methodology-optimized method for the extraction of phenolic compounds from hazelnut skin. *Molecules*, 26:2652.
- FAOSTAT** (2022a). Crops and Livestock Products. <https://www.fao.org/faostat/en/#data/QCL>. Accessed: 2022-12-01.
- FAOSTAT** (2022b). Food and Agricultural Organization of the United Nations 2022. <https://www.fao.org/faostat/en/data/QCL/visualize>, Accessed on 08 Aug 2022.

- Ferraro, V., Madureira, A. R., Sarmento, B., Gomes, A., Pintado, M. E.** (2015). Study of the interactions between rosmarinic acid and bovine milk whey protein α -lactalbumin, β -lactoglobulin and lactoferrin. *Food Research International*, 77:450–459.
- Ferrero, F.** (2007). Dye removal by low cost adsorbents: Hazelnut shells in comparison with wood sawdust. *Journal of Hazardous Materials*, 142:144–152.
- Fuso, A., Risso, D., Rosso, G., Rosso, F., Manini, F., Manera, I., Caligiani, A.** (2021). Potential valorization of hazelnut shells through extraction, purification and structural characterization of prebiotic compounds: A critical review. *Foods*, 10:1197.
- Ge, Z., Zhang, Y., Jin, X., Wang, W., Wang, X., Liu, M., Zhang, L., Zong, W.** (2021). Effects of dynamic high-pressure microfluidization on the physicochemical, structural and functional characteristics of eucommia ulmoides oliv. seed meal proteins. *LWT*, 138:110766.
- Geow, C. H. Tan, M. C.** (2021). Pretreatment effect of osmotic dehydration on ultrasound-assisted solvent extraction: Functional properties of defatted hazelnut meal. *Journal of Food Processing and Preservation*, 45.
- Ghanghas, N., Prabhakar, P. K., Sharma, S., Mukilan, M.** (2021). Microfluidization of fenugreek (*trigonella foenum graecum*) seed protein concentrate: Effects on functional, rheological, thermal and microstructural properties. *LWT*, 149:111830.
- Ghribi, A. M., Gafsi, I. M., Sila, A., Blecker, C., Danthine, S., Attia, H., Bougatef, A., Besbes, S.** (2015). Effects of enzymatic hydrolysis on conformational and functional properties of chickpea protein isolate. *Food Chemistry*, 187:322–330.
- Gorissen, S. H. M., Crombag, J. J. R., Senden, J. M. G., Waterval, W. A. H., Bierau, J., ... van Loon, L.** (2018). Protein content and amino acid composition of commercially available plant-based protein isolates. *Amino Acids*, 50:1685–1695.
- Gozaydin, G. Yuksel, A.** (2017). Valorization of hazelnut shell waste in hot compressed water. *Fuel Processing Technology*, 166:96–106.
- Green, R. J., Murphy, A. S., Schulz, B., Watkins, B. A., Ferruzzi, M. G.** (2007). Common tea formulations modulate in vitro digestive recovery of green tea catechins. *Molecular Nutrition & Food Research*, 51:1152–1162.
- Grosso, A. L., Riveros, C., Asensio, C. M., Grosso, N. R., Nepote, V.** (2020). Improving walnuts' preservation by using walnut phenolic extracts as natural antioxidants through a walnut protein-based edible coating. *Journal of Food Science*, 85:3043–3051.

- Gu, P., Liu, W., Hou, Q., Ni, Y.** (2021). Lignocellulose-derived hydrogel/aerogel-based flexible quasi-solid-state supercapacitors with high-performance: a review. *Journal of Materials Chemistry A*, 9:14233–14264.
- Gul, O., Atalar, I., Mortas, M., Saricaoglu, F. T., Besir, A., Gul, L. B., Yazici, F.** (2022). Potential use of high pressure homogenized hazelnut beverage for a functional yoghurt-like product. *Anais da Academia Brasileira de Ciências*, 94.
- Gul, O., Saricaoglu, F. T., Besir, A., Atalar, I., Yazici, F.** (2018). Effect of ultrasound treatment on the properties of nano-emulsion films obtained from hazelnut meal protein and clove essential oil. *Ultrasonics Sonochemistry*, 41:466–474.
- Göksu, A. G., Çakır, B., Gülseren, I.** (2022a). Hazelnut peptide fractions preserve their bioactivities beyond industrial manufacture and simulated digestion of hazelnut cocoa cream. *Food Research International*, 161:111865.
- Göksu, A. G., Çakır, B., Gülseren, I.** (2022b). Industrial utilization of bioactive hazelnut peptide fractions in the manufacture of functional hazelnut paste: Ace-inhibition and allergy suppression. *Waste and Biomass Valorization*, 13:3561–3572.
- Gülseren, I.** (2018). In silico methods to identify ace and dpp-iv inhibitory activities of ribosomal hazelnut proteins. *Journal of Food Measurement and Characterization*, 12:2607–2614.
- Gülseren, I., Çakır, B.** (2019). Soğuk pres findik posalarından Üretilmiş triptik peptitlerin in vitro ace inhibe edici aktiviteleri Üzerine on incelemeler. *The Journal of Food*, 44:309–317.
- Günel-Köroğlu, D., Turan, S., Capanoglu, E.** (2022). Interaction of lentil protein and onion skin phenolics: Effects on functional properties of proteins and in vitro gastrointestinal digestibility. *Food Chemistry*, 372:130892.
- Han, L., Lu, K., Zhou, S., Zhang, S., Xie, F., Qi, B., Li, Y.** (2021). Development of an oil-in-water emulsion stabilized by a black bean protein-based nanocomplex for co-delivery of quercetin and perilla oil. *LWT*, 138:110644.
- Harrysson, H., Hayes, M., Eimer, F., Carlsson, N. G., Toth, G. B., Undeland, I.** (2018). Production of protein extracts from swedish red, green, and brown seaweeds, porphyra umbilicalis kützing, ulva lactuca linnaeus, and saccharina latissima (linnaeus) j. v. lamouroux using three different methods. *Journal of Applied Phycology*, 30:3565–3580.
- Hasni, I., Bourassa, P., Hamdani, S., Samson, G., Carpentier, R., Tajmir-Riahi, H.-A.** (2011). Interaction of milk α - and β -caseins with tea polyphenols. *Food Chemistry*, 126:630–639.

- He, J., Xing, Y.-F., Huang, B., Zhang, Y.-Z., Zeng, C.-M.** (2009). Tea catechins induce the conversion of preformed lysozyme amyloid fibrils to amorphous aggregates. *Journal of Agricultural and Food Chemistry*, 57:11391–11396.
- Herrera, R., Hemming, J., Smeds, A., Gordobil, O., Willför, S., Labidi, J.** (2020). Recovery of bioactive compounds from hazelnuts and walnuts shells: Quantitative–qualitative analysis and chromatographic purification. *Biomolecules*, 10:1363.
- Hosgun, E. Bozan, B.** (2014). Effect of temperature and time on the steam pretreatment of hazelnut shells for the enzymatic saccharification. *Chemical Engineering Transactions*, 37:379–384.
- Hoşgün, E. Z., Ay, S. B., Bozan, B.** (2021). Effect of sequential pretreatment combinations on the composition and enzymatic hydrolysis of hazelnut shells. *Preparative Biochemistry Biotechnology*, 51:570–579.
- Hoşgün, E. Z., Berikten, D., Kıvanç, M., Bozan, B.** (2017). Ethanol production from hazelnut shells through enzymatic saccharification and fermentation by low-temperature alkali pretreatment. *Fuel*, 196:280–287.
- Hoşgün, E. Z. Bozan, B.** (2020). Effect of different types of thermochemical pretreatment on the enzymatic hydrolysis and the composition of hazelnut shells. *Waste and Biomass Valorization*, 11:3739–3748.
- Hu, X., Zhao, M., Sun, W., Zhao, G., Ren, J.** (2011). Effects of microfluidization treatment and transglutaminase cross-linking on physicochemical, functional, and conformational properties of peanut protein isolate. *Journal of Agricultural and Food Chemistry*, 59:8886–8894.
- Hunsakul, K., Laokuldilok, T., Sakdatorn, V., Klangpetch, W., Brennan, C. S., Utama-ang, N.** (2022). Optimization of enzymatic hydrolysis by alcalase and flavourzyme to enhance the antioxidant properties of jasmine rice bran protein hydrolysate. *Scientific Reports*, 12:12582.
- Imura, T., Nakayama, M., Taira, T., Sakai, H., Abe, M., Kitamoto, D.** (2015). Interfacial and emulsifying properties of soybean peptides with different degrees of hydrolysis. *Journal of Oleo Science*, 64:183–189.
- Ivanović, S., Avramović, N., Dojčinović, B., Trifunović, S., Novaković, M., Tešević, V., Mandić, B.** (2020). Chemical composition, total phenols and flavonoids contents and antioxidant activity as nutritive potential of roasted hazelnut skins (*corylus avellana* l.). *Foods*, 9:430.
- Jakobek, L.** (2015). Interactions of polyphenols with carbohydrates, lipids and proteins. *Food Chemistry*, 175:556–567.
- Jamali, H. A., Mahvi, A. H., Nazmara, S.** (2009). Removal of cadmium from aqueous solutions by hazel nut shell. *Adsorption*, 2(4).

- JAO, C.-L. KO, W.-C.** (2002). 1,1-diphenyl-2-picrylhydrazyl (dpph) radical scavenging by protein hydrolyzates from tuna cooking juice. *Fisheries Science*, 68:430–435.
- Jia, J., Gao, X., Hao, M., Tang, L.** (2017). Comparison of binding interaction between β -lactoglobulin and three common polyphenols using multi-spectroscopy and modeling methods. *Food Chemistry*, 228:143–151.
- Jiang, J., Zhang, Z., Zhao, J., Liu, Y.** (2018). The effect of non-covalent interaction of chlorogenic acid with whey protein and casein on physicochemical and radical-scavenging activity of in vitro protein digests. *Food Chemistry*, 268:334–341.
- Kanakis, C., Hasni, I., Bourassa, P., Tarantilis, P., Polissiou, M., Tajmir-Riahi, H.-A.** (2011). Milk β -lactoglobulin complexes with tea polyphenols. *Food Chemistry*, 127:1046–1055.
- Karamać, M., Kosińska-Cagnazzo, A., Kulczyk, A.** (2016). Use of different proteases to obtain flaxseed protein hydrolysates with antioxidant activity. *International Journal of Molecular Sciences*, 17:1027.
- Kato, H., Volterman, K. A., West, D. W. D., Suzuki, K., Moore, D. R.** (2018). Nutritionally non-essential amino acids are dispensable for whole-body protein synthesis after exercise in endurance athletes with an adequate essential amino acid intake. *Amino Acids*, 50:1679–1684.
- Kavipriya, J. Ravitchandirane, V.** (2021). Nutritional composition and ft-ir functional group analysis of pharaoh cuttlefish (*sepia pharaonis*) from puducherry coastal waters, india. *Notulae Scientia Biologicae*, 13:10904.
- Kazemipour, M., Ansari, M., Tajrobehkar, S., Majdzadeh, M., Kermani, H. R.** (2008). Removal of lead, cadmium, zinc, and copper from industrial wastewater by carbon developed from walnut, hazelnut, almond, pistachio shell, and apricot stone. *Journal of Hazardous Materials*, 150:322–327.
- Koby, M.** (2004). Adsorption, kinetic and equilibrium studies of cr(vi) by hazelnut shell activated carbon. *Adsorption Science Technology*, 22:51–64.
- Kong, J. Yu, S.** (2007). Fourier transform infrared spectroscopic analysis of protein secondary structures. *Acta Biochimica et Biophysica Sinica*, 39:549–559.
- Konieczny, D., Stone, A. K., Korber, D. R., Nickerson, M. T., Tanaka, T.** (2020). Physicochemical properties of enzymatically modified pea protein-enriched flour treated by different enzymes to varying levels of hydrolysis. *Cereal Chemistry*, 97:326–338.

- Košťálová, Z. Hromádková, Z.** (2019). Structural characterisation of polysaccharides from roasted hazelnut skins. *Food Chemistry*, 286:179–184.
- Król, K. Gantner, M.** (2020). Morphological traits and chemical composition of hazelnut from different geographical origins: A review. *Agriculture*, 10:375.
- Król, K., Gantner, M., Piotrowska, A., Hallmann, E.** (2020). Effect of climate and roasting on polyphenols and tocopherols in the kernels and skin of six hazelnut cultivars (*corylus avellana* L.). *Agriculture*, 10:36.
- Kumaran, A. karunakaran, R. J.** (2006). Antioxidant and free radical scavenging activity of an aqueous extract of *coleus aromaticus*. *Food Chemistry*, 97:109–114.
- Köksal, A. I., Artik, N., Şimşek, A., Güneş, N.** (2006). Nutrient composition of hazelnut (*corylus avellana* L.) varieties cultivated in turkey. *Food Chemistry*, 99:509–515.
- Labuckas, D. O., Maestri, D. M., Perelló, M., Martínez, M. L., Lamarque, A. L.** (2008). Phenolics from walnut (*juglans regia* L.) kernels: Antioxidant activity and interactions with proteins. *Food Chemistry*, 107(2):607–612.
- Laemmli, U. K.** (1970). Cleavage of structural proteins during the assembly of the head of bacteriophage t4. *Nature*, 227:680–685.
- Lainas, K., Alasalvar, C., Bolling, B. W.** (2016). Effects of roasting on proanthocyanidin contents of turkish tombul hazelnut and its skin. *Journal of Functional Foods*, 23:647–653.
- Lakowicz, J. R.** (2006). *Principles of Fluorescence Spectroscopy*. Springer US.
- Lelli, V., Molinari, R., Merendino, N., Timperio, A. M.** (2021). Detection and comparison of bioactive compounds in different extracts of two hazelnut skin varieties, tonda gentile romana and tonda di giffoni, using a metabolomics approach. *Metabolites*, 11:296.
- Leni, G., Soetemans, L., Caligiani, A., Sforza, S., Bastiaens, L.** (2020). Degree of hydrolysis affects the techno-functional properties of lesser mealworm protein hydrolysates. *Foods*, 9:381.
- Lewicka, K.** (2017). Activated carbons prepared from hazelnut shells, walnut shells and peanut shells for high CO₂ adsorption. *Polish Journal of Chemical Technology*, 19:38–43.
- Li, C., Qi, R., Yuan, J., Han, L., Wang, S., Li, W., Han, W.** (2021). In silico study to predict potential precursors of human dipeptidyl peptidase-IV inhibitors from hazelnut. *Journal of Biomolecular Structure and Dynamics*, Early access:1–12.

- Li, D., Zhao, Y., Wang, X., Tang, H., Wu, N., Wu, F., Yu, D., Elfalleh, W.** (2020). Effects of (+)-catechin on a rice bran protein oil-in-water emulsion: Droplet size, zeta-potential, emulsifying properties, and rheological behavior. *Food Hydrocolloids*, 98:105306.
- Li, X., Deng, J., Shen, S., Li, T., Yuan, M., Yang, R., Ding, C.** (2015). Antioxidant activities and functional properties of enzymatic protein hydrolysates from defatted camellia oleifera seed cake. *Journal of Food Science and Technology*, 52:5681–5690.
- Li, X. Hao, Y.** (2015). Probing the binding of (+)-catechin to bovine serum albumin by isothermal titration calorimetry and spectroscopic techniques. *Journal of Molecular Structure*, 1091:109–117.
- Li, X. Wang, S.** (2015). Study on the interaction of (+)-catechin with human serum albumin using isothermal titration calorimetry and spectroscopic techniques. *New Journal of Chemistry*, 39:386–395.
- Li, Y., Jiang, B., Zhang, T., Mu, W., Liu, J.** (2008). Antioxidant and free radical-scavenging activities of chickpea protein hydrolysate (cph). *Food Chemistry*, 106:444–450.
- Lin, C., Kegang, W., Xianghua, C., Lin, Y.** (2015). Microfluidization pretreatment improving enzymatic hydrolysis of soy isolated protein and emulsifying properties of hydrolysates. *Transactions of the Chinese Society of Agricultural Engineering*, 31(5).
- Linarès, E., Larré, C., Lemeste, M., Popineau, Y.** (2000). Emulsifying and foaming properties of gluten hydrolysates with an increasing degree of hydrolysis: Role of soluble and insoluble fractions. *Cereal Chemistry Journal*, 77:414–420.
- Liu, B., Zhu, Y., Tian, J., Guan, T., Li, D., Bao, C., Norde, W., Wen, P., Li, Y.** (2019). Inhibition of oil digestion in pickering emulsions stabilized by oxidized cellulose nanofibrils for low-calorie food design. *RSC Advances*, 9:14966–14973.
- Liu, C., He, W., Chen, S., Chen, J., Zeng, M., Qin, F., He, Z.** (2017a). Interactions of digestive enzymes and milk proteins with tea catechins at gastric and intestinal ph. *International Journal of Food Science & Technology*, 52:247–257.
- Liu, F.-F., Li, Y.-Q., Wang, C.-Y., Liang, Y., Zhao, X.-Z., He, J.-X., Mo, H.-Z.** (2022). Physicochemical, functional and antioxidant properties of mung bean protein enzymatic hydrolysates. *Food Chemistry*, 393:133397.
- Liu, M.-C., Yang, S.-J., Hong, D., Yang, J.-P., Liu, M., Lin, Y., ... Wang, C.** (2016). A simple and convenient method for the preparation of antioxidant peptides from walnut (*Juglans regia* L.) protein hydrolysates. *Chemistry Central Journal*, 10:39.

- Liu, X., Liu, Y.-Y., Guo, J., Yin, S.-W., Yang, X.-Q.** (2017b). Microfluidization initiated cross-linking of gliadin particles for structured algal oil emulsions. *Food Hydrocolloids*, 73:153–161.
- Longato, E., Meineri, G., Peiretti, P. G., Gai, F., Viuda-Martos, M., Pérez-Álvarez, J., ... Fernández-López, J.** (2019). Effects of hazelnut skin addition on the cooking, antioxidant and sensory properties of chicken burgers. *Journal of Food Science and Technology*, 56:3329–3336.
- Lopes, L. C., Martins, J., Esteves, B., De Lemos, L. T.** (2012). New products from hazelnut shell. In *Proceedings of the ECOWOOD*.
- Lunn, J. Theobald, H.** (2006). The health effects of dietary unsaturated fatty acids. *Nutrition Bulletin*, 31(3):178–224.
- López, L., Rivas, S., Moure, A., Vila, C., Parajó, J.** (2020). Development of pretreatment strategies for the fractionation of hazelnut shells in the scope of biorefinery. *Agronomy*, 10:1568.
- Malherbe, S. Cloete, T.** (2002). Lignocellulose biodegradation: Fundamentals and applications. *Reviews in Environmental Science and Bio/Technology*, 1:105–114.
- Masullo, M., Cerulli, A., Mari, A., de Souza Santos, C. C., Pizza, C., Piacente, S.** (2017). Lc-ms profiling highlights hazelnut (nocciola di giffoni pgi) shells as a byproduct rich in antioxidant phenolics. *Food Research International*, 101:180–187.
- Michele, A. D., Pagano, C., Allegrini, A., Blasi, F., Cossignani, L., Raimo, E. D., ... Perioli, L.** (2021). Hazelnut shells as source of active ingredients: Extracts preparation and characterization. *Molecules*, 26:6607.
- Milenković, D., Dašić, P., Veljković, V.** (2009). Ultrasound-assisted adsorption of copper(ii) ions on hazelnut shell activated carbon. *Ultrasonics Sonochemistry*, 16:557–563.
- Minekus, M., Alminger, M., Alvito, P., Ballance, S., Bohn, T., Bourlieu, C., ... Brodkorb, A.** (2014). A standardised static in vitro digestion method suitable for food - an international consensus. *Food Funct.*, 5:1113–1124.
- Mocciaro, G., Bresciani, L., Tsiountsioura, M., Martini, D., Mena, P., ... Ray, S.** (2019). Dietary absorption profile, bioavailability of (poly)phenolic compounds, and acute modulation of vascular/endothelial function by hazelnut skin drink. *Journal of Functional Foods*, 63:103576.
- Mohamed, M., Jaafar, J., Ismail, A., Othman, M., Rahman, M.** (2017). Fourier transform infrared (ftir) spectroscopy. pages 3–29. Elsevier.

- Mohan, A., Rajendran, S. R. C. K., He, Q. S., Bazinet, L., Udenigwe, C. C.** (2015). Encapsulation of food protein hydrolysates and peptides: a review. *RSC Advances*, 5:79270–79278.
- Monsen, E. R.** (2000). Dietary reference intakes for the antioxidant nutrients: vitamin c, vitamin e, selenium, and carotenoids. *Journal of the Academy of Nutrition and Dietetics*, 100(6):637.
- Montella, R., Coisson, J. D., Travaglia, F., Locatelli, M., Bordiga, M., Meyrand, M., ... Arlorio, M.** (2013a). Identification and characterisation of water and alkali soluble oligosaccharides from hazelnut skin (*corylus avellana* l.). *Food Chemistry*, 140:717–725.
- Montella, R., Coisson, J. D., Travaglia, F., Locatelli, M., Malfa, P., Martelli, A., Arlorio, M.** (2013b). Bioactive compounds from hazelnut skin (*corylus avellana* l.): Effects on *lactobacillus plantarum* p17630 and *lactobacillus crispatus* p17631. *Journal of Functional Foods*, 5:306–315.
- Moreno, C., Mojica, L., de Mejía, E. G., Ruiz, R. M. C., Luna-Vital, D. A.** (2020). Combinations of legume protein hydrolysates synergistically inhibit biological markers associated with adipogenesis. *Foods*, 9:1678.
- Moure, A., Dominguez, H., Zúñiga, M. E., Soto, C., Chamy, R.** (2002). Characterisation of protein concentrates from pressed cakes of guevina avellana (chilean hazelnut). *Food Chemistry*, 78:179–186.
- Nazzaro, M., Mottola, M. V., La Cara, F., Del Monaco, G., Aquino, R. P., Volpe, M. G.** (2012). Extraction and characterization of biomolecules from agricultural wastes. *Chem. Eng. Trans*, 27.
- Ni, H., Hayes, H., Stead, D., Liu, G., Yang, H., Li, H., Raikos, V.** (2020). Interaction of whey protein with polyphenols from salal fruits (*Gaultheria shallon*) and the effects on protein structure and hydrolysis pattern by Flavourzyme®. *International Journal of Food Science & Technology*, 55:1281–1288.
- Nielsen, P., Petersen, D., Dambmann, C.** (2001). Improved method for determining food protein degree of hydrolysis. *Journal of Food Science*, 66:642–646.
- Niki, E., Traber, M. G.** (2012). A history of vitamin e. *Annals of Nutrition and Metabolism*, 61:207–212.
- Norazalina, S., Norhaizan, M. E., Hairuszah, I., Nurul, H. S.** (2011). Optimization of optimum condition for phytic acid extraction from rice bran. *African Journal of Plant Science*, 5(3):168–175.

- Odabaş, H. İ. Koca, I.** (2016). Application of response surface methodology for optimizing the recovery of phenolic compounds from hazelnut skin using different extraction methods. *Industrial Crops and Products*, 91:114–124.
- Ozdal, T., Capanoglu, E., Altay, F.** (2013). A review on protein–phenolic interactions and associated changes. *Food Research International*, 51(2):954–970.
- Ozdemir, F. Akinci, I.** (2004). Physical and nutritional properties of four major commercial turkish hazelnut varieties. *Journal of Food Engineering*, 63:341–347.
- Ozdemir, K. S., Yilmaz, C., Durmaz, G., Gökmen, V.** (2014). Hazelnut skin powder: A new brown colored functional ingredient. *Food Research International*, 65:291–297.
- Papadopoulou, A., Green, R. J., Frazier, R. A.** (2005). Interaction of flavonoids with bovine serum albumin: A fluorescence quenching study. *Journal of Agricultural and Food Chemistry*, 53:158–163.
- Papirio, S.** (2020). Coupling acid pretreatment and dosing of ni and se enhances the biomethane potential of hazelnut skin. *Journal of Cleaner Production*, 262:121407.
- Pearce, K. N. Kinsella, J. E.** (1978). Emulsifying properties of proteins: evaluation of a turbidimetric technique. *Journal of Agricultural and Food Chemistry*, 26:716–723.
- Pehlivan, E., Altun, T., Cetin, S., Bhangar, M. I.** (2009). Lead sorption by waste biomass of hazelnut and almond shell. *Journal of Hazardous Materials*, 167:1203–1208.
- Pelvan, E., Öktem Olgun, E., Karadağ, A., Alasalvar, C.** (2018). Phenolic profiles and antioxidant activity of turkish tombul hazelnut samples (natural, roasted, and roasted hazelnut skin). *Food Chemistry*, 244:102–108.
- Perna, S., Giacosa, A., Bonitta, G., Bologna, C., Isu, A., Guido, D., Rondanelli, M.** (2016). Effects of hazelnut consumption on blood lipids and body weight: A systematic review and bayesian meta-analysis. *Nutrients*, 8:747.
- Petrucci, R., Herring, F., Madura, J., Bissonnette, C.** (2011). Spontaneous change: Entropy and gibbs energy. pages 819–862. Pearson.
- Puliga, F., Leonardi, P., Minutella, F., Zambonelli, A., Francioso, O.** (2022). Valorization of hazelnut shells as growing substrate for edible and medicinal mushrooms. *Horticulturae*, 8:214.
- Pérez-Armada, L., Rivas, S., González, B., Moure, A.** (2019). Extraction of phenolic compounds from hazelnut shells by green processes. *Journal of Food Engineering*, 255:1–8.

- Pérez-Jiménez, J., Neveu, V., Vos, F., Scalbert, A.** (2010). Identification of the 100 richest dietary sources of polyphenols: an application of the phenol-explorer database. *European Journal of Clinical Nutrition*, *64*:S112–S120.
- Quaglia, G. B. Orban, E.** (1990). Influence of enzymatic hydrolysis on structure and emulsifying properties of sardine (*sardina pilchardus*) protein hydrolysates. *Journal of Food Science*, *55*:1571–1573.
- Rajan, L., Palaniswamy, D., Mohankumar, S. K.** (2020). Targeting obesity with plant-derived pancreatic lipase inhibitors: A comprehensive review. *Pharmacological Research*, *155*:104681.
- Rauf, A., Imran, M., Abu-Izneid, T., Iahtisham-Ul-Haq, Patel, S., Pan, X., ...Suleria, H.** (2019). Proanthocyanidins: A comprehensive review. *Biomedicine Pharmacotherapy*, *116*:108999.
- Rawel, H. M. Rohn, S.** (2010). Nature of hydroxycinnamate-protein interactions. *Phytochemistry Reviews*, *9*:93–109.
- Renna, M., Lussiana, C., Malfatto, V., Gerbelle, M., Turille, G., Medana, C., ...Cornale, P.** (2020). Evaluating the suitability of hazelnut skin as a feed ingredient in the diet of dairy cows. *Animals*, *10*:1653.
- Rivas, S., Moure, A., Parajó, J. C.** (2020). Pretreatment of hazelnut shells as a key strategy for the solubilization and valorization of hemicelluloses into bioactive compounds. *Agronomy*, *10*:760.
- Rohn, S.** (2014). Possibilities and limitations in the analysis of covalent interactions between phenolic compounds and proteins. *Food Research International*, *65*:13–19.
- Ross, P. D. Subramanian, S.** (1981). Thermodynamics of protein association reactions: forces contributing to stability. *Biochemistry*, *20*:3096–3102.
- Salem, M. A., Aborehab, N. M., Al-Karmalawy, A. A., Fernie, A. R., Alseekh, S., Ezzat, S. M.** (2022). Potential valorization of edible nuts by-products: Exploring the immune-modulatory and antioxidants effects of selected nut shells extracts in relation to their metabolic profiles. *Antioxidants*, *11*:462.
- Saricaoglu, F. T., Gul, O., Besir, A., Atalar, I.** (2018). Effect of high pressure homogenization (hph) on functional and rheological properties of hazelnut meal proteins obtained from hazelnut oil industry by-products. *Journal of Food Engineering*, *233*:98–108.
- Sarmadi, B. H. Ismail, A.** (2010). Antioxidative peptides from food proteins: A review. *Peptides*, *31*:1949–1956.
- Schneider, C.** (2005). Chemistry and biology of vitamin e. *Molecular Nutrition Food Research*, *49*:7–30.

- Seedher, N. Agarwal, P.** (2010). Complexation of fluoroquinolone antibiotics with human serum albumin: A fluorescence quenching study. *Journal of Luminescence*, 130:1841–1848.
- Sen, D. Kahveci, D.** (2020). Production of a protein concentrate from hazelnut meal obtained as a hazelnut oil industry by-product and its application in a functional beverage. *Waste and Biomass Valorization*, 11:5099–5107.
- Sencan, A., Karaboyacı, M., Kılıç, M.** (2015). Determination of lead(ii) sorption capacity of hazelnut shell and activated carbon obtained from hazelnut shell activated with zncl₂. *Environmental Science and Pollution Research*, 22:3238–3248.
- Sert, S., Çelik, A., Tirtom, V. N.** (2017). Removal of arsenic (iii) ions from aqueous solutions by modified hazelnut shell. *DESALINATION AND WATER TREATMENT*, 75:115–123.
- Shahidi, F., Alasalvar, C., Liyana-Pathirana, C. M.** (2007). Antioxidant phytochemicals in hazelnut kernel (*corylus avellana* l.) and hazelnut byproducts. *Journal of Agricultural and Food Chemistry*, 55:1212–1220.
- Shahidi, F. Miraliakbari, H.** (2006). Tree nut oils and byproducts: Compositional characteristics and nutraceutical applications. In *Nutraceutical and specialty lipids and their co-products*, pages 173–182. CRC Press.
- Shen, X. Sun, R.** (2021). Recent advances in lignocellulose prior-fractionation for biomaterials, biochemicals, and bioenergy. *Carbohydrate Polymers*, 261:117884.
- Shi, M., Huang, L.-Y., Nie, N., Ye, J.-H., Zheng, X.-Q., Lu, J.-L., Liang, Y.-R.** (2017). Binding of tea catechins to rice bran protein isolate: Interaction and protective effect during in vitro digestion. *Food Research International*, 93:1–7.
- Shim, S.-M., Yoo, S.-H., Ra, C.-S., Kim, Y.-K., Chung, J.-O., Lee, S.-J.** (2012). Digestive stability and absorption of green tea polyphenols: Influence of acid and xylitol addition. *Food Research International*, 45:204–210.
- Simsek, A., Artik, N., Konar, N.** (2017). Phenolic profile of meals obtained from defatted hazelnut (*corylus avellana* l.) varieties. *International Journal of Life Sciences Biotechnology and Pharma Research*, 6.
- Simsek, S.** (2021). Angiotensin i-converting enzyme, dipeptidyl peptidase-iv, and -glucosidase inhibitory potential of hazelnut meal protein hydrolysates. *Journal of Food Measurement and Characterization*, 15:4490–4496.
- Slatnar, A., Mikulic-Petkovsek, M., Stampar, F., Veberic, R., Solar, A.** (2014). Hplc-msn identification and quantification of phenolic compounds in hazelnut kernels, oil and bagasse pellets. *Food Research International*, 64:783–789.

- Spagnuolo, L., Posta, S. D., Fanali, C., Dugo, L., Gara, L. D.** (2021). Antioxidant and antiglycation effects of polyphenol compounds extracted from hazelnut skin on advanced glycation end-products (ages) formation. *Antioxidants*, 10:424.
- Stressler, T., Eisele, T., Ewert, J., Kranz, B., Fischer, L.** (2019). Proving the synergistic effect of alcalase, pepx and pepn during casein hydrolysis by complete degradation of the released opioid precursor peptide vpyfpgpipn. *European Food Research and Technology*, 245:61–71.
- Stévigny, C., Rolle, L., Valentini, N., Zeppa, G.** (2007). Optimization of extraction of phenolic content from hazelnut shell using response surface methodology. *Journal of the Science of Food and Agriculture*, 87:2817–2822.
- Su, S., Wan, Y., Guo, S., Zhang, C., Zhang, T., Liang, M.** (2018). Effect of peptide–phenolic interaction on the antioxidant capacity of walnut protein hydrolysates. *International Journal of Food Science & Technology*, 53(2):508–515.
- Surek, E. Buyukkileci, A. O.** (2017). Production of xylooligosaccharides by autohydrolysis of hazelnut (*corylus avellana* l.) shell. *Carbohydrate Polymers*, 174:565–571.
- Surek, E., Buyukkileci, A. O., Yegin, S.** (2021). Processing of hazelnut (*corylus avellana* l.) shell autohydrolysis liquor for production of low molecular weight xylooligosaccharides by *aureobasidium pullulans* nr1 y–2311–1 xylanase. *Industrial Crops and Products*, 161:113212.
- Szewczyk, K., Chojnacka, A., Górnicka, M.** (2021). Tocopherols and tocotrienols—bioactive dietary compounds; what is certain, what is doubt? *International Journal of Molecular Sciences*, 22:6222.
- Tamm, F., Herbst, S., Brodkorb, A., Drusch, S.** (2016). Functional properties of pea protein hydrolysates in emulsions and spray-dried microcapsules. *Food Hydrocolloids*, 58:204–214.
- Tang, B., Huang, Y., Ma, X., Liao, X., Wang, Q., Xiong, X., Li, H.** (2016). Multispectroscopic and docking studies on the binding of chlorogenic acid isomers to human serum albumin: Effects of esteryl position on affinity. *Food Chemistry*, 212:434–442.
- Tatar, F., Tunç, M. T., Kahyaoglu, T.** (2015). Turkish tombul hazelnut (*corylus avellana* l.) protein concentrates: functional and rheological properties. *Journal of Food Science and Technology*, 52:1024–1031.
- Taş, N. G. Gökmen, V.** (2015). Bioactive compounds in different hazelnut varieties and their skins. *Journal of Food Composition and Analysis*, 43:203–208.

- Taş, N. G., Yılmaz, C., Gökmen, V.** (2019). Investigation of serotonin, free and protein-bound tryptophan in turkish hazelnut varieties and effect of roasting on serotonin content. *Food Research International*, 120:865–871.
- Thakur, M. Hurburgh, C. R.** (2007). Quality of us soybean meal compared to the quality of soybean meal from other origins. *Journal of the American Oil Chemists' Society*, 84:835–843.
- Thurkill, R. L., Grimsley, G. R., Scholtz, J. M., Pace, C. N.** (2006). pk values of the ionizable groups of proteins. *Protein Science*, 15:1214–1218.
- Tunçil, Y. E.** (2020). Dietary fibre profiles of turkish tombul hazelnut (*corylus avellana* l.) and hazelnut skin. *Food Chemistry*, 316:126338.
- Turkmen, N., Sari, F., Velioglu, Y. S.** (2006). Effects of extraction solvents on concentration and antioxidant activity of black and black mate tea polyphenols determined by ferrous tartrate and folin–ciocalteu methods. *Food Chemistry*, 99:835–841.
- USDA** (2022). Food Composition Database. <https://ndb.nal.usda.gov/ndb/search/list>. Accessed on 2022-12-01.
- Uyan, M., Alptekin, F. M., Cebi, D., Celiktaş, M. S.** (2020). Bioconversion of hazelnut shell using near critical water pretreatment for second generation biofuel production. *Fuel*, 273:117641.
- Uzuner, S. Cekmecelioglu, D.** (2014). Hydrolysis of hazelnut shells as a carbon source for bioprocessing applications and fermentation. *International Journal of Food Engineering*, 10:799–808.
- Uzuner, S., Sharma-Shivappa, R. R., Cekmecelioglu, D., Kolar, P.** (2018). A novel oxidative destruction of lignin and enzymatic digestibility of hazelnut shells. *Biocatalysis and Agricultural Biotechnology*, 13:110–115.
- Uzuner, S., Shivappa, R. R. S., Cekmecelioglu, D.** (2017). Bioconversion of alkali pretreated hazelnut shells to fermentable sugars for generation of high value products. *Waste and Biomass Valorization*, 8:407–416.
- Velickovic, T. D. C. Stanic-Vucinic, D. J.** (2018). The role of dietary phenolic compounds in protein digestion and processing technologies to improve their antinutritive properties. *Comprehensive Reviews in Food Science and Food Safety*, 17:82–103.
- Vermeirssen, V., Camp, J. V., Verstraete, W.** (2004). Bioavailability of angiotensin i converting enzyme inhibitory peptides. *British Journal of Nutrition*, 92:357–366.
- Villamonte, G., Pottier, L., de Lamballerie, M.** (2016). Influence of high-pressure processing on the physicochemical and the emulsifying properties of sarcoplasmic proteins from hake (*merluccius merluccius*). *European Food Research and Technology*, 242:667–675.

- Vogelsang-O'Dwyer, M., Sahin, A. W., Arendt, E. K., Zannini, E.** (2022). Enzymatic hydrolysis of pulse proteins as a tool to improve techno-functional properties. *Foods*, 11:1307.
- Wang, J., Zhou, M., Wu, T., Fang, L., Liu, C., Min, W.** (2020). Novel anti-obesity peptide (rllph) derived from hazelnut (*corylus heterophylla fisch*) protein hydrolysates inhibits adipogenesis in 3t3-l1 adipocytes by regulating adipogenic transcription factors and adenosine monophosphate-activated protein kinase (ampk) activation. *Journal of Bioscience and Bioengineering*, 129:259–268.
- Wang, L., Mao, X., Cheng, X., Xiong, X., Ren, F.** (2010). Effect of enzyme type and hydrolysis conditions on the in vitro angiotensin i-converting enzyme inhibitory activity and ash content of hydrolysed whey protein isolate. *International Journal of Food Science & Technology*, 45:807–812.
- Wang, S., Wang, T., Sun, Y., Cui, Y., Yu, G., Jiang, L.** (2021a). Effects of high hydrostatic pressure pretreatment on the functional and structural properties of rice bran protein hydrolysates. *Foods*, 11:29.
- Wang, X., Ai, X., Zhu, Z., Zhang, M., Pan, F., Yang, Z., Wang, O., Zhao, L., Zhao, L.** (2022). Pancreatic lipase inhibitory effects of peptides derived from sesame proteins: In silico and in vitro analyses. *International Journal of Biological Macromolecules*, 222:1531–1537.
- Wang, X.-Y. Tang, C.-H.** (2012). Physicochemical and antioxidant properties of buckwheat protein isolates with different polyphenolic content modified by limited hydrolysis with trypsin. *Food Technology and Biotechnology*, 50(1):17.
- Wang, Y.-Y., Wang, C.-Y., Wang, S.-T., Li, Y.-Q., Mo, H.-Z., He, J.-X.** (2021b). Physicochemical properties and antioxidant activities of tree peony (*paeonia suffruticosa andr.*) seed protein hydrolysates obtained with different proteases. *Food Chemistry*, 345:128765.
- WHO** (2021). Health topics/obesity. Available online: https://www.who.int/health-topics/obesity#tab=tab_2 (accessed on 4 November 2022).
- WHO World Health Statistics** (2021). Monitoring health for the sdgs sustainable development goals. World Health Organization: Geneva.
- Wien, M.** (2017). Nut intake and health. In *Vegetarian and Plant-Based Diets in Health and Disease Prevention*, pages 271–292. Elsevier.
- Wu, X., Wu, H., Liu, M., Liu, Z., Xu, H., Lai, F.** (2011). Analysis of binding interaction between (-)-epigallocatechin (egc) and β -lactoglobulin by multi-spectroscopic method. *Spectrochimica Acta Part A: Molecular and Biomolecular Spectroscopy*, 82:164–168.

- Xie, Y., Kosińska, A., Xu, H., Andlauer, W.** (2013). Milk enhances intestinal absorption of green tea catechins in vitro digestion/caco-2 cells model. *Food Research International*, 53:793–800.
- Xu, J., Cheng, J. J., Sharma-Shivappa, R. R., Burns, J. C.** (2010). Lime pretreatment of switchgrass at mild temperatures for ethanol production. *Bioresource Technology*, 101:2900–2903.
- Xu, Y. Hanna, M. A.** (2011). Nutritional and anti-nutritional compositions of defatted nebraska hybrid hazelnut meal. *International Journal of Food Science Technology*, 46:2022–2029.
- Xu, Y., Sismour, E. N., Parry, J., Hanna, M. A., Li, H.** (2012). Nutritional composition and antioxidant activity in hazelnut shells from us-grown cultivars. *International Journal of Food Science Technology*, 47:940–946.
- Yalçın, S., Oğuz, F., Yalçın, S.** (2005). Effect of dietary hazelnut meal supplementation on the meat composition of quails. *Turkish Journal of Veterinary & Animal Sciences*, 29(6):1285–1290.
- Yan, S., Xu, J., Zhang, X., Xie, F., Zhang, S., Jiang, L., Qi, B., Li, Y.** (2021). Effect of ph-shifting treatment on the structural and functional properties of soybean protein isolate and its interactions with (–)-epigallocatechin-3-gallate. *Process Biochemistry*, 101:190–198.
- Yuan, B., Lu, M., Eskridge, K. M., Hanna, M. A.** (2018). Valorization of hazelnut shells into natural antioxidants by ultrasound-assisted extraction: Process optimization and phenolic composition identification. *Journal of Food Process Engineering*, 41:e12692.
- Yılmaz, H., Lee, S., Chronakis, I. S.** (2021). Interactions of β -lactoglobulin with bovine submaxillary mucin vs. porcine gastric mucin: The role of hydrophobic and hydrophilic residues as studied by fluorescence spectroscopy. *Molecules*, 26:6799.
- Yılmaz, T. Şebnem Tavman** (2016). Ultrasound assisted extraction of polysaccharides from hazelnut skin. *Food Science and Technology International*, 22:112–121.
- Zarai, Z., Balti, R., Sila, A., Ali, Y. B., Gargouri, Y.** (2016). Helix aspersa gelatin as an emulsifier and emulsion stabilizer: functional properties and effects on pancreatic lipolysis. *Food & Function*, 7:326–336.
- Zeppa, G., Belviso, S., Bertolino, M., Cavallero, M. C., Bello, B. D., Ghirardello, D., ... Gerbi, V.** (2015). The effect of hazelnut roasted skin from different cultivars on the quality attributes, polyphenol content and texture of fresh egg pasta. *Journal of the Science of Food and Agriculture*, 95:1678–1688.

- Zhang, H., Yu, D., Sun, J., Liu, X., Jiang, L., Guo, H., Ren, F.** (2014). Interaction of plant phenols with food macronutrients: characterisation and nutritional–physiological consequences. *Nutrition Research Reviews*, 27:1–15.
- Zhang, L., Chen, X., Wang, Y., Guo, F., Hu, S., Hu, J., Xiong, H., Zhao, Q.** (2021). Characteristics of rice dreg protein isolate treated by high-pressure microfluidization with and without proteolysis. *Food Chemistry*, 358:129861.
- Zhang, Y., Chen, S., Qi, B., Sui, X., Jiang, L.** (2018). Complexation of thermally-denatured soybean protein isolate with anthocyanins and its effect on the protein structure and in vitro digestibility. *Food Research International*, 106:619–625.
- Zhang, Y., Tang, X., Li, F., Zhang, J., Zhang, B., Yang, X., ... Zhang, B.** (2022). Inhibitory effects of oat peptides on lipolysis: A physicochemical perspective. *Food Chemistry*, 396:133621.
- Zheng, Z., Wei, X., Shang, T., Huang, Y., Hu, C., Zhang, R.** (2018). Bioconversion of duck blood cell: process optimization of hydrolytic conditions and peptide hydrolysate characterization. *BMC Biotechnology*, 18:67.
- Zhu, Q. Y., Huang, Y., Tsang, D., Chen, Z.-Y.** (1999). Regeneration of α -tocopherol in human low-density lipoprotein by green tea catechin. *Journal of Agricultural and Food Chemistry*, 47:2020–2025.

CURRICULUM VITAE

Name Surname: Fatma Duygu CEYLAN

EDUCATION :

- **B.Sc.** : 2012, Ege University, Faculty of Engineering, Department of Food Engineering
- **M.Sc.** : 2015, Istanbul Technical University, Institute of Science, Engineering, and Technology, Department of Food Engineering

PUBLICATIONS AND PRESENTATIONS ON THE THESIS:

- **Ceylan, F. D.**, Adrar, N., Günal-Köroğlu, D., Gültekin-Subaşı, B., Capanoglu, E. (2022, accepted). Combined Neutralse-Alcalase Protein Hydrolysates from Hazelnut Meal, a Potential Functional Food Ingredient. Submitted to ACS Omega.
- **Ceylan, F. D.**, Yılmaz, H., Adrar, N., Günal Köroğlu, D., Gultekin Subasi, B., & Capanoglu, E. (2022). Interactions between Hazelnut (*Corylus avellana* L.) Protein and Phenolics and In Vitro Gastrointestinal Digestibility. *Separations*, 9(12), 406.
- **Ceylan, F. D.**, Adrar, N., Bolling, B.W., Capanoglu, E. (2022, submitted) Valorisation of Hazelnut By-products: Current Applications and Future Potential. Submitted.
- **Ceylan, F. D.**, Adrar, N., Gültekin-Subaşı, B., Capanoglu, E. (2022). Neutralse-Alcalase Combined Hydrolysis of Protein Isolates from Hazelnut Meal: Transforming Waste to Functional Food Ingredient. Presented Orally in 2022 Annual Conference and Exhibition, Functional Foods, Nutraceuticals, Natural Health Products and Dietary Supplements, October 2-5, Istanbul, Turkey.

OTHER PUBLICATIONS AND PRESENTATIONS:

- Ale, E. C., Ibáñez, R. A., Wilbanks, D., Peralta, G. H., **Ceylan, F. D.**, Binetti, A. G., ... & Lucey, J. A. (2022). Technological role and metabolic profile of two probiotic EPS-producing strains with potential application in yoghurt: impact on rheology and release of bioactive peptides. *International Dairy Journal*, 105533.

- Adrar, N., Bahadori, F., **Ceylan, F. D.**, Topçu, G., Bedjou, F., & Capanoglu, E. (2021). Stability evaluation of interdigitated liposomes prepared with a combination of 1, 2-d istearoyl-sn-glycero-3-phosphocholine and 1, 2-dilauroyl-sn-glycero-3-phosphocholine. *Journal of Chemical Technology & Biotechnology*, 96(9), 2537-2546.
- Salehi, B., Quispe, C., Butnariu, M., Sarac, I., Marmouzi, I., Kamle, M., ... & Martorell, M. (2021). Phytotherapy and food applications from Brassica genus. *Phytotherapy Research*, 35(7), 3590-3609.
- Guldiken, B., Catalkaya, G., Ozkan, G., **Ceylan, F. D.**, & Capanoglu, E. (2021). Toxicological effects of commonly used herbs and spices. In *Toxicology* (pp. 201-213). Academic Press.
- Liu, X., Raghuvanshi, R., **Ceylan, F. D.**, & Bolling, B. W. (2020). Quercetin and its metabolites inhibit recombinant human angiotensin-converting enzyme 2 (ACE2) activity. *Journal of Agricultural and Food Chemistry*, 68(47), 13982-13989.
- Catalkaya, G., **Ceylan, F. D.**, Ozkan, G., Guldiken, B., & Capanoglu, E. (2020). Consumption, Bioaccessibility, Bioavailability of Anthocyanins and Their Interactions with Gut Microbiota. *Anthocyanins: Antioxidant Properties, Sources and Health Benefits*. New York, USA: Nova Science Publishers, Inc, 107-39.
- Bakir, S., Catalkaya, G., **Ceylan, F. D.**, Khan, H., Guldiken, B., Capanoglu, E., & Kamal, M. A. (2020). Role of dietary antioxidants in neurodegenerative diseases: Where are we standing?. *Current Pharmaceutical Design*, 26(7), 714-729.
- Ozdal, T., **Ceylan, F. D.**, Eroglu, N., Kaplan, M., Olgun, E. O., & Capanoglu, E. (2019). Investigation of antioxidant capacity, bioaccessibility and LC-MS/MS phenolic profile of Turkish propolis. *Food Research International*, 122, 528-536.
- Guldiken, B., Ozkan, G., Catalkaya, G., **Ceylan, F. D.**, Yalcinkaya, I. E., & Capanoglu, E. (2018). Phytochemicals of herbs and spices: Health versus toxicological effects. *Food and Chemical Toxicology*, 119, 37-49.
- Perk, A. A., **Ceylan, F. D.**, Yanar, O., Boztas, K., & Capanoglu, E. (2016). Investigating the antioxidant properties and rutin content of Sea buckthorn (*Hippophae rhamnoides* L.) leaves and branches. *African Journal of Biotechnology*, 15(5), 118-124.